THE UNIVERSITY OF MICHIGAN

INDUSTRY PROGRAM OF THE COLLEGE OF ENGINEERING

THE INTEGRAL ISOBARIC HEAT OF VAPORIZATION OF MIXTURES

Fred P. Stein

A dissertation submitted in partial fulfillment
of the requirements for the degree of
Doctor of Philosophy in The
University of Michigan
1960

September, 1960

IP-456

ACKNOWLEDGEMENTS

The author gratefully acknowledges and offers his sincere thanks for the valuable assistance, in the various forms described below, which he received from both organizations and individuals.

The Department of Chemical and Metallurgical Engineering provided funds for the purchase of equipment and supplies used in the experimental work. Three predoctoral fellowships granted by the National Science Foundation afforded personal financial assistance. The duPont Fundamental Research in Chemical Engineering Fund provided a tuition grant for one semester. The Industry Program of the College of Engineering aided in the preparation and reproduction of the dissertation.

Professor Joseph J. Martin's guidance in the formulation of the thesis problem, his counsel and encouraggement at various stages of the work, and his service as doctoral committee chairman were indispensable. The doctoral committee composed of Professors Lee O. Case, Stuart W. Churchill, Donald L. Katz, and G. Brymer Williams gave of their time and counsel to the author. Professor Williams is to be singled out for his service as committee chairman during the period of Professor Martin's leave. Frank B. Drogosz and Cleatis Bolen of the departmental shop rendered competent assistance in the construction of parts of the apparatus. A number of fellow students offered helpful suggestions for and constructive criticism of the work.

Finally, the moral and financial support of Monica B. Stein, Ethel H. Stein, and Paul E. Stein, members of the author's immediate family, must be recognized. Without this support the author's undergraduate and graduate training would have been in serious jeopardy.

TABLE OF CONTENTS

TABLE OF CONTENTS CONT'D

TABLE OF CONTENTS CONT'D

LIST OF TABLES

LIST OF TABLES CONT'D

LIST OF FIGURES

LIST OF FIGURES CONT'D

ABSTRACT

The integral isobaric heats of vaporization of the isopropyl alcohol-water system and the acetone-water system have been measured in an essentially adiabatic flow calorimeter at atmospheric pressure. The integral isobaric heat of vaporization is defined to be the enthalpy change which occurs when a mixture is totally vaporized under isobaric conditions - the initial state being saturated liquid at the bubble point and the final state being saturated vapor at the dew point. The data obtained have been used to construct accurate enthalpy-concentration diagrams for the systems studied and to serve as the criteria for evaluating methods of predicting integral isobaric heats of vaporization. In addition to the enthalpy data the vapor-liquid equilibria for the two binaries were determined, simultaneously in the same apparatus, and compared to similar data published in the literature.

The flow calorimeter consisted primarily of a small, thermally insulated vaporizer in which vaporization was effected by the consumption of electrical energy in a submerged heater. A constant liquid level was maintained in the vaporizer by the gravitational flow of liquid from a large, constant-head preheater. The vapors which escaped from the vaporizer passed through externally heated lines to a condenser and returned to the preheater as liquid. The rate of cycling from the preheater, to the vaporizer, through the condenser, and back to the preheater was controlled by the amount of power supplied to the heater located in the vaporizer. The principal measurements which were required for determining the integral isobaric heat of vaporization were the power supplied to the heater and the amount of material vaporized in a given interval of time.

The analyses for both systems were determined by density measurements in calibrated pycnometers. Analyses of the condensate (vapor) and the preheater liquid, which were identical, provided the composition of the mixture for which the enthalpy data were taken. A sample of the liquid contents of the vaporizer, in conjunction with the condensate (vapor) sample and the temperature and pressure in the vaporizer during the run, provided the necessary data to determine the vapor-liquid equilibria for the mixture.

Heat transfer between the vaporizer and the surroundings was minimized by a reduction of both the heat-transfer coefficients and the temperature difference. The coefficients were reduced by conventional means. The elimination of the temperature difference was effected by carrying out, in a chamber which surrounded the vaporizer, a vaporization process identical to the one in the vaporizer.

The integral isobaric heats of vaporization obtained for the two binaries studied in this investigation are estimated to be reliable within plus or minus 0.3 per cent. The data were correlated by an equation of the form

$$\lambda_P = z_j L_{j,T_1} + z_k L_{k,T_1} + (z_j \overline{C}^{\circ}_{P,j} + z_k \overline{C}^{\circ}_{P,k})(T_2 - T_1)$$

where λ_P is the integral isobaric heat of vaporization; z_j and z_k are the mole fractions of j and k, respectively; T_1 and T_2 are the bubble-point and dew-point temperatures of the mixture, respectively; L_{j,T_1} and L_{k,T_1} are the heats of vaporization of pure j and pure k, respectively, taken at the bubble-point temperature of the mixture; and $\overline{C}^{\circ}_{P,j}$ and $\overline{C}^{\circ}_{P,k}$

are the ideal-gas specific heats of pure j and pure k, respectively, taken at the average temperature between the bubble point and dew point. This equation is quite simple to use. The average difference, without regard to sign, between the experimental data and the heats of vaporization calculated from the above equation was 0.8 per cent for isopropyl alcohol-water mixtures and 0.3 per cent for acetone-water mixtures.

Application of the above equation to experimental data for methyl alcohol-benzene, acetone-benzene, methyl alcohol-water, ethyl alcohol-water, n-propyl alcohol-water and nitrogen-oxygen mixtures also produced satisfactory results.

INTRODUCTION

The heat of vaporization of mixtures is a particular subject which is encompassed by the broader classification of enthalpy of mixtures. Most studies or calculations involving the enthalpy of mixtures soon lead to questions concerning the heat effects which accompany a liquid-vapor phase change. Any chemical processing step which involves either vaporization or condensation of mixtures, such as distillation and liquefaction operations, requires knowledge of the enthalpy difference between the two phases.

The emphasis of this investigation was on the integral isobaric heat of vaporization, which is the most important type of vaporization from a practical viewpoint; however, this emphasis is not restrictive because the various heats of vaporization are interrelated.

The experimental objectives involved the design, construction, and operation of an adiabatic flow calorimeter for the precise measurement of the integral isobaric heat of vaporization. Heat leaks, which are the bane of all calorimetric measurements, received special attention in the design of the apparatus with the forethought to operation of the calorimeter with mixtures which have a large temperature difference between the bubble point and the dew point. The integral isobaric heat of vaporization was measured at atmospheric pressure for the acetone-water binary, which has large temperature differences between the bubble point and dew point over most of the concentration range, and for the isopropyl alcohol-water binary, which in addition to large bubble-point - dew-point temperature differences at some concentrations also contains

a minimum boiling azeotrope. A secondary experimental objective was to determine, simultaneously with the heat-of-vaporization data and in the same apparatus, the vapor-liquid equilibria for the mixtures and to compare these data with those published in the literature. The experimental data were used to prepare enthalpy-concentration diagrams for both binaries.

The theoretical objectives concerned the development of new methods for predicting integral isobaric heat of vaporization and the evaluation of existing methods. The experimental data served as criteria for evaluation of the reliability of these predictive methods.

THEORETICAL BACKGROUND

Enthalpy Change Accompanying a Liquid-Vapor Phase Change

In reference to a pure material the term "heat of vaporization" defines a single phenomenon. The liquid-vapor phase change is both isothermal and isobaric, and the amount of heat required to change a unit quantity of the material from its saturated-liquid state to its saturated-vapor state is the heat of vaporization.

The heat of vaporization of a mixture, unlike that of a pure compound, is not unique. A mixture can be vaporized in a number of ways, and the heat of vaporization depends on the method chosen. Consider the pressure-temperature diagram of a hypothetical mixture shown in Figure 1 on page 4. Point 1 represents the mixture in its saturated-liquid state at a pressure of P_{1-2} and a temperature of T_{1-3}.

A unit quantity of the mixture in the state represented by point 1 could be completely vaporized by adding heat to it while holding the pressure constant. This vaporization would proceed along a line of constant pressure and increasing temperature from point 1 to point 2. At point 2 the mixture would be in a saturated-vapor state at a pressure of P_{1-2} and a temperature of T_{2-4}. The amount of heat required to effect this type of phase change is known as the integral isobaric heat of vaporization. The word "integral" is included because the mixture is completely vaporized.

From point 1 the vaporization could also proceed along an isothermal line. That is, heat could be added to the mixture along a line of constant temperature and decreasing pressure from point 1 to point 3.

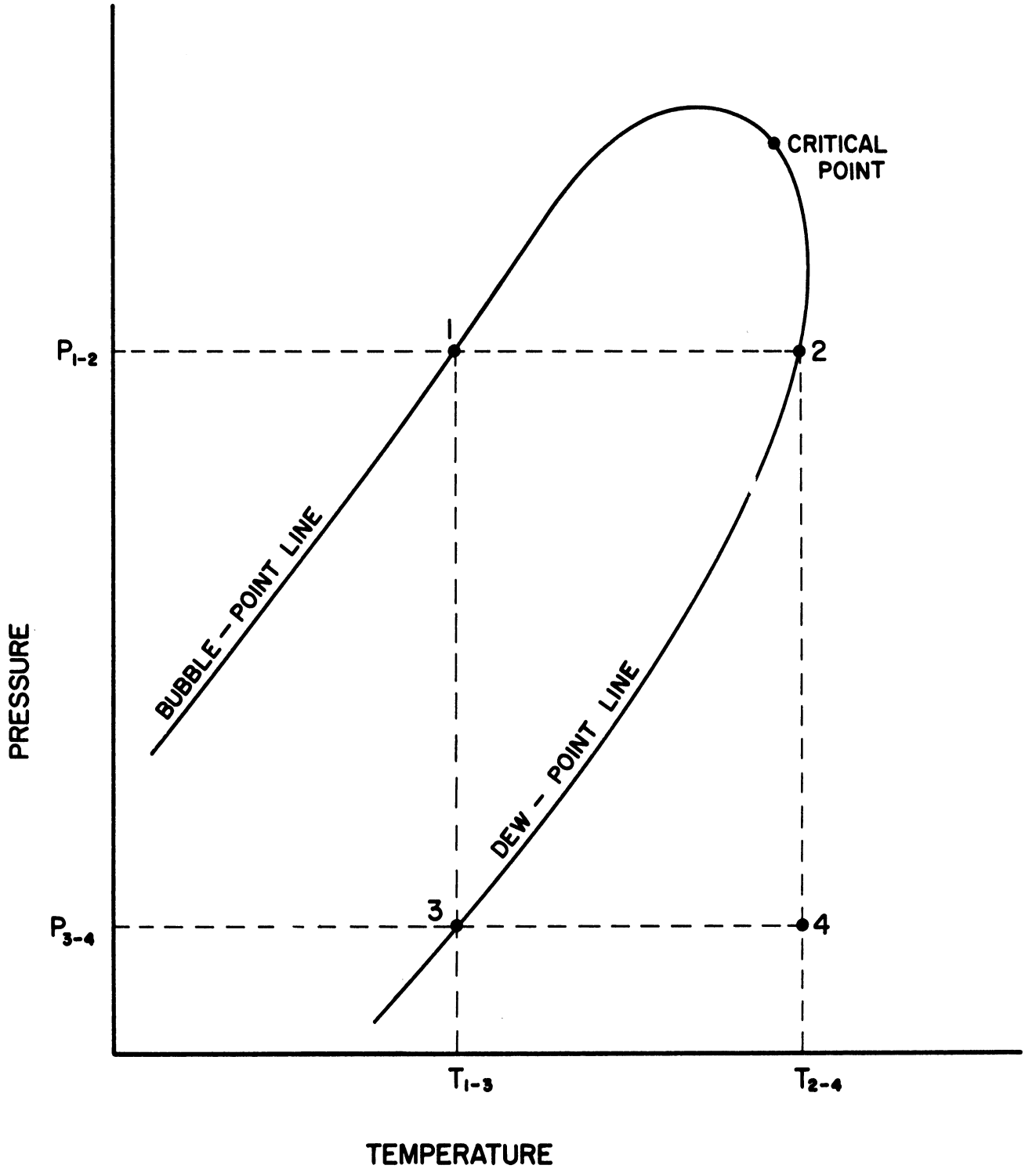

Figure 1. Pressure-Temperature Diagram for a Hypothetical Mixture. (Constant Composition)

At point 3 the entire mixture would be in a saturated-vapor state at a pressure of P_{3-4} and a temperature of T_{1-3}. The amount of heat required to effect this type of phase change for a unit quantity of the mixture is known as the integral isothermal heat of vaporization.

Still another type of vaporization could begin with a mixture in the state represented by point 1. A differential amount of material could be vaporized from this saturated-liquid mixture at both constant pressure and constant temperature. In order for the vapor formed to be in a saturated state at a pressure of P_{1-2} and a temperature of T_{1-3}, the vapor must be of different composition than the liquid, and in particular this composition must be that of the vapor in equilibrium with the liquid. The amount of heat required to effect this type of physical change is known as the differential heat of vaporization. An entirely equivalent procedure would be to begin with an essentially infinite quantity of the mixture in the condition described by point 1 and to vaporize from that a unity quantity of vapor in equilibrium with the liquid. It is difficult to accurately determine the differential heat of vaporization experimentally; for, the task of producing a small amount of equilibrium vapor from an amount of liquid so large that its composition is effectively unchanged does not lend itself to precise experimental technique.

Each of the three types of vaporization described above began with a common saturated liquid denoted by point 1, but each terminated with a saturated vapor under the different conditions denoted by point 2, by point 3, and by the vapor in equilibrium with the point-1 liquid.

The heat required for the integral vaporizations is the difference in enthalpy between the initial and final states; therefore, the integral heats of vaporization are definitely of different magnitude. The differential heat of vaporization, since it involves a vapor of different composition from the liquid, is not in general equal in magnitude to either of the integral heats of vaporization.

Both types of integral heat of vaporization have corresponding integral heats of condensation of exactly the same magnitude but of opposite sign. No such corresponding heat of condensation exists for the differential heat of vaporization because of the differences in the composition and the amount of material involved in each phase. However, a differential heat of condensation can be defined analogously to the differential heat of vaporization. It is the amount of heat which must be removed from an infinite amount of a saturated vapor in order to condense a unit quantity of liquid in equilibrium with the vapor.

Whereas the difference in enthalpies involved with the two integral heats of vaporization is obvious, for example $\lambda_P = \underline{H}^{sat.v.} - \underline{H}^{sat.l.}$, the difference in enthalpies involved with the differential heat of vaporization is not obvious. The enthalpy of the final state is simply that of a unit quantity of the equilibrium vapor, but the enthalpy of this material in its initial state is not immediately apparent. It is not the enthalpy of a unit quantity of the infinite amount of liquid, because this liquid is of a different composition than the vapor. Hence, some of the less volatile material in a unit quantity of the liquid would

not be vaporized while some of the more volatile material that was actually vaporized would have to be drawn from outside of the original unit quantity of liquid.

Further insight into the enthalpies involved can be gained from the consideration of heat and mass balances around a hypothetical, perfectly insulated, flow calorimeter. Consider a binary mixture in a saturated-liquid state which flows to the calorimeter at a rapid rate, F. This stream has a composition, x, and an enthalpy, $\underline{H}_x^{sat.l.}$. A small amount of heat at a rate, Δh, is assumed to be released in the calorimeter. The release of heat energy produces a saturated vapor at a small rate, ΔF. The vapor, which is in equilibrium with the liquid, is of composition y and has an enthalpy of $\underline{H}_y^{sat.v.}$. The liquid flows from the calorimeter at a rate of $F - \Delta F$. This exit liquid has a composition of $x + \Delta x$ and an enthalpy of $\underline{H}_x^{sat.l.} + \Delta\underline{H}^l$. Thus, there is one stream which enters the calorimeter, but two streams which leave.

The enthalpy input to the calorimeter is given by $F\underline{H}_x^{sat.l.} + \Delta h$. The enthalpy output in the vapor stream is $\Delta F\ \underline{H}_y^{sat.v.}$ and in the liquid stream is $(F - \Delta F)(\underline{H}_x^{sat.l.} + \Delta\underline{H}^l)$.

Equating the input and output yields

$$F\ \underline{H}_x^{sat.l.} + \Delta h = \Delta F\ \underline{H}_y^{sat.v.} + (F - \Delta F)(\underline{H}_x^{sat.l.} + \Delta\underline{H}^l) \qquad (1)$$

Multiplying, collecting terms, and dividing through by ΔF yields

$$\frac{\Delta h}{\Delta F} = \underline{H}_y^{sat.v.} - \underline{H}_x^{sat.l.} + F\,\frac{\Delta\underline{H}^l}{\Delta F} - \Delta\underline{H}^l \qquad (2)$$

As Δh approaches zero, as required by the definition of the differential heat of vaporization, the process proceeds at both constant temperature

and pressure, and $\Delta\underline{H}^{l}$ and ΔF also approach zero. Equation (2) then becomes

$$\frac{dh}{dF} = \lambda_{T,P} = \underline{H}_{y}^{sat.v.} - \underline{H}_{x}^{sat.l.} + F\left(\frac{\partial \underline{H}^{l}}{\partial F}\right)_{T,P} \tag{3}$$

Equation (3) is undesirable because it is dependent on the flow rate, F. However, a mass balance around the hypothetical calorimeter produces another equation which permits the elimination of F.

Equating the rate of influx of one component, Fx, to the rate of efflux in the vapor stream, ΔFy, plus the liquid stream, $(F-\Delta F)(x+\Delta x)$, yields

$$Fx = \Delta Fy + (F - \Delta F)(x + \Delta x) \tag{4}$$

Multiplying, collecting terms, and dividing through by ΔF yields

$$x - y = F\frac{\Delta x}{\Delta F} - \Delta x \tag{5}$$

In the limit as Δh approaches zero, Δx and ΔF also approach zero and Equation (5) becomes

$$x - y = F\frac{dx}{dF} \tag{6}$$

A slight rearrangement of Equation (3) yields

$$\lambda_{T,P} = \underline{H}_{y}^{sat.v.} - \underline{H}_{x}^{sat.l.} + F\left(\frac{\partial x}{\partial F}\right)_{T,P}\left(\frac{\partial \underline{H}^{l}}{\partial x}\right)_{T,P} \tag{7}$$

Substitution of Equation (6) into the last term of Equation (7) yields the final result for a binary

$$\lambda_{T,P} = \underline{H}_{y}^{sat.v.} - \underline{H}_{x}^{sat.l.} + (x - y)\left(\frac{\partial \underline{H}^{l}}{\partial x}\right)_{T,P} \tag{8}$$

Equation (8) shows exactly which enthalpy terms are involved in the differential latent heat. The derivative is to be evaluated at the saturation point at composition x.

An analogous expression can be derived for the differential heat of condensation. If a unit quantity of the equilibrium liquid of composition x is considered to be condensed from a large quantity of saturated vapor of composition y, then the differential heat of condensation is given by

$$\Lambda_{T,P} = \underline{H}_x^{sat.l.} - \underline{H}_y^{sat.v.} + (y - x)\left(\frac{\partial H^V}{\partial y}\right)_{T,P} \qquad (9)$$

Here, the derivative is to be evaluated at the saturated-vapor point at composition y.

Relationships Among the Heats of Vaporization of Mixtures

Of the three heats of vaporization of a mixture described in the previous section, the integral isobaric heat of vaporization is of primary interest. In practice most vaporization processes are conducted at constant pressure and on non-differential quantities of material. Furthermore, the method adopted for this investigation makes the integral isobaric heat of vaporization the easiest of the three to accurately determine experimentally. However, the heats of vaporization are related, so that if data for one exist over the range of conditions of interest then the others may be calculated.

The relationship between the two integral heats of vaporization is easily explained in terms of the pressure-temperature diagram shown in Figure 1 on page 4 . As previously defined, the integral

isothermal heat of vaporization is the enthalpy difference between the mixture in a state defined by point 3 and the same mixture in a state defined by point 1. Because enthalpy is a state function, the path traversed in going from point 1 to point 3 is inconsequential. Thus, the sum of the enthalpy changes in traversing the route 1-2-4-3 is identically the integral isothermal heat of vaporization. By definition the enthalpy difference between point 2 and point 1 is the integral isobaric heat of vaporization. The path from point 2 to point 4 represents the isothermal expansion at T_{2-4} of the vapor from a saturation pressure of P_{1-2} to a pressure P_{3-4}. This enthalpy difference is given by

$$\Delta H^{V}_{Exp} = \int_{P_{1-2}}^{P_{3-4}} [\underline{V} - T(\frac{\partial \underline{V}}{\partial T})]dP \qquad (10)$$

The path from point 4 to point 3 represents an isobaric cooling at P_{3-4} of the vapor from a temperature of T_{2-4} to a saturation temperature of T_{1-3}. This enthalpy difference is given by

$$\Delta H^{V}_{Cool} = \int_{T_{2-4}}^{T_{1-3}} C^{V}_{P,m} dT \qquad (11)$$

The summation of the above enthalpy terms gives the relationship between the two integral heats of vaporization

$$\lambda_T = \lambda_P + \Delta H^{V}_{Cool} + \Delta H^{V}_{Exp} \qquad (12)$$

It is doubtful if the second and third terms on the right-hand side of Equation (12) can be evaluated rigorously for any mixture because of

the lack of the required data. Fortunately, however, the first term is quite large in comparison to the latter two, and as a result, suitable estimates of the latter terms permit calculation of the integral isothermal heat of vaporization with very nearly the same degree of accuracy as is embodied in the first term, the integral isobaric heat of vaporization. The enthalpy change resulting from the expansion step can be evaluated - if, indeed, it is significant at all - with sufficient accuracy by use of generalized charts and the pseudo-critical concept for mixtures. The specific heat for the vapor mixture can be obtained by averaging the specific heats of the pure components for the pressure P_{3-4} pursuant to the concentration of each component in the mixture. The specific heats for the vapor are additive in this manner except at extreme conditions where the heat of mixing in the vapor phase becomes significant. If it is not desirable to average the pure-component specific heats or if none are available for a pressure of P_{3-4}, then the enthalpy change for the step which involved the isothermal expansion would have to be evaluated for an expansion to zero pressure, where the specific heat of the mixture can be determined rigorously by a molal average of the ideal-gas specific heats. This procedure, of course, would require the additional evaluation of the enthalpy change for the isothermal compression of the vapor from zero pressure to the final pressure of P_{3-4}.

The relationship between the integral isobaric heat of vaporization and the differential heat of condensation is simpler, and in practice it is easier to apply, than the relationship which involves the

differential heat of vaporization. If the composition of the mixture shown on Figure 1 on page 4 is denoted by x, then in order to produce by differential condensation a unit quantity of x in the saturated-liquid state described by point 1, one must start with an infinite amount of saturated vapor which has a composition y, a temperature of T_{1-3}, and a pressure of P_{1-2}. An entirely equivalent procedure which would produce the same end result is as follows: (1) separate from the large amount of vapor of composition y a unit quantity of vapor of composition x at a constant temperature of T_{1-3} and a constant pressure of P_{1-2}, (2) isobaricly heat the unit quantity of vapor of composition x from T_{1-3} to T_{2-4}, (3) totally condense the unit quantity of vapor of composition x under isobaric conditions. The enthalpy change accompanying step 1 is the same magnitude as the vapor-phase differential heat of mixing, ΔH_M^v, for a unit quantity of composition x in an infinite quantity of composition y; however, the sign on the differential heat of mixing is reversed. It is doubtful if such data exist for any mixture, but, fortunately, the heat effects accompanying the mixing of vapors are quite small and can safely be neglected except at extreme conditions. This term will be neglected in further discussions. The enthalpy change accompanying step 2 is given by

$$\Delta H_{heat}^v = \int_{T_{1-3}}^{T_{2-4}} C_{P,m}^v \, dT \qquad (13)$$

where $C_{P,m}^v$ is the specific heat of the vapor of composition x at a pressure of P_{1-2}. It is doubtful if this piece of data is available for mixtures, but a molal average of the specific heats of the pure

components will give a reliable answer for all conditions where the vapor-phase heat of mixing is small. Step 3 by definition is the negative of the integral isobaric heat of vaporization. The sum of the enthalpy changes involved in the three steps is the differential heat of condensation.

$$\Lambda_{T,P} = - \Delta\underline{H}^{V}_{M} + \Delta\underline{H}^{V}_{heat} - \lambda_{P} \tag{14}$$

Since the integral isobaric heat of vaporization has been related to both of the other heats of vaporization by Equations (12) and (14), a combination of these equations yields the relationship between the differential heat of condensation and the integral isothermal heat of vaporization. It is

$$\Lambda_{T,P} = - \Delta\underline{H}^{V}_{M} + \Delta\underline{H}^{V}_{heat} - \lambda_{T} + \Delta\underline{H}^{V}_{cool} + \Delta\underline{H}^{V}_{Exp} \tag{15}$$

Since the terms $\Delta\underline{H}^{V}_{heat}$ and $\Delta\underline{H}^{V}_{cool}$ refer to heating and cooling the same material over the same temperature range, one is the negative of the other; hence, they cancel, and Equation (15) becomes

$$\Lambda_{T,P} = - \lambda_{T} + \Delta\underline{H}^{V}_{Exp} - \Delta\underline{H}^{V}_{M} \tag{16}$$

METHODS OF PREDICTING HEATS OF VAPORIZATION OF MIXTURES

Summary

The subsequent sections in this chapter deal with relationships between the heats of vaporization of mixtures and other properties of both the mixtures and the pure components. The data available in the literature for these "other properties" are much more abundant than heat of vaporization data; therefore, the available data in conjunction with the relationships developed hereinafter serve as a means of predicting heats of vaporization of mixtures. The emphasis is on relationships involving the integral isobaric heat of vaporization; however, this emphasis is not restrictive because, as shown in the previous chapter, the heats of vaporization are interrelated.

The possible predictions range in complexity from the assumption of a constant molal heat of vaporization for an entire range of compositions to the rigorous application of two-phase, P-V-T-x data for the evaluation of the heat of vaporization of a single mixture. Each method has its own merits; consequently, for a specific case the most rigorous method which is consistent with both the data and the time available should be chosen. Predictive methods which require, as a fundamental part, data on the behavior of mixtures (with the exception of data on vapor-liquid equilibria) are more limited in application than methods which require only data on pure materials, because the available data on mixtures are scarce relative to those for the pure components. Integral heat of mixing in the liquid phase at temperatures above ambient temperatures and the specific heat of liquid mixtures as

a function of temperature are examples of frequently needed mixture data which are quite scarce. In addition, long, tedious calculations to adjust available data to fit the requirements of a predictive technique tend to cast suspicion on the reliability of the adjusted data and, thereafter, the results of the prediction.

In the section entitled "The Enthalpy-Temperature-Diagram Approach" particular emphasis is given to the development of an equation for the prediction of the integral isobaric heat of vaporization. This equation permits prediction of the integral isobaric heat of vaporization by much shorter and much less tedious computations than those required for construction of an enthalpy-concentration diagram, which seems to be the most used and most frequently recommended method. In addition, the aforementioned equation requires less data on mixture behavior than the enthalpy-concentration diagram; consequently, the results, which are a function of the reliability of the data used, can reasonably be expected to be more accurate, or at least of equal accuracy to those obtained from the diagram.

The Enthalpy-Temperature-Diagram Approach

Figure 2 on page 16 is an enthalpy-temperature diagram for a hypothetical mixture. The diagram is for a constant composition; every composition would have its own envelope on the H-T plane. The isobar, P_{1-2}, represents the enthalpy-temperature relationship for the addition of heat to the mixture at constant pressure, beginning in the subcooled-liquid region and extending through the two-phase region into the superheated-vapor region. The straight isobar through the two-phase

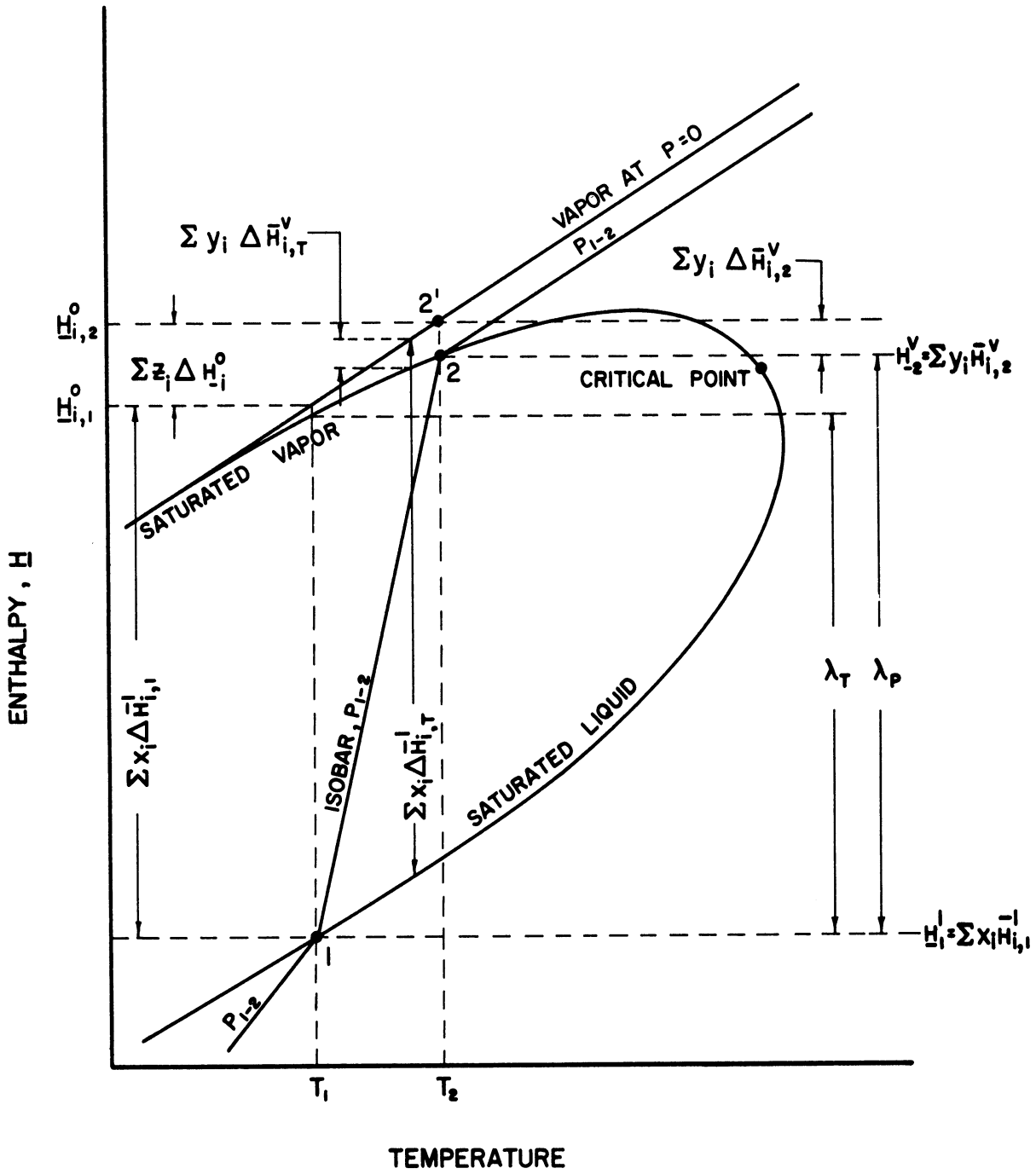

Figure 2. Enthalpy-Temperature Diagram for a Hypothetical Mixture. (Constant Composition $x_i = y_i = z_i$)

envelope is simply a connection of points 1 and 2 and is not intended to construe that an isobaric vaporization must or does proceed along that path. The straight isobars in the superheated-vapor region and the subcooled-liquid region imply that the specific heats of the vapor and the liquid are independent of temperature, an assumption which is valid only for small temperature ranges. From the definitions of the heats of vaporization and with the aid of the isobar, P_{1-2}, it is easy to identify the distances, λ_P and λ_T, to be the integral isobaric heat of vaporization and the integral isothermal heat of vaporization, respectively. Reference is made in subsequent paragraphs of this section to the quantities shown on the figure, during the process of developing an equation for the prediction of the integral isobaric heat of vaporization.

From the definition of integral isobaric heat of vaporization and the properties of partial enthalpies one can write

$$\lambda_P = (\underline{H}_2^v - \underline{H}_1^l)_{P_{1-2}} = \sum_i y_i \bar{H}_{i,2}^v - \sum_i x_i \bar{H}_{i,1}^l \qquad (17)$$

In Equation (17) the mole fractions, x_i and y_i, are equal; the $\bar{H}$'s are partial molal enthalpies; subscripts 1 and 2 refer to points 1 and 2, respectively; and the superscripts, l and v, refer to the liquid and vapor phases, respectively. The definition of a new term, $\underline{H}_{i,T}^o$, equal to the enthalpy of component i in the ideal-gas state at temperature T permits one to write Equation (17) in the form

$$\lambda_P = -\sum_i y_i \underline{H}_{i,2}^o + \sum_i y_i \bar{H}_{i,2}^v + \sum_i x_i \underline{H}_{i,1}^o - \sum_i x_i \bar{H}_{i,1}^l + \sum_i y_i \underline{H}_{i,2}^o - \sum x_i \underline{H}_{i,1}^o \qquad (18)$$

The newly defined term was inserted by simply adding and subtracting both $\sum_i y_i \underline{H}^0_{i,2}$ and $\sum_i x_i \underline{H}^0_{i,1}$ to the right-hand side of the equation. Here again $x_i = y_i$. Rearranging Equation (18) yields

$$\lambda_P = -\sum_i y_i(\underline{H}^0_{i,2} - \overline{H}^V_{i,2}) + \sum_i x_i(\underline{H}^0_{i,1} - \overline{H}^l_{i,1}) + \sum_i z_i(\underline{H}^0_{i,2} - \underline{H}^0_{i,1}) \quad (19)$$

where $x_i = y_i = z_i$. The definition of three more new terms for the bracketed terms, $\Delta\overline{H}^V_{i,2} = \underline{H}^0_{i,2} - \overline{H}^V_{i,2}$, $\Delta\overline{H}^l_{i,1} = \underline{H}^0_{i,1} - \overline{H}^l_{i,1}$, and $\Delta\underline{H}^0_i = \underline{H}^0_{i,2} - \underline{H}^0_{i,1}$, permits one to write Equation (19) in the shorter form

$$\lambda_P = \sum_i x_i(\Delta\overline{H}^l_{i,1}) + \sum_i z_i(\Delta\underline{H}^0_i) - \sum_i y_i(\Delta\overline{H}^V_{i,2}) \quad (20)$$

Equation (20) is the basic equation to be considered in this development; it is rigorous, and its various terms are illustrated on the $\underline{H}$-T plane. The terms are considered individually for evaluation.

The last term, $\sum_i y_i(\Delta\overline{H}^V_{i,2})$, is the enthalpy change for the isothermal expansion at the dew-point temperature, T_2, of the vapor from the saturation pressure, $P_{1\text{-}2}$, to zero pressure. For ideal gases the enthalpy change is zero, and even for a non-ideal gas at moderate pressures it is quite small in comparison to the other enthalpy terms. It can be estimated from the generalized charts in conjunction with the pseudo-critical concept, if it can not be safely neglected. However, for the purposes at hand it will be assumed that

$$\sum_i y_i(\Delta\overline{H}^V_{i,2}) \cong 0 \quad (21)$$

Equation (21) is tantamount to making points 2 and 2' on the figure coincide.

The term $\sum_i z_i(\Delta\underline{H}_i^0)$ represents the enthalpy change on heating the ideal-gas mixture from the bubble-point temperature, T_1, to the dew-point temperature, T_2. It is given by

$$\sum_i z_i(\Delta\underline{H}_i^0) = \int_{T_1}^{T_2} C_{P,m}^0 \, dT = \sum_i \int_{T_1}^{T_2} y_i C_{P,i}^0 \, dT \qquad (22)$$

where $C_{P,i}^0$ is the heat capacity of component i in the ideal-gas state.

$\sum_i x_i(\Delta\overline{H}_{i,1}^l)$ is the enthalpy change accompanying the vaporization of the mixture at constant temperature T_1 and the isothermal expansion of the resulting vapor to zero pressure. The evaluation of this term is not accomplished as directly as the others. The thermodynamic equation which gives the temperature variation of the fugacity function is

$$\underline{H}_{i,T}^0 - \overline{H}_{i,T} = RT^2\left(\frac{\partial \ln \overline{f}_i}{\partial T}\right)_{P,N} \qquad (23)$$

This equation is derived in many thermodynamic texts, for example Hougen and Watson.[30] It represents the partial molal enthalpy difference for component i in a mixture which undergoes a change from any initial state to a final state of zero pressure and the same temperature as the original state. The restrictions on the derivative are constant total pressure P and constant total composition N. Since the entire $\underline{H}$-T diagram is for constant total composition, the subscript N will be dropped henceforth. $\overline{f}_i$ is the fugacity of species i in the mixture in its original state. In the notation of this development Equation (23) becomes

$$\sum_i x_i(\Delta\overline{H}_{i,1}^l) = RT_1^2 \sum x_i\left(\frac{\partial \ln \overline{f}_i^l}{\partial T}\right)_{P_{1\text{-}2}} \qquad (24)$$

The fugacity, $\bar{f}_i^l$, is given by

$$\bar{f}_i^l = \gamma_i \, x_i \, p_i \tag{25}$$

where γ_i is the activity coefficient, which is a corrective factor for the non-ideality of the liquid mixture; x_i is the mole fraction of species i; and p_i is the vapor pressure of i at the temperature of interest. If one takes logarithms of both sides of Equation (25) and substitutes the result for $\ln \bar{f}_i^l$ into Equation (24) the result is

$$\sum_i x_i (\Delta \bar{H}_{i,l}^l) = RT_l^2 \sum_i x_i \left[\left(\frac{\partial \ln \gamma_i}{\partial T}\right)_{P_{l-2}} + \left(\frac{\partial \ln x_i}{\partial T}\right)_{P_{l-2}} + \left(\frac{\partial \ln p_i}{\partial T}\right)_{P_{l-2}} \right] \tag{26}$$

where all derivatives are to be evaluated at T_l. Consider the term, $\sum_i x_i \left(\frac{\partial \ln x_i}{\partial T}\right)_{P_{l-2}}$, in Equation (26). If this term is written out for a binary, and if it is observed that $dx_j + dx_k = 0$ for a binary the result is

$$\begin{aligned} \sum_i x_i \left(\frac{\partial \ln x_i}{\partial T}\right)_{P_{l-2}} &= x_j \left(\frac{\partial \ln x_j}{\partial T}\right)_{P_{l-2}} + x_k \left(\frac{\partial \ln x_k}{\partial T}\right)_{P_{l-2}} \\ &= x_j \frac{1}{x_j} \left(\frac{\partial x_j}{\partial T}\right)_{P_{l-2}} + x_k \frac{1}{x_k} \left(\frac{\partial x_k}{\partial T}\right)_{P_{l-2}} \\ &= \left(\frac{\partial x_j}{\partial T}\right)_{P_{l-2}} - \left(\frac{\partial x_j}{\partial T}\right)_{P_{l-2}} = 0 \end{aligned} \tag{27}$$

thus, Equation (26) becomes

$$\sum_i x_i (\Delta \bar{H}_{i,l}^l) = RT_l^2 \sum_i x_i \left[\left(\frac{\partial \ln p_i}{\partial T}\right)_{P_{l-2}} + \left(\frac{\partial \ln \gamma_i}{\partial T}\right)_{P_{l-2}} \right] \tag{28}$$

The combination of Equations (21), (22), and (28) according to the basic Equation (20) yields

$$\lambda_P = \sum_i x_i(\Delta\bar{H}^l_{i,1}) + \sum_i z_i(\Delta\bar{H}^0_i) - \sum_i y_i(\Delta\bar{H}^v_{i,2}) \tag{20}$$

$$= RT_1^2 \sum_i x_i\left[\left(\frac{\partial \ln p_i}{\partial T}\right)_{P_{1-2}} + \left(\frac{\partial \ln \gamma_i}{\partial T}\right)_{P_{1-2}}\right] + \int_{T_1}^{T_2} \sum_i y_i C^0_{P,i}\,dT \tag{29}$$

Equation (29) written out for a binary becomes

$$\lambda_P = x_j RT_1^2 \left(\frac{\partial \ln p_j}{\partial T}\right)_{P_{1-2}} + x_k RT_1^2 \left(\frac{\partial \ln p_k}{\partial T}\right)_{P_{1-2}}$$

$$+ RT_1^2 \left[x_j\left(\frac{\partial \ln \gamma_j}{\partial T}\right)_{P_{1-2}} + x_k\left(\frac{\partial \ln \gamma_k}{\partial T}\right)_{P_{1-2}}\right]$$

$$+ y_j \int_{T_1}^{T_2} C^0_{P,j}\,dT + y_k \int_{T_1}^{T_2} C^0_{P,k}\,dT \tag{30}$$

where all the derivatives are to be evaluated at T_1.

The terms in Equation (30) will be examined further in pairs. The term, $RT_1^2 \left(\frac{\partial \ln p_j}{\partial T}\right)_{P_{1-2}}$, is the Clausius-Clapeyron equation for the heat of vaporization, L_{j,T_1}, of component j at temperature T_1. The restriction of constant total pressure on the derivative has no significance here. The substitution of the heat of vaporization for the Clausius-Clapeyron equation involves the assumption that the ratio $RT_1/P_{1-2}\,\Delta\underline{V}$ is essentially equal to unity. With this substitution the first two terms of Equation (30) become

$$x_j L_{j,T_1} + x_k L_{k,T_1} \tag{31}$$

Each mixture of j and k has a different bubble point, T_1; therefore the L's, as well as the x's, will be different for every composition.

The limits on the integrals of the last pair of terms in Equation (30) are the bubble-point and the dew-point temperatures. If these temperatures are not widely separated, the ideal-gas specific heat, $\overline{C}^{o}_{P,j}$, at the average temperature should be a good approximation. Thus, the last two terms in Equation (30) can be reduced to

$$(y_j \overline{C}^{o}_{P,j} + y_k \overline{C}^{o}_{P,k})(T_2 - T_1) \tag{32}$$

The middle pair of terms of Equation (30) can not be reduced as straightforwardly as the others. Rearrangement and collection of terms for this pair yields

$$RT_1^2 \left[x_j \left(\frac{\partial \ln \gamma_j}{\partial T}\right)_{P_{1-2}} + x_k \left(\frac{\partial \ln \gamma_k}{\partial T}\right)_{P_{1-2}}\right]$$

$$= RT_1^2 \left[x_j \left(\frac{\partial \ln \gamma_j}{\partial x_j}\right)_{P_{1-2}} \left(\frac{\partial x_j}{\partial T}\right)_{P_{1-2}} + x_k \left(\frac{\partial \ln \gamma_k}{\partial x_j}\right)_{P_{1-2}} \left(\frac{\partial x_j}{\partial T}\right)_{P_{1-2}}\right]$$

$$= RT_1^2 \left(\frac{\partial x_j}{\partial T}\right)_{P_{1-2}} \left[x_j \left(\frac{\partial \ln \gamma_j}{\partial x_j}\right)_{P_{1-2}} + x_k \left(\frac{\partial \ln \gamma_k}{\partial x_j}\right)_{P_{1-2}}\right] \cong 0 \tag{33}$$

The terms in the brackets are almost equivalent to the Duhem[15] relationship; however, in the Duhem relationship the derivatives carry the additional restriction of constant temperature. In spite of the lack of rigor the Duhem equation has been used extensively under isobaric and varying-temperature conditions, and it has been found satisfactory in many cases under these conditions (see for example Dodge[13]). Therefore, the bracketed terms are set equal to zero by the Duhem equation; hence, the entire expression becomes zero. Additional discussion of these relationships appears in subsequent paragraphs of this section.

Rewriting Equation (30) according to Statements (31) and (32) and Equation (33) and recalling that throughout the development $x_j = y_j = z_j$ (The different letters were used merely to avoid confusion as to which phase was under consideration at the time.) yields the final working equation for the prediction of the integral isobaric heat of vaporization of a binary

$$\lambda_P = z_j L_{j,T_1} + z_k L_{k,T_1} + (z_j \bar{C}^0_{P,j} + z_k \bar{C}^0_{P,k})(T_2 - T_1) . \qquad (34)$$

Throughout the development of this equation the composition terms had to be in mole fractions and the temperatures in absolute degrees in order to use a unique value for the gas constant, R. However, R does not appear in the final working equation so that any consistent set of units, such as mass fractions, calories per gram, and degrees centigrade may be used successfully. The following data are required for the prediction of integral isobaric heats of vaporization from Equation (34): (1) isobaric vapor-liquid equilibria, (2) the heat of vaporization of the pure components as a function of temperature in the temperature range covered by the bubble points of the mixtures, (3) the ideal-gas specific heat of the pure components as a function of temperature in the temperature range covered by the bubble points and dew points of the mixture. The computations required by this equation are both simple and short. The inherent assumptions involved in the derivation of Equation (34) are not restrictive, but they are noted here in case estimates of the magnitude of their effect are desired. The assumptions are (1) the mixture under isobaric and varying-temperature conditions obeys the Duhem equation, (2) the ratio $RT_1/P_{1-2}\Delta\underline{V}$ is essentially equal to unity for both

pure components, (3) the pressure effect on the enthalpy of the vapor between P_{1-2} and zero pressure is negligible.

An investigation of the terms in Equation (33) with respect to their relationship to the Duhem equation adds additional information to the properties of the mixtures. First, however, it should be pointed out that direct evaluation of Equation (33) is tedious and not likely to produce satisfactory results. Graphical differentiation of the activity-coefficient data is apt to introduce larger errors than the assumption of applicability of the Duhem equation. Differentiation of most of the correlating equations for activity coefficients, including the Redlich-Kister[55] equations, produces identically zero results because the Duhem equation is inherent in their derivations.

Ibl and Dodge[32] have shown that the rigorous Duhem equation for isobaric and varying-temperature conditions is given by

$$\left[\frac{\partial \ln \gamma_j}{\partial \ln x_j}\right]_P - \left[\frac{\partial \ln \gamma_k}{\partial \ln (1-x_j)}\right]_P = - \Delta H_M^1 \frac{1}{RT^2} \left(\frac{\partial T}{\partial x_j}\right)_P \qquad (35)$$

or in the form used herein

$$x_j \left(\frac{\partial \ln \gamma_j}{\partial x_j}\right)_P + x_k \left(\frac{\partial \ln \gamma_k}{\partial x_j}\right)_P = - \Delta H_M^1 \frac{1}{RT^2} \left(\frac{\partial T}{\partial x_j}\right)_P \qquad (36)$$

where ΔH_M^1 is the integral heat of mixing at the bubble point. Substitution of this relationship for the bracketed terms in Equation (33) yields

$$RT_1^2 \left(\frac{\partial x_j}{\partial T}\right)_{P_{1-2}} \left[x_j \left(\frac{\partial \ln \gamma_j}{\partial x_j}\right)_{P_{1-2}} + x_k \left(\frac{\partial \ln \gamma_k}{\partial x_j}\right)_{P_{1-2}}\right]$$

$$= RT_1^2 \left(\frac{\partial x_j}{\partial T}\right)_{P_{1-2}} \left[- \Delta H_M^1 \frac{1}{RT_1^2} \left(\frac{\partial T}{\partial x_j}\right)_{P_{1-2}}\right] = - \Delta H_M^1 \qquad (37)$$

Thus, Equation (34) might be written

$$\lambda_P = z_j L_{j,T_1} + z_k L_{k,T_1} + (z_j \overline{C}^{O}_{P,j} + z_k \overline{C}^{O}_{P,k})(T_2 - T_1) - \Delta\underline{H}^{1}_{M} . \quad (38)$$

Whereas the addition of this new term enhances the knowledge about the original assumption of zero for the expression involving the Duhem equation, it does not greatly enhance the ability to predict integral isobaric heats of vaporization, because integral heat of mixing data at temperatures near the bubble point of the mixture are practically nonexistent. It would be unrealistic to assume that heat of mixing data taken at temperatures well below the bubble points would be applicable at the bubble point. If, however, sufficient specific heat data for the liquid mixture as a function of temperature up to the bubble point are available, the integral heat of mixing data might be adjusted to the bubble point temperature. It should be added, however, that such specific heat information for mixtures is not readily available in the literature.

The definition of the integral heat of mixing at temperature T is

$$\Delta\underline{H}_{M,T} = \underline{H}_{m,T} - x_j \underline{H}_{j,T} - x_k \underline{H}_{k,T} \quad (39)$$

Differentiation of Equation (39) with respect to temperature at constant pressure and composition and observation of the definition of specific heat yields the variation of the integral heat of mixing with temperature.

$$\left[\frac{\partial \Delta\underline{H}_{M,T}}{\partial T}\right]_{P,x_j} = \left(\frac{\partial \underline{H}_m}{\partial T}\right)_{P,x_j} - x_j\left(\frac{\partial \underline{H}_j}{\partial T}\right)_{P,x_j} - x_k\left(\frac{\partial \underline{H}_k}{\partial T}\right)_{P,x_j}$$

$$= C_{P,m} - x_j C_{P,j} - x_k C_{P,k} \quad (40)$$

The integral heat of mixing in, say, the liquid phase at any temperature in relation to the integral heat of mixing at some base temperature, say 25°C, is obtained by integrating Equation (40).

$$\underline{\Delta H}^{l}_{M,T} = \underline{\Delta H}^{l}_{M,25} + \int_{25}^{T} (C^{l}_{P,m} - x_j C^{l}_{P,j} - x_k C^{l}_{P,k})\, dT \qquad (41)$$

Data on the specific heat of the mixture are necessary because, as can be seen in Equation (41), an assumption that a molal average of the specific heats of the pure components can be used for the specific heat of the mixture is equivalent to assuming that the integral heat of mixing is the same at all temperatures.

Figure 3 on page 27 shows the comparison of the integral heat of mixing of the acetone-water binary at the bubble-point temperatures and at the constant temperature of 25°C. The 25°C data are those of Kister and Waldman.[36] Specific-heat data for the mixtures[36] and both pure components[33,46,64] were used in Equation (41) in conjunction with bubble-point data[49] for the computation of the integral heats of mixing at the bubble-point temperatures. It can easily be seen on the figure that it is unrealistic to assume a constant integral heat of mixing for this system. The heats of mixing, without regard to sign, are on the whole much smaller at the elevated temperatures and can be safely neglected in the prediction of integral isobaric heats of vaporization from Equation (38).

Application of Equilibrium-K Values

Edmister[16] derived an equation for the calculation of integral isobaric heat of vaporization by reasoning from an enthalpy-temperature

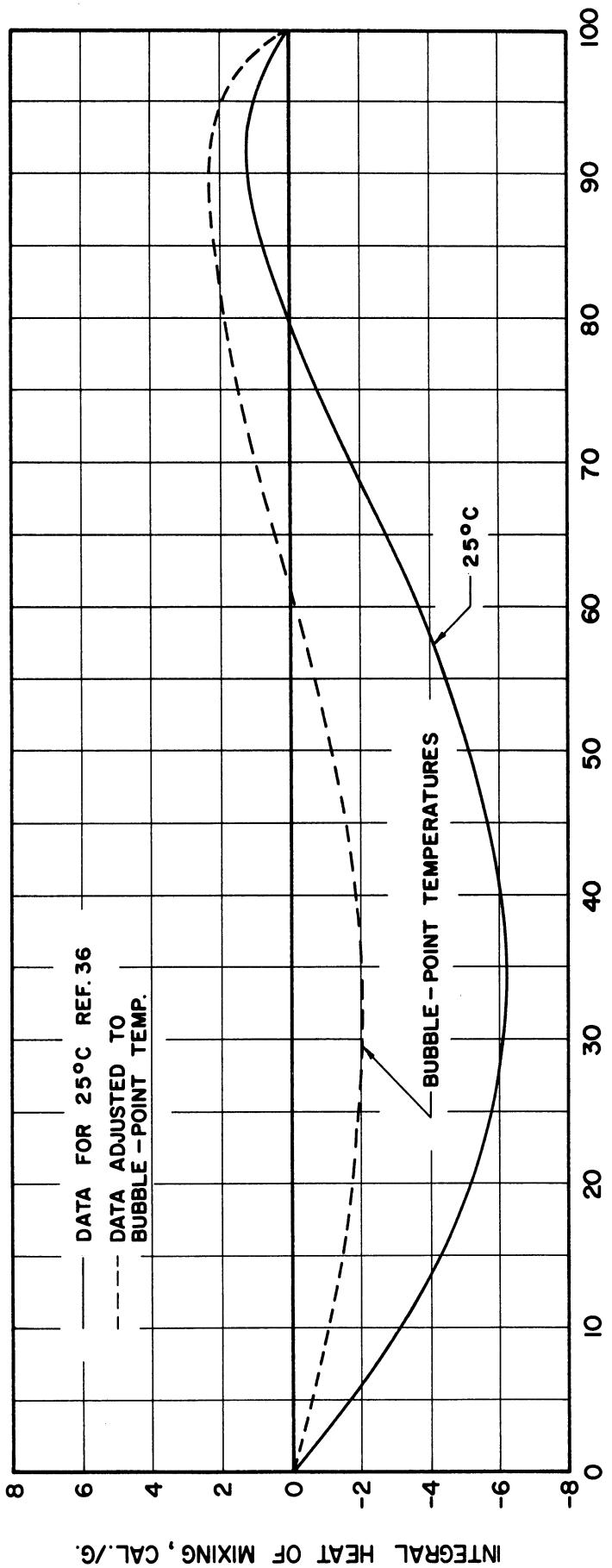

Figure 3. Integral Heat of Mixing for Acetone-Water.

diagram similar to the one shown in Figure 2 on page 16 of the previous section. His final equation requires knowledge of equilibrium-ratio-K values and the ideal-gas specific heats of the pure components. The equation is

$$\lambda_P = \frac{RT_1T_2}{T_2-T_1} \sum_i z_i \ln \frac{K_{i,2}}{K_{i,1}} + \sum_i z_i \Delta\bar{H}_i^0 \qquad (42)$$

where R is the gas constant; T_1 and T_2 are the bubble-point and dew-point temperatures, respectively; z_i is the mole fraction of component i in the mixture of interest; $K_{i,2}$ is to be evaluated at T_2 and is defined as $y_{i,2}/x^*_{i,2}$, where $y_{i,2}$ is the concentration of i in the mixture of interest in the vapor phase (numerically equal to z_i) and $x^*_{i,2}$ is the concentration of i in the liquid mixture which would be in equilibrium with a vapor of composition y_i at temperature T_2; $K_{i,1}$ is to be evaluated at T_1 and is defined as $y^*_{i,1}/x_{i,1}$, where $x_{i,1}$ is the concentration of i in the mixture of interest in the liquid phase (numerically equal to z_i) and $y^*_{i,1}$ is the concentration of i in the vapor mixture which would be in equilibrium with a liquid of composition $x_{i,1}$ at temperature T_1; $\Delta\bar{H}_i^0$ is the difference in the ideal-gas enthalpies between T_1 and T_2. The derivation embodies the assumption of the applicability of the Duhem equation to the mixture of interest, and the assumption that the terms $\sum_i y_i \Delta\bar{H}^V_{i,T}$ and $\sum_i x_i \Delta\bar{H}^l_{i,T}$ shown in Figure 2 on page 16 are constant over the range T_1 to T_2 and equal to $\sum_i y_i \Delta\bar{H}^V_{i,2}$ and $\sum_i x_i \Delta\bar{H}^l_{i,1}$, respectively, over that temperature range.

A modified version of Edmister's equation is developed in the subsequent paragraphs. The view point taken and the method of approach

are similar to those of Edmister; however, additional terms are included to more adequately define the variation of $\sum_i x_i \, \Delta\bar{H}^l_{i,T}$ over the temperature interval between T_1 and T_2. The final result is an equation which contains the two terms already present in Edmister's equation plus one additional term.

Equations (20) and (23) have been given previously on pages 18 and 19 where the salient features of each have been discussed.

$$\lambda_P = \sum_i x_i (\Delta\bar{H}^l_{i,1}) + \sum_i z_i (\Delta H^0_i) - \sum_i y_i (\Delta\bar{H}^v_{i,2}) \qquad (20)$$

$$\Delta\bar{H}_{i,T} = H^0_{i,T} - \bar{H}_{i,T} = RT^2 \left(\frac{\partial \ln \bar{f}_i}{\partial T}\right)_P \qquad (23)$$

In order to substitute a difference form of Equation (23), instead of its present differential form, into Equation (20) for the quantities $\Delta\bar{H}^v_{i,2}$ and $\Delta\bar{H}^l_{i,1}$, Edmister integrated Equation (23) over the range from T_1 to T_2 under the assumption that $\Delta\bar{H}^v_{i,T}$ and $\Delta\bar{H}^l_{i,T}$ were constant and equal to $\Delta\bar{H}^v_{i,2}$ and $\Delta\bar{H}^v_{i,1}$, respectively, for any point between T_1 and T_2.

This assumption is followed here, exactly, for the integration involving the vapor phase. The immediate result is

$$\Delta\bar{H}^v_{i,2} = -\frac{RT_1T_2}{T_2-T_1} \ln \frac{\bar{f}^v_{i,1}}{\bar{f}^v_{i,2}} \qquad (43)$$

For the integration involving the liquid phase a deviation from the course taken by Edmister is made. The term $\Delta\bar{H}^l_{i,T}$ for any point between T_1 and T_2 can be expressed by

$$\Delta\bar{H}^l_{i,T} = H^0_{i,T} - \bar{H}^l_{i,1} - \Delta\bar{H}^l_{Com,i,1}(P) - \int_{T_1}^{T} \bar{C}^l_{P,i} \, dT \qquad (44)$$

where $\bar{H}^{l}_{i,1}$ is the partial molal enthalpy of i in the liquid mixture at the bubble point; $\Delta\bar{H}^{l}_{Com,(P)_{i,1}}$ is the partial molal enthalpy difference involved in the isothermal compression at T_1 of the liquid from P_{1-2} to P (here (P) serves as a reminder that this expression is a function of the terminal pressure, P, which in turn is a function of the terminal temperature, T); the term containing the integral sign is the partial molal enthalpy change involved in the isobaric heating of the liquid from T_1 to T at a pressure of P. $\underline{H}^{0}_{i,T}$ in Equation (44) is the ideal-gas enthalpy at temperature T and is given by

$$\underline{H}^{0}_{i,T} = \underline{H}^{0}_{i,1} + \left(\frac{T - T_1}{T_2 - T_1}\right) \Delta\underline{H}^{0}_{i} \tag{45}$$

if the ideal-gas heat capacity is assumed to be independent of temperature for the T_1-to-T_2 temperature range. Substituting $\underline{H}^{0}_{i,T}$ from Equation (45) into Equation (44) yields

$$\Delta\bar{H}^{l}_{i,T} = \underline{H}^{0}_{i,1} + \left(\frac{T - T_1}{T_2 - T_1}\right) \Delta\underline{H}^{0}_{i} - \bar{H}^{l}_{i,1} - \Delta\bar{H}^{l}_{Com,(P)_{i,1}} - \int_{T_1}^{T} \bar{C}^{l}_{P,i}\, dT \tag{46}$$

Neglecting the effect of pressure on the enthalpy of the liquid phase and assuming that $\bar{C}^{l}_{P,i}$, the partial molal specific heat of i in the liquid phase, is independent of temperature between T_1 and T_2, Equation (46) becomes

$$\Delta\bar{H}^{l}_{i,T} = \underline{H}^{0}_{i,1} + C^{0}_{P,i}(T - T_1) - \bar{H}^{l}_{i,1} - \bar{C}^{l}_{P,i}(T - T_1) \tag{47}$$

since $\Delta\underline{H}^{0}_{i}/(T_2 - T_1)$ is equal to $C^{0}_{P,i}$ according to the assumption given following Equation (45). Collecting terms yields

$$\Delta\bar{H}^{l}_{i,T} = \Delta\bar{H}^{l}_{i,1} - (T - T_1)(\bar{C}^{l}_{P,i} - C^{0}_{P,i}) \tag{48}$$

Substituting $\Delta\bar{H}^{l}_{i,T}$ from Equation (48) into Equation (23) and integrating between T_1 and T_2 yields

$$\Delta\bar{H}^{l}_{i,1}\int_{T_1}^{T_2}\frac{dT}{T^2} - (\bar{C}^{l}_{P,i} - C^{0}_{P,i})\int_{T_1}^{T_2}\frac{(T-T_1)}{T^2}\,dT = R\int_{\bar{f}^{l}_{i,1}}^{\bar{f}^{l}_{i,2}} d\ln \bar{f}^{l}_{i} \qquad (49)$$

$$\Delta\bar{H}^{l}_{i,1}\left(\frac{T_2 - T_1}{T_1T_2}\right) - (\bar{C}^{l}_{P,i} - C^{0}_{P,i})\left[\ln\frac{T_2}{T_1} + \frac{T_1 - T_2}{T_2}\right] = -R\ln\frac{\bar{f}^{l}_{i,1}}{\bar{f}^{l}_{i,2}} \qquad (50)$$

$$\Delta\bar{H}^{l}_{i,1} = -\frac{RT_1T_2}{T_2-T_1}\ln\frac{\bar{f}^{l}_{i,1}}{\bar{f}^{l}_{i,2}} + (\bar{C}^{l}_{P,i} - C^{0}_{P,i})\left(\frac{T_1\,T_2}{T_2-T_1}\ln\frac{T_2}{T_1} - T_1\right) \qquad (51)$$

From this point the development is the same as that used by Edmister. Substituting Equations (43) and (51) into Equation (20) and recalling that for the constant-composition system $x_i = y_i = z_i$ yields

$$\lambda_P = \frac{RT_1T_2}{T_2-T_1}\sum_i z_i\left[\ln\frac{\bar{f}^{v}_{i,1}/y_{i,1}}{\bar{f}^{v}_{i,2}/y_{i,2}} - \ln\frac{\bar{f}^{l}_{i,1}/x_{i,1}}{\bar{f}^{l}_{i,2}/x_{i,2}}\right]$$

$$+ \left(\frac{T_1\,T_2}{T_2-T_1}\ln\frac{T_2}{T_1} - T_1\right)\sum_i z_i\,(\bar{C}^{l}_{P,i} - C^{0}_{P,i}) + \sum_i z_i\,\Delta\bar{H}^{0}_{i} \qquad (52)$$

The definitions for $K_{i,2}$ and $K_{i,1}$ are given on page 28 following Equation (42). These definitions in conjuction with the fact that at equilibrium, $\bar{f}^{l}_{i,T} = \bar{f}^{v}_{i,T}$, yield the following expression for the equilibrium-ratio K's.

$$K_{i,2} = \frac{\bar{f}^{l}_{i,2}/x^{*}_{i,2}}{\bar{f}^{v}_{i,2}/y_{i,2}} \qquad (53)$$

$$K_{i,1} = \frac{\bar{f}^{l}_{i,1}/x_{i,1}}{\bar{f}^{v}_{i,1}/y^{*}_{i,1}} \qquad (54)$$

Substituting these K's into the first term on the right-hand side of Equation (52) yields

$$\frac{RT_1T_2}{T_2-T_1}\sum_i z_i\left[\ln\frac{K_{i,2}\,\bar{f}^{v}_{i,1}/y_{i,1}}{\bar{f}^{l}_{i,2}/x^{*}_{i,2}}-\ln\frac{K_{i,1}\,\bar{f}^{v}_{i,1}/y^{*}_{i,1}}{\bar{f}^{l}_{i,2}/x_{i,2}}\right] \tag{55}$$

Collecting terms and rearranging yields

$$\frac{RT_1T_2}{T_2-T_1}\sum_i z_i\left[\ln\frac{K_{i,2}}{K_{i,1}}+\ln\frac{\bar{f}^{v}_{i,1}/y_{i,1}}{\bar{f}^{v}_{i,1}/y^{*}_{i,1}}+\ln\frac{\bar{f}^{l}_{i,2}/x_{i,2}}{\bar{f}^{l}_{i,2}/x^{*}_{i,2}}\right] \tag{56}$$

The latter two terms inside the brackets of Statement (56) can be eliminated by application of the Duhem equation; one form of which is

$$\sum_i z_i\, d\ln\bar{f}_i = 0 \tag{57}$$

Observing that $\sum z_i = 1$ and writing the Duhem relationship in difference form rather than in differential form yields

$$\sum_i z_i\,\Delta\ln(\bar{f}_i/z_i) = 0 \tag{58}$$

The term $\Delta\ln(\bar{f}_i/z_i)$ can be expressed as

$$\Delta\ln(\bar{f}_i/z_i) = \ln(\bar{f}_i/z_i)' - \ln(\bar{f}_i/z_i)'' = \ln\frac{(\bar{f}_i/z_i)'}{(\bar{f}_i/z_i)''} \tag{59}$$

where the prime and double prime indicate two different compositions for the same phase, temperature, and pressure. This equation is applicable to either the vapor or liquid phase. Thus, substituting Equation (59) into Equation (58) yields

$$\sum_i z_i\ln\frac{(\bar{f}_i/z_i)'}{(\bar{f}_i/z_i)''} = 0 \tag{60}$$

Application of Equation (60) to the latter two terms inside the brackets of Statement (56) eliminates them. Under these restrictions Equation (52) becomes

$$\lambda_P = \frac{RT_1T_2}{T_2-T_1} \sum_i z_i \ln \frac{K_{i,2}}{K_{i,1}} + \sum_i z_i \Delta\underline{H}_i^0$$

$$+ \left(\frac{T_1T_2}{T_2 - T_1} \ln \frac{T_2}{T_1} - T_1\right) \sum_i z_i \left(\overline{C}_{P,i}^{1} - C_{P,i}^{0}\right) \qquad (61)$$

This equation differs from that given by Edmister, Equation (42), only by the inclusion of the last term.

The Enthalpy-Concentration-Diagram Approach

Figure 4 on page 34 is an enthalpy-concentration diagram for a hypothetical binary mixture. The conditions on the $\underline{H}$-x plane are constant pressure and varying temperature. The integral isobaric heat of vaporization for any composition is the vertical distance between the saturated-liquid line and the saturated-vapor line at that composition. The saturated-vapor and saturated-liquid lines, as shown in the figure, are in general not straight. The frequently used McCabe-Thiele type of distillation calculation, for example see Brown,[3] embodies the assumption of constant molal heat of vaporization; that is, it is assumed that on a molal basis the heat of vaporization of both pure components and the integral isobaric heat of vaporization of all mixtures thereof are equal. The McCabe-Thiele assumption is tantamount to the assumption that on the enthalpy-concentration diagram the saturated-liquid and saturated-vapor lines are not only straight, but also parallel. If these lines are assumed to be straight, but not parallel, then the integral isobaric heat of vaporization of any mixture of the pure components

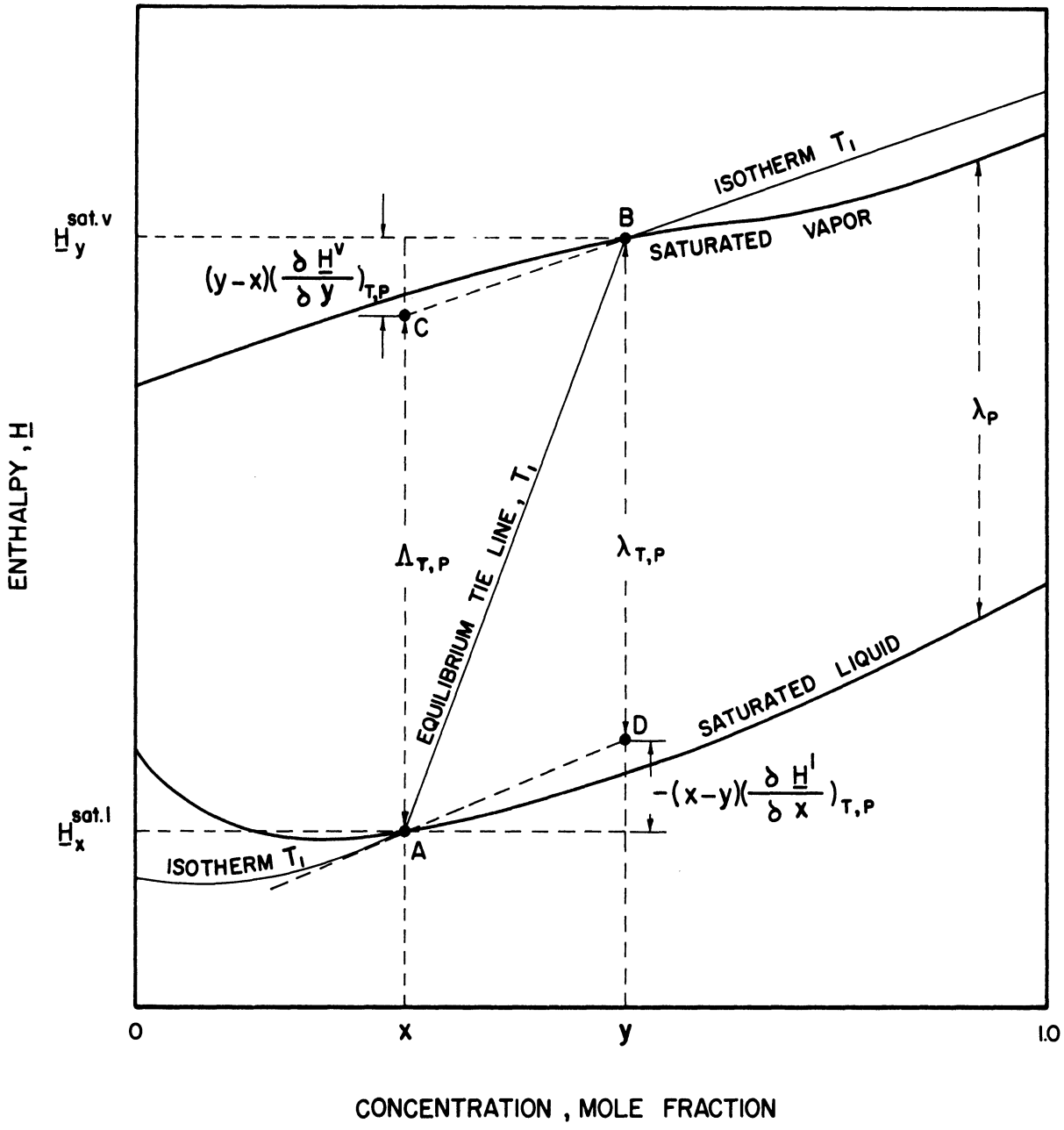

Figure 4. Enthalpy-Concentration Diagram for a Hypothetical Mixture. (Constant Pressure)

is given by a molal average of the heats of vaporization of the pure components, each taken at the pressure of interest.

The method of construction of an enthalpy-concentration diagram when the integral isobaric heat of vaporization data are not available has been given by several authors, for example Dodge.[12] It is reviewed here quite briefly. A datum level for the enthalpies, usually the pure materials in their normal state at 0°C and the pressure of interest, is chosen first. The end points of the saturated-vapor line are fixed by marking on the ordinate of each pure component its saturated-vapor enthalpy. The remainder of the saturated-vapor line is then established as follows: (1) on both pure-component ordinates the vapor enthalpies are marked for various temperatures above the saturation temperature - and in the case of the less volatile component are also marked at temperatures below saturation, neglecting pressure effects on the enthalpy, (2) straight isotherms are then drawn connecting the pure-component ordinates, (3) the dew-point temperatures for a number of mixtures are determined from vapor-liquid equilibrium data and are located on the H-x plane by interpolation between the isotherms, (4) these saturated-vapor values and the previously determined end points are joined by a smooth curve, which is the saturated-vapor line. The use of straight isotherms in the vapor region assumes zero heat of mixing in that phase, which is a reasonable assumption.

It is not likely that the isotherms in the liquid region will be straight. The temperature at which the integral heat of mixing data in the liquid phase are available serves as the starting point for the constructions. The enthalpies of both pure liquids at this temperature

are marked off on the respective ordinates to fix the end points of the isotherm. The end points are joined temporarily by a straight line. The integral heats of mixing for a number of compositions are then represented by their proper distances above or below the temporary line, according to sign. These points are joined by a smooth curve, which is the base isotherm. Other isotherms are established at higher temperatures by determining the enthalpy change accompanying an isobaric heating of the liquid mixture. The bubble-point temperatures for a number of mixtures are determined from vapor-liquid equilibrium data; the sensible-heat terms are then calculated up to these temperatures and marked on the $\underline{H}$-x plane. A smooth curve through these points establishes the saturated-liquid line.

The foregoing graphical construction yields the entire enthalpy-concentration diagram. However, if only a few integral isobaric heats of vaporization are needed, it would be convenient to have the construction features described in equations. These equations are

$$\underline{H}^{\text{sat.v.}} = \sum_i z_i \left[\int_0^{t_{bp,i}} C^l_{P,i}\, dt + L_{i,P} + \int_{t_{bp,i}}^{t_{DP,m}} C^v_{P,i}\, dt \right] + \Delta\underline{H}^v_M \qquad (62)$$

$$\underline{H}^{\text{sat.l.}} = \sum_i z_i \left[\int_0^{25} C^l_{P,i}\, dt \right] + \Delta\underline{H}^l_{M,25} + \int_{25}^{t_{BP,m}} C^l_{P,m}\, dt \qquad (63)$$

The integral isobaric heat of vaporization is the difference between Equations (62) and (63).

$$\lambda_P = \underline{H}^{\text{sat.v.}} - \underline{H}^{\text{sat.l.}} \qquad (64)$$

The assumptions involved in writing Equations (62) and (63), none of which affect the rigor of the equations but which do involve the number of terms

used and some of the limits on the integrals, are as follows: (1) both pure components are liquids at the reference temperature (0°C), (2) the integral heat of mixing data are available at only one temperature, that being 25°C.

If the heat of mixing in the vapor phase is neglected, the following data are required for the calculation of the integral isobaric heat of vaporization by using the enthalpy-concentration-diagram approach: (1) isobaric vapor-liquid equilibria, (2) specific heat of the pure components in the liquid phase as a function of temperature from 0°C to the boiling point, (3) the heat of vaporization of the pure components at the pressure of interest, (4) the specific heat of the pure components in the vapor phase as a function of temperature in the vicinity of the boiling point, (5) the integral heat of mixing in the liquid phase, (6) the specific heat of the mixture in the liquid phase as a function of temperature up to the bubble point. The calculations involved are simple, but tedious.

The relationships between the saturated-liquid and saturated-vapor enthalpies and both the differential heat of vaporization and the differential heat of condensation, which were described with equations in the chapter entitled "Theoretical Background", can be illustrated graphically on Figure 4 on page 34 with the aid of an equilibrium tie line and the isotherms. The tie line joins a saturated liquid of composition x with a saturated vapor of composition y. Isotherms in both the liquid and vapor regions terminate at these saturation points. Equation (9) from the previous chapter gives the differential heat of

condensation as

$$\Lambda_{T,P} = \underline{\underline{H}}_x^{\text{sat.l.}} - \underline{\underline{H}}_y^{\text{sat.v.}} + (y - x) \left(\frac{\partial \underline{\underline{H}}^V}{\partial y}\right)_{T,P} \qquad (9)$$

The distance $-(\underline{\underline{H}}_y^{\text{sat.v.}} - \underline{\underline{H}}_x^{\text{sat.l.}})$ is easily located on the figure. The derivative is given by the slope of the vapor-phase isotherm at point B; however, since these isotherms are straight, simply an extension of the T_1 isotherm beyond the saturation point for a horizontal distance of $(y - x)$ yields a vertical rise of $(y - x) \left(\frac{\partial \underline{\underline{H}}^V}{\partial y}\right)_{T,P}$. Thus, the differential heat of condensation from a vapor of composition y is represented by the distance A - C. A similar procedure applies for the differential heat of vaporization, which as given by Equation (8) in the previous chapter is

$$\lambda_{T,P} = \underline{\underline{H}}_y^{\text{sat.v.}} - \underline{\underline{H}}_x^{\text{sat.l.}} + (x - y) \left(\frac{\partial \underline{\underline{H}}^l}{\partial x}\right)_{T,P} \qquad (8)$$

The difference between the saturated enthalpies is the same; however, the liquid-phase isotherm is not straight so, consequently, a tangent must be drawn to it at point A. If the tangent is extended beyond the saturation point for a horizontal distance of $-(x - y)$ the resultant vertical rise of $-(x - y) \left(\frac{\partial \underline{\underline{H}}^l}{\partial x}\right)_{T,P}$ shows that the distance B - D represents the differential heat of vaporization. It can be seen from these illustrations that the essential data for making enthalpy balances for distillation calculations are not differential heats of vaporization or condensation, as suggested occasionally in the literature, but are saturated-liquid and saturated-vapor enthalpies, which are most readily obtained from integral-isobaric-heat-of-vaporization data.

Approximately 17 enthalpy-concentration diagrams have been published in the literature for various liquid-vapor systems. Most are on large enough graphs to be useful or are supported by tabular values. A literature survey by Lemlich et al.[39] lists references to the original diagrams.

Rigorous Application of Two-Phase, P-V-T-x Data

The integral isothermal heat of vaporization can be computed from a rigorous application of the two-phase, P-V-T-x data for a mixture. A combination of the first and second laws of thermodynamics in conjunction with the definition of enthalpy produces the general expression

$$d\underline{H} = Td\underline{S} + \underline{V}dP \tag{65}$$

At constant temperature the entropy term, $d\underline{S}$, can be expressed in terms of pressure, volume, and temperature by use of the Maxwell relationship

$$\left(\frac{\partial \underline{S}}{\partial \underline{V}}\right)_T = \left(\frac{\partial P}{\partial T}\right)_{\underline{V}} \tag{66}$$

Substitution of this expression into Equation (65) for $d\underline{S}$ yields

$$d\underline{H}_T = T\left(\frac{\partial P}{\partial T}\right)_{\underline{V}} d\underline{V} + \underline{V}dP \tag{67}$$

Equation (67) can be integrated from the bubble point to the dew point along a reversible isothermal path.

$$\lambda_T = \int_{B.P.}^{D.P.} d\underline{H}_T = T \int_{\underline{V}_{BP}}^{\underline{V}_{DP}} \left(\frac{\partial P}{\partial T}\right)_{\underline{V}} d\underline{V} + \int_{P_{BP}}^{P_{DP}} \underline{V}\, dP \tag{68}$$

In order to carry out the indicated integrations a large amount of precise P-V-T-x data for the two-phase region are required. The computations

are tedious, and precision is required because the data must first be differentiated, then cross plotted, and finally integrated. Although this method is outlined several places in the literature, for example Hobson and Weber,[29] it has rarely been carried out because of the scarcity of the data required and the computational difficulties involved.

Bahlke and Kay[2] performed this type of calculation for a commercial gasoline and a narrow-boiling-range naphtha. They began the computation by plotting the pressure-volume isotherms for the two phase region. The volumes involved are, of course, the combined volumes of the equilibrium vapor-liquid mixtures which would be present during a reversible, isothermal vaporization. From these pressure-volume isotherms a number of the corresponding pressures and temperatures were read off for a series of different volumes. The pressures and temperatures so obtained were plotted as log pressure versus reciprocal temperature with the different volumes as parameters. The slopes, $(\frac{d \log P}{d\, 1/T})_{\underline{V}}$, were taken at the temperature of the vaporization from each of the constant-volume curves in the series. The slopes in this form - $(\frac{d \log P}{d\, 1/T})_{\underline{V}}$ - could then be easily transformed to $(\frac{\partial P}{\partial T})_{\underline{V}}$ and plotted against the corresponding volumes. The area under the resulting $(\frac{\partial P}{\partial T})_{\underline{V}}$-$\underline{V}$ curve between the saturated-liquid volume and the saturated-vapor volume is the value of the first integral on the right-hand side of Equation (65). In comparison to the above computation the second integral on the right-hand side is simple to evaluate. Only the area under the pressure-volume curve, which was previously plotted, for the temperature of interest between the bubble-point pressure and the dew-point pressure need be determined.

Strickland-Constable[66] has carried out the evaluation of two-phase, P-V-T-x data for the prediction of the heat of vaporization of an equimolecular mixture of propylene and carbon dioxide at 0°C.

Equation (65) is not adaptable to the prediction of the integral isobaric heat of vaporization because the restriction of constant pressure eliminates the second term on the right-hand side and reduces the equation to an identity.

Clapeyron Equation for Mixtures

The Clapeyron equation, which is often used to predict the latent heat of vaporization of pure materials, can be applied to mixtures to relate the differential heat of vaporization or condensation to the vapor pressure and specific volumes of the mixture. The differential processes occur both isothermally and isobaricly - conditions which are requisites for the applicability of the Clapeyron equation. This equation has been outlined in the literature, for example Hobson and Weber,[29] as a possible method of predicting heats of vaporization of mixtures, but in practice it is seldom used because of the scarcity of the required data on mixture behavior.

The Clapeyron equation for the differential heat of vaporization for the removal of a vapor of composition y from an infinite amount of liquid of composition x is given by

$$\lambda_{T,P} = T \Delta \underline{V} \left(\frac{\partial P}{\partial T}\right)_x \qquad (69)$$

The terms look identical to those appearing in the Clapeyron equation for a pure material; however, a closer examination in view of the actual

phase change being considered reveals that they are slightly more complicated. T is simply the absolute temperature of the differential vaporization. $\Delta \underline{V}$ is not the difference between the volume of the saturated vapor y and the volume of the saturated liquid x because the molecules constituting a mole of the vapor y did not occupy in the liquid phase the same volume as was occupied by a mole of the liquid x. The exact expression for the volume difference can be derived in a manner analogous to that used on pages 7 through 9, Equations (1) through (8), to derive the relationship for the enthalpies involved in the differential heat of vaporization. If one merely uses the appropriate volume terms in place of the enthalpies in that development, the equation for the volume difference is obtained. Thus, for a binary

$$\Delta \underline{V} = \underline{V}_y^{\text{sat.v.}} - \underline{V}_x^{\text{sat.l.}} + (x - y) \left(\frac{\partial V^l}{\partial x}\right)_{T,P} \tag{70}$$

The last term, $\left(\frac{\partial P}{\partial T}\right)_x$, in the Clapeyron equation is the slope of the pressure-temperature curve for the bubble points of a mixture of composition x taken at the temperature, T, of the vaporization.

The analogous equation for the differential heat of condensation for the removal of a liquid of composition x from an infinite amount of vapor of composition y is given by

$$\Lambda_{T,P} = T \Delta \underline{V} \left(\frac{\partial P}{\partial T}\right)_y \tag{71}$$

where T is the absolute temperature; $\left(\frac{\partial P}{\partial T}\right)_y$ is the slope of the pressure-temperature curve for the dew points of a mixture of composition y taken at T; and $\Delta \underline{V}$ is given by

$$\Delta \underline{V} = \underline{V}_x^{\text{sat.l.}} - \underline{V}_y^{\text{sat.v.}} + (y - x) \left(\frac{\partial V^v}{\partial y}\right)_{T,P} \tag{72}$$

Stiehl et al.,[65] Hobson and Weber,[28] and Weber,[75] used Equations (71) and (72) to calculate the differential heat of condensation of a number of hydrocarbon binaries at pressures ranging from 100 to 600 psia. They used precise dew-point-pressure-temperature, volumetric, and equilibrium data in conjunction with an equation of state for the vapor-phase mixtures to make the calculations. The derivative in Equation (72) was determined from a graph of $\underline{V}^V$ versus y at constant pressure. The $\underline{V}^V$ - y isotherms for the superheated-vapor region on this graph were determined from an equation of state for mixtures, and the saturated-vapor envelope was established with the aid of vapor-liquid equilibrium data. From the $\underline{V}^V$ - y graph the slope of the isotherm taken at the saturation point for the temperature of interest furnished the $(\frac{\partial \underline{V}^V}{\partial y})_{T,P}$ term. Experimental data and a graphical differentiation of the dew-point - pressure-temperature data yielded the other information required by Equations (71) and (72).

The usual assumptions can be made to reduce the Clapeyron equation to the simpler Clausius-Clapeyron equation. That is, if one assumes that only the volume of the vapor in Equations (70) and (72) is significant and that, furthermore, the vapor volume can be expressed with sufficient accuracy by the ideal-gas law, then the equation for the differential heat of vaporization becomes

$$\lambda_{T,P} = RT^2 \left(\frac{\partial \ln P}{\partial T}\right)_x \qquad (73)$$

A similar equation applies to the differential heat of condensation. The evaluation of Equation (73) requires only the pressure-temperature relationship for the bubble points of the mixture. Equation (73) also

presents a simple relationship whereby vapor pressures of mixtures could be computed, if differential heat of vaporization data were available over a wide range of conditions. The latter, however, are not prevelant enough to make the technique of much practical value.

Simpler Approximations

A number of simple approximations, which are relatively easy to apply, have been used to estimate heats of vaporization for mixtures. Most methods have been directed toward the estimation of the integral isobaric heat of vaporization, because it is this quantity which is most often required in design calculations. Hydrocarbon mixtures have received the bulk of the attention of those attempting to establish rapid approximate techniques.

The most common approximation is the use of a mass average or a molal average of the pure-component latent heats taken at the pressure of interest. Another common approximation is based on the fact that on a molal basis the latent heats of a number of pure materials are roughly equal. On this premise it has been customary to assume constant molal heat of vaporization for many types of mixtures. That is, an arithmetic average of the pure-component latent heats is assumed to be a satisfactory representation of the heat of vaporization for all mixtures thereof.

Hougen and Watson[31] have published a chart for the heat of vaporization of hydrocarbons and petroleum fractions which uses the molal-average boiling point in degrees Fahrenheit and the molecular weight or the A.P.I. gravity as correlating variables. The chart gives the heat of vaporization at atmospheric pressure in Btu's per pound.

Hydrocarbon mixtures sometimes have been characterized as being equivalent to a hypothetical pure component for which the heat of vaporization can be established. Edmister[17] refined this technique somewhat for the integral isothermal heat of vaporization. He proposed that the calculation be made in two parts. The heat of vaporization of the equivalent pure component at atmospheric pressure is first estimated from Meissner's generalized chart[42] using the pseudo-critical concept to determine the reduced properties. A pressure correction calculated for isothermal conditions is then added to the hypothetical pure-component latent heat to determine the integral isothermal heat of vaporization for the mixture.

EXPERIENCE OF PREVIOUS EXPERIMENTERS

Earliest Investigations

The first attempts to measure latent heats of vaporization of mixtures were reported in the early nineteen hundreds.[20,59] These early investigations were concerned with the vaporization of liquid air. The investigators failed to recognize that the heat of vaporization of a mixture is not a unique phenomenon. However, Shearer[59] noted, "There seemed to be a distinct increase in the heat of vaporization as the liquid boiled away." At the time these experiments were conducted, the heat of vaporization of one of the pure components, oxygen, had not been determined. These first investigations suffered from three important deficiencies. Firstly, the experiments were not disciplined by a guiding definition of the heat of vaporization which was to be measured. Secondly, the experiments suffered inherently from attempts to use the same calorimetric equipment which was then used for latent heat measurements on pure materials. Thirdly, the heat leaks were large.

In the early 1910's Tyrer[70,71,72] and Fletcher and Tyrer[22] published heat of vaporization data for several mixtures. The integral isothermal heat of vaporization was adequately defined (Tyrer called it vaporization at constant composition.), and Fletcher and Tyrer[22] designed an experiment to measure the defined quantity. Attempts were made to develop a formula relating the so-called "vaporization at constant composition" to a so-called "vaporization at constant pressure," an ill-defined term somewhat like the differential heat of vaporization. The calorimetric equipment and procedures employed by these investigators

did not lend themselves to highly accurate measurements; consequently their data are not sufficiently reliable for present use.

Recent Investigations

In 1925 Dana[8] published an excellent paper on the heat of vaporization of liquid nitrogen-oxygen mixtures. In this work Dana measured the integral isobaric heat of vaporization. Large steps were taken toward the correction of the aforementioned deficiencies of the pioneering investigators. Adequate thermodynamic definitions of the latent heats of interest were used as a guide for designing calorimetric equipment suitable for the measurement of these quantities. Cognizance of the heat leaks to the low temperature system was taken, and efforts were made to reduce them. The basic features of Dana's flow calorimeter have been used in more recent calorimeters constructed by other investigators.

Recently, Tallmadge et al.[67,68] and Plewes et al.[52,53,54] used modified versions of Dana's calorimetric equipment for the measurement of the integral isobaric heat of vaporization of mixtures which have boiling points above room temperature. The systems studied by these investigators are listed in Table I.

Tallmadge et al.[67,68] gave considerable attention to heat leaks in their apparatus. Calibrated heaters external to the unsilvered, vacuum-jacketed calorimeter prevented conductive heat losses from the system. A temperature difference between the calorimeter and its immediate surroundings, the magnitude of which was governed essentially by the difference between the bubble point and the dew point of a given mixture,

was an inherent liability of their apparatus. Radiative heat losses from the calorimeter to the surroundings, resulting from this temperature difference, were estimated, and the necessary corrections were applied to the latent heats. In two of the systems studied[67] the maximum temperature difference probably did not exceed six centigrade degrees, thus rendering the corrective terms for the radiative heat losses rather small percentages of the latent heats. However, in the other system studied[68] the temperature difference between the calorimeter and its surroundings was probably as high as seventeen centigrade degrees. The high precision of their latent heat data attests to the accuracy with which they were able to estimate the radiative heat leak.

Plewes et al.[52,53,54] did not discuss the possibility of heat leaks in their apparatus. Their apparatus was similar to that of Tallmadge et al. in that a dew-point - bubble-point temperature difference between the calorimeter and the surroundings was an inherent feature. They had to deal with heat losses similar to those of Tallmadge et al., but probably to a somewhat lesser degree because the silvered, vacuum-jacketed calorimeter they used provided a smaller emissive coefficient for radiative heat transfer than that experienced by Tallmadge et al. in their unsilvered calorimeter. In their initial paper Plewes et al.[53] reported studies of systems which produced maximum temperature differences between the calorimeter and its immediate surroundings of about fifteen centigrade degrees. However, the important measurement of the amount of power delivered to the calorimeter was made with only moderate precision; consequently, the heat-leak effects were

probably masked by the uncertainties in the power measurements. In subsequent studies[52,54] their technique of power measurement attained a high precision. However, the systems studied never produced an inherent temperature difference between the calorimeter and its surroundings of greater than about three centigrade degrees. These small temperature differences would, of course, have produced only small heat leaks. The high precision of the latent heat data presented in their latter papers probably vindicates ignoring the heat leaks for those systems.

Stallaid and Amis[63] have published differential latent heat measurements for the system dioxane-water. As was mentioned in a previous section, the differential latent heat of vaporization is the most difficult to deal with experimentally. Wrewsky[82] measured the differential heat of vaporization of one sulfuric acid-water mixture.

Table I lists the systems studied and reported in the literature referred to hereinbefore.

TABLE I

MIXTURES FOR WHICH RELIABLE, EXPERIMENTALLY DETERMINED, LATENT-HEAT-OF-VAPORIZATION DATA ARE AVAILABLE

Mixture	Type of Data	Reference	Remarks
Water-Formic Acid	Int. Isobaric	(54)	760mm Hg
Water-Acetic Acid	Int. Isobaric	(52)	760mm Hg
Methanol-Benzene	Int. Isobaric	(68)	735mm Hg (avg.)
Acetone-Chloroform	Int. Isobaric	(67)	738mm Hg
Acetone-Benzene	Int. Isobaric	(67)	738mm Hg
Methanol-Water	Int. Isobaric	(53)	300 & 760mm Hg
Ethanol-Water	Int. Isobaric	(53)	300 & 760mm Hg
n-Propanol-Water	Int. Isobaric	(53)	300 & 760mm Hg
Water-Dioxane	Differential	(63)	760mm Hg
Sulfuric Acid-Water	Differential	(82)	Only one conc.
Nitrogen-Oxygen	Int. Isobaric	(8)	Avg. atm. press.

Other investigators have made enthalpy measurements on petroleum fractions and other mixtures.[19,35,41,43,76] In most of these investigations the emphasis was on measurements of moderate accuracy over wide ranges of temperature and pressure, including measurements in the superheated-vapor region and in the subcooled-liquid region, as well as in the two-phase region.

EXPERIMENTAL APPARATUS

Summary

A thermally insulated flow calorimeter which operated at a steady state was used for the precise measurement of the integral isobaric heat of vaporization. A continuous flow of the liquid mixture to the calorimeter was vaporized by the consumption of electrical energy in the heater. The vapor which escaped was condensed and collected for an accurately timed interval. The mass of vapor collected and the energy consumed by the heater during the timed interval were the principal measurements required for the determination of the latent heats.

The Flow System

A modified version of a flow system, which was used in cryogenic work by Dana and originally reported by him in the literature,[8] was constructed for this investigation. The apparatus was designed for operation at atmospheric pressure on mixtures with bubble points above ambient temperatures. Steady-state operation of the apparatus is considered first. A discussion of the approach to the steady-state condition is taken up in the latter part of this section.

Figure 5 on page 52 is a schematic diagram of the calorimetric apparatus, showing the items in the same relative positions as in the photograph, Figure 6 on page 53. Only the functions and purposes of the components are discussed herein. Details of the individual components are given in subsequent sections.

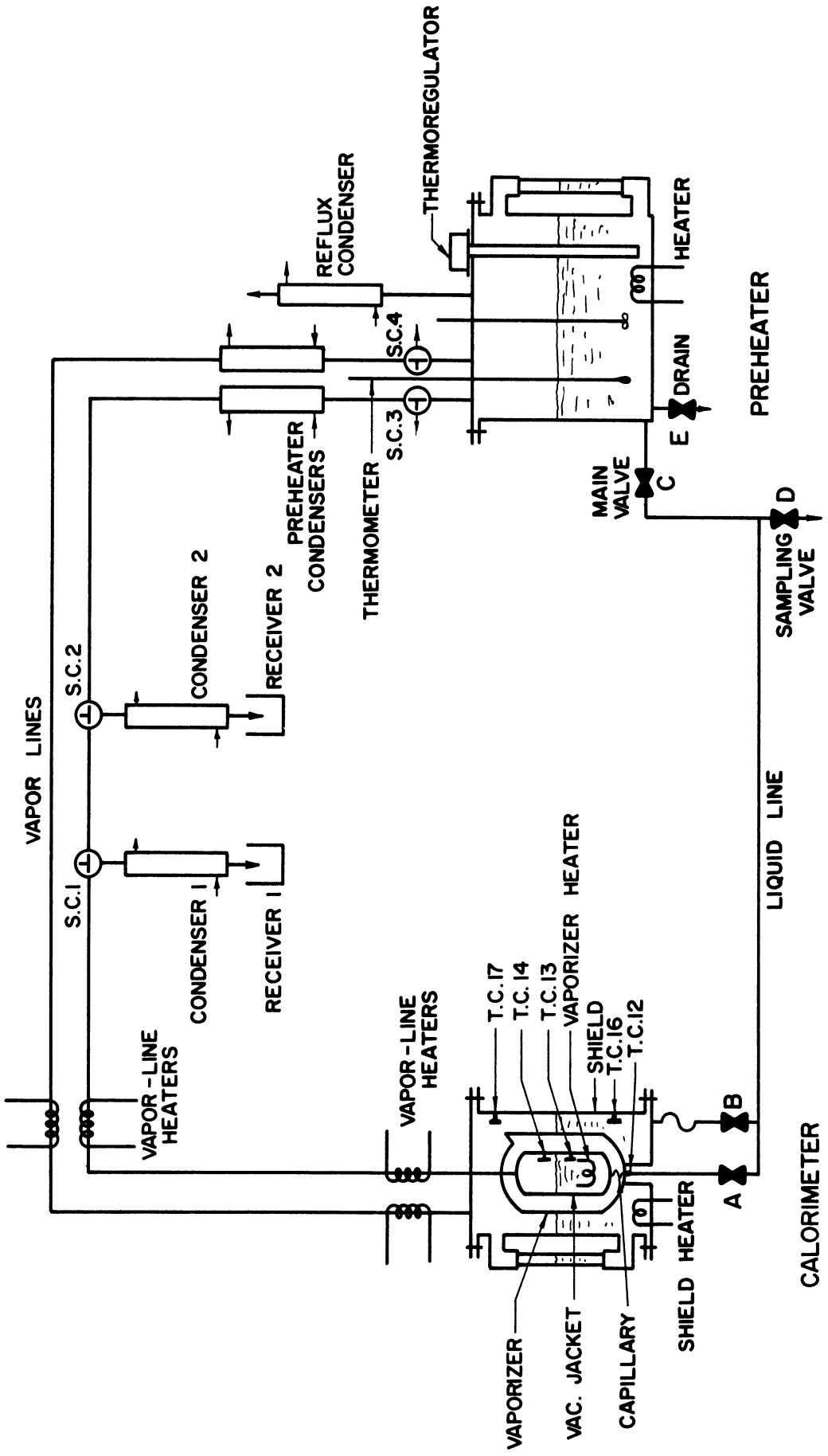

Figure 5. Schematic Diagram of the Flow System.

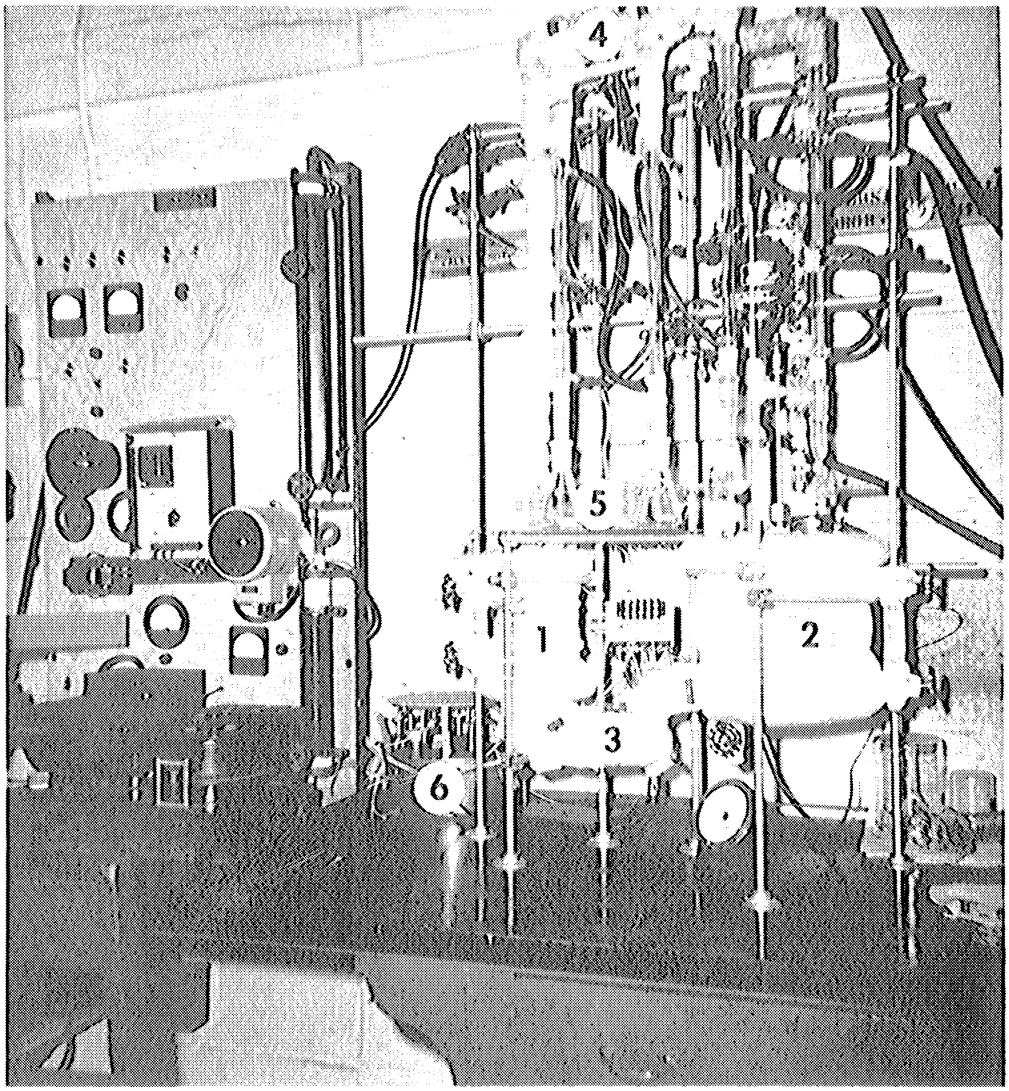

1. Calorimeter
2. Preheater
3. Liquid Lines
4. Vapor Lines
5. Receivers
6. Standard Resistors

Figure 6. Photograph of the Apparatus.

Consider the steady-state flow of a mixture, as it passed through the apparatus, beginning at the preheater. The function of the preheater was to maintain a relatively large, liquid inventory of constant composition at a temperature only slightly below the bubble point of the mixture. To accomplish this mission the preheater was equipped with a thermoregulator, heater, thermometer, and stirrer. The liquid mixture, near its bubble point, flowed by gravity to the calorimeter through the heavily insulated liquid line. Near the calorimeter the liquid line split into two branches. One branch fed the vaporizer; the other fed the shield.

Consider, first, the branch which led to the vaporizer. The liquid feed entered the vaporizer through a capillary tube in the bottom. The capillary served to prevent any sporadic "kick back" of the vaporizer contents into the liquid line which might have been caused by boiling action in the vaporizer. The liquid feed, upon entering the vaporizer, immediately mixed with the vigorously boiling contents, was vaporized, and escaped from the vaporizer via the vapor line at the top. Heat for vaporization of the feed was supplied by consumption of electrical energy in the vaporizer heater.

An identical vaporization process was carried out in the shield. The purpose of the shield was to thermally insulat the vaporizer from heat exchange with its surroundings. This aspect is discussed in more detail in a subsequent section entitled "Thermal Shielding." In order to accomplish its mission the shield performed the same functions as the vaporizer; that is, it provided a place for vaporization

to take place, housed the heater, and provided a volume for the necessary liquid holdup. When in subsequent discussions, a given condition is said to apply to the vaporizer, it should be recalled that the same condition also must apply to the shield because identical processes occurred in each.

The vapor which left both the vaporizer and the shield passed through externally heated vapor lines to the preheater condensers. External heat to the vapor lines was required to prevent the above-ambient-temperature vapor from condensing on cold lines and falling back into the containers. The vapor was then totally condensed in the preheater condensers and returned to the preheater, thus completing the cycle.

In summary, the steady-state cycle was as follows: (1) liquid at its bubble point flowed by gravity from the preheater to the vaporizer, (2) in the vaporizer it mixed with the contents, was vaporized, and escaped via the vapor line, (3) the vapor was condensed and returned to the preheater.

Control of the flow system rested with the vaporizer heater. The power supplied to this heater determined the rate of vaporization, which in turn set the rate of liquid flow by gravity to the vaporizer.

A most important feature of the calorimeter was that under steady-state operating conditions the composition of the liquid mixture which entered the vaporizer was identical to the composition of the vapor which left it. This condition can, of course, be confirmed by an elementary material balance around the vaporizer, which at steady state had a constant liquid level with only one entering stream, the liquid, and

only one exiting stream, the vapor. Yet, this condition may seem paradoxical in view of the fact that vapor which rises from a boiling, binary mixture is richer in the more-volatile component, than is the liquid. Both statements are correct, because during the approach to steady state from the initial state, where liquid of the same composition pervaded the preheater, liquid line, and vaporizer, the liquid holdup in the vaporizer became progressively richer in the less-volatile component. Finally, a composition was reached in the vaporizer such that the vapor which rose from the boiling contents was of identical composition to the incoming liquid. The liquid contents of the vaporizer had thus attained a composition exactly equal, or at least very nearly equal, to that of the equilibrium composition. For a more detailed discussion of the unsteady-state operating period, the reader is referred to Appendix A where an intuitive illustration and a time-varying material balance around the vaporizer are presented.

A steady-state operation of the type described above is not unfamiliar to chemical engineers. The similar performance of the reboiler of an equilibrium distillation column which is operating at total reflux, a hypothetical situation - but a much studied one, is familiar to most. The popular Othmer still[47] used for the determination of vapor-liquid equilibrium data operates in a similar fashion.

Required Measurements

The flow system described in the previous section was ideally suited for calorimetric determinations of the integral isobaric heat of vaporization for a number of reasons. Firstly, it permitted an almost

direct measurement of the latent heat, as defined. Secondly, it permitted operation at a steady-state condition which eliminated the problem of having to cope with time-varying temperatures and compositions. Thirdly, it permitted simultaneous determination of isobaric, vapor-liquid equilibrium data for the mixtures under study with only a small expenditure of additional effort.

A considerable cycling period was required to bring the apparatus to its steady-state operating condition. Once this condition had been reached, the inlet and outlet conditions of the vaporizer corresponded almost exactly to the defined initial and final states involved in the integral isobaric heat of vaporization - the initial state was defined to be liquid of a given composition at its bubble point under a given pressure, and the final state was defined to be vapor of the same composition at its dew point under the same pressure. The liquid feed, however, was not delivered to the vaporizer exactly at its bubble-point temperature, but usually a few degrees lower. Thus, the electrical energy consumed by the vaporizer heater, while used almost entirely for the heat of vaporization, had to make up this small amount of sensible heat. Equation (74) indicates the important measurements which were required for arriving at the integral isobaric heat of vaporization.

$$\text{Integral Isobaric Heat of Vaporization} = \frac{(\text{Power})(\text{Time})}{(\text{Mass of Condensate})} - \text{Sensible Heat Correction} \qquad (74)$$

Reference is again made to Figure 5 on page 52. The flow system was brought to a steady-state condition and operated in that manner

for a period of time prior to making the latent-heat measurements. The actual measurements were begun by simultaneously starting a timer and turning stopcock number 2 so as to divert the cycling vapor into condenser number 2 and its attached, tared receiver. During the timed interval of the determination, several accurate current and voltage readings were made on the vaporizer-heater circuit. The inlet temperature at point TC 12 was measured several times during this interval, as were the other temperatures at points marked TC 13, TC 14, TC 16, and TC 17. The measurements were terminated by simultaneously stoping the timer and turning stopcock number 2 to a straight-through position. A similar, check determination was immediately made with the use of the number 1 stopcock, condenser, and tared receiver. These measurements constituted all that were required for application of Equation (74).

During the unsteady-state operating period the temperatures at all points were recorded at intervals. Several consecutive, unvarying temperature readings indicated that the apparatus had reached steady state. Temperatures, however, served only as an indication; in all cases the steady-state condition was verified by analysis of samples taken from the liquid feed and the condensate.

It has been pointed out in the preceding section that the liquid contents of the vaporizer attained a composition which was in equilibrium with the departing vapor. The temperature of the vaporizer and the vapor composition were determined during the latent-heat measurements as a matter of course. In order to obtain the vapor-liquid equilibrium data only the composition of the liquid contents of the vaporizer remained to be determined. At the conclusion of each determination

a sample of this liquid was removed for analysis. Proper technique and manipulation of valves A, B, C, and D permitted independent sampling of any of the liquid contents of the system.

Thermal Shielding

In order to make precise calorimetric determinations of latent heat, it is imperative that the measurements be made in a thermodynamic system which is adiabatic, or in one in which the heat exchange with the surroundings is accurately known. In the ideal calorimeter accurate measurements of energy, mass, and time are made with no heat exchange occuring between the calorimeter and its surroundings. For adiabatic operation the ideal calorimeter must have either zero heat transfer coefficients or zero temperature difference between it and the surroundings.

A variety of methods have been reported in the literature for maintaining thermal shields at the same temperature as their associated calorimeters. These methods have all been applied to calorimeters used to determine the latent heats of pure substances, but many of the methods would be applicable, probably with more difficulty, to calorimeters used for mixtures. Several investigators[44,45] have used shields which were heated externally by small electrical heaters attached to the surface. Temperature sensing devices detected differences in temperature between the calorimeter and the shield. These differences were then corrected, either manually or automatically by adjustment of the shield heaters. Manual adjustment would demand a considerable portion of the operator's time and attention and distract him from other

essential tasks. As a consequence, a number of complex, automatic temperature-regulating-and-recording shields have been developed.[7,9,78,81,83] Other investigators[21,40,41,43,46,58,74] have used constant-temperature baths of boiling liquids, condensing vapors, or heated liquids of suitable viscosity and vapor pressure to establish shield temperatures.

All previous calorimeters used by other investigators for the determination of integral isobaric heats of vaporization and reported in the literature[8,53,68] operated with an inherent temperature difference between the calorimeter proper and its surroundings. The magnitude of the difference was essentially that of the dew-point - bubble-point temperature difference for a given mixture. For many mixtures this difference is rather small, but for the acetone-water and isopropyl alcohol-water mixtures studied in this investigation the temperature differences would have been large and would have caused large heat leaks in calorimeters of the previous design. Thus, in the calorimeter designed for this investigation, the temperature difference between the calorimeter proper (vaporizer) and its surroundings had to be eliminated, and in addition, the conductive, convective and radiative coefficients for heat transfer had to be made as small as practicable.

Figure 7 on page 63 is a cross-section of the calorimeter used in this investigation. In this calorimeter a temperature difference between the vaporizer and its surroundings was eliminated by setting up, in the shield, a steady-state vaporization process identical to the one which was occurring in the vaporizer. This method was well suited for calormetric work with mixtures, and especially for the type of flow apparatus used in this investigation, in that, the correct shield temperature

was easily and automatically guaranteed regardless of the exact, final, steady-state composition. Furthermore, no complex, automatically controlled apparatus was required to maintain the temperature, and only a minimum of the operator's attention was required to achieve excellent results. Heat transfer by all modes was practically eliminated by this technique.

In addition to the aforementioned precaution for temperature control, the heat-transfer coefficients were reduced to a minimum by conventional methods. The jacket immediately adjacent to the vaporizer was evacuated to reduce the convective coefficient, and both the outer surface of the vaporizer and the inner surface of the jacket were silvered in order to reduce the radiative coefficient. The electrical leads and the lines carrying material to and from the vaporizer provided a means by which conductive heat transfer occurred. The associated conductive coefficients were reduced by the use of electrical leads as small as possible, consistent with the limits of electrical resistance tolerable in them, and by construction of the lines from thin material of low thermal conductivity.

The heat leak along the liquid-feed capillary at the bottom of the vaporizer which resulted from a higher temperature at the vaporizer end of the capillary than at the inlet end of the capillary was reduced by the rapid flow of the liquid feed through the capillary in the opposite direction. In addition, the low thermal conductivity of the glass and its thin wall, were favorable to the reduction of this heat leak to a small quantity.

A quantitative discussion of the effect of the very small, but ever present, heat leaks on the results is taken up in a subsequent section entitled "Effects of Flow Rate."

The Calorimeter

The word calorimeter is used here to refer to all of the apparatus, except the flow lines, shown on the left-hand portion of the schematic flow diagram, Figure 5 on page 52. The calorimeter consisted of two main components. The vaporizer and its vacuum jacket formed the heart of the calorimeter; the shield constituted the other main component. Figure 7 on page 63 is a cross section of the calorimeter.

The vaporizer and its vacuum jacket constituted a single unit constructed of standard-wall Pyrex glass. The outside surface of the vaporizer and the inside surface of the jacket were silvered; the jacket was then evacuated to a very low pressure by a mercury diffusion pump and sealed off. Both the vaporizer and the vacuum jacket were cylindrical in shape. The vapor outlet tube at the top was 14mm in inside diameter and extended approximately 3/4 inch beyond the top of the jacket. The outside surface of this tube was tapered toward the top. A spiral-wound capillary tube extended from the bottom of the vaporizer through the evacuated space to the bottom of the jacket where it joined the inlet tube. This capillary was thin walled with an inside diameter of 1.3mm and a passage length of approximately 6 inches. The inlet tube was 6mm in outside diameter and extended approximately 2-1/2 inches below the jacket.

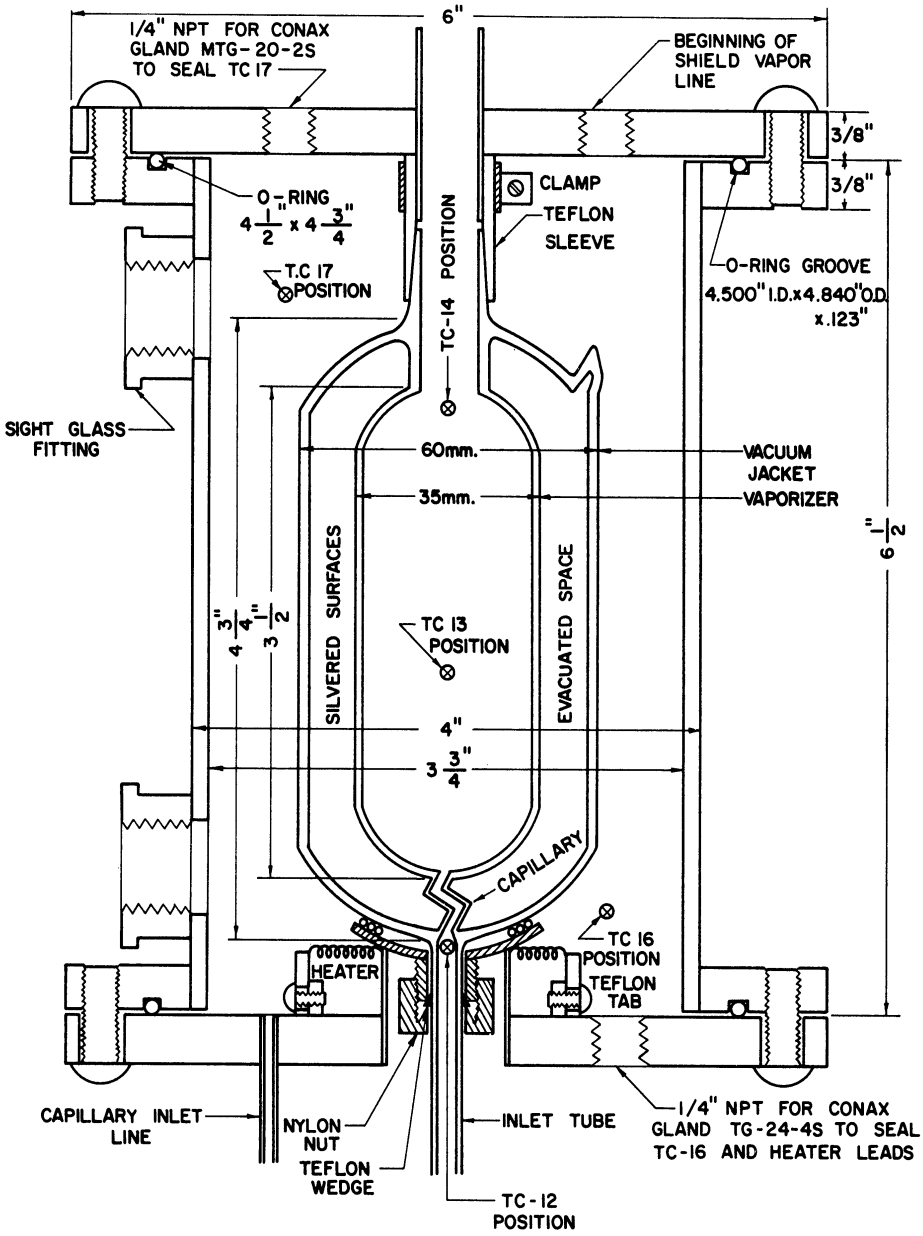

Figure 7. The Calorimeter.

The shield was constructed for the most part from brass and consisted primarily of a cylinder with two removable ends. A brass flange was silver-soldered to each end of the cylinder, and a groove was machined into each annulus to accommodate a Teflon O-ring which formed the seal between the flange and the top or bottom. The flanges each contained eight tapped holes for the accommodation of the machine screws which secured the top and bottom. A sight glass was installed on one side of the cylinder. Two, 1/2-inch, brass pipe fittings, which were milled to fit the wall curvature, were silver-soldered to the wall over 3/4-inch holes. Standard brass fittings for 5/8-inch gauge glass and the glass, itself, were installed. The pipe threads were sealed with soft solder. The stem packings in the fittings were replaced with packings cut from Teflon sheet, and the gauge-glass packings were replaced with modified Teflon V-rings (nominal size: 1/2 inch by 1 inch).

The top of the shield contained the openings for the beginning of both vapor lines and an outlet for thermocouple wires. A 1/2-inch copper tube which extended from 1/2 inch below the bottom of the plate, where it met the outlet tube of the vaporizer, to 5/8 inch above the top was silver-soldered into the center of the plate. The top of the copper tube was tapped to accommodate a 1/4-inch brass nipple to which was attached a 1/4-inch brass cross. The left side of the cross was fitted with a gland (Conax MTG-20-2S Teflon sealant) which sealed thermocouples number 13 and 14. The right side was fitted with a gland (Conax TG-24-A4 Teflon sealant) which sealed the vaporizer heater leads. The top of the cross accomodated a brass compression fitting which contained a short length of 3/8-inch copper tubing for the beginning of

the vapor line. All threads and joints were adequately sealed with soft solder. The vapor line from the shield originated directly behind the line from the vaporizer as one looks at Figure 7; however, the shield line was purposely misplaced to the right on the figure for illustrative purposes. The top of the shield was tapped for the accomodation of a brass compression fitting which contained a short length of 3/8-inch copper tubing for the beginning of the shield vapor line.

The bottom of the shield provided openings for the capillary inlet line to the shield and the vaporizer inlet tube, as well as, an outlet for thermocouple wires and the shield-heater leads. In addition, it furnished support for the shield heater and the vacuum-jacketed vaporizer. A coil of 1/8-inch copper tubing with a passage length of 8 inches was silver-soldered into an inlet hole to one side of the bottom. Five, 1/8-inch brass nuts were soft-soldered in an upright position to the inside of the bottom of the shield in a pentagonal configuration to form the base for the shield heater supports. Brass machine screws held Teflon tabs (approximately 1/4 inch by 1/2 inch by 1/8 inch) to the nuts. Slots cut into the top of the Teflon tabs firmly secured the bare wire of the shield heater. A recessed space, which permitted liquid to flow through the inlet tube to the vaporizer unaffected by the temperature of the shield contents, was formed by a one-inch brass tube extending 1/2 inch into the shield. This tube was silver-soldered to the bottom of the shield, and it supported, at its top, a circular piece of copper 1-1/2 inches in diameter which had the same contour as the bottom of the vacuum jacket. This dished piece, which contained a 3/8-inch hole at its center, was silver-soldered to

the top of the tube. A 1/4-inch, brass, flared tubing connector was cut in half, drilled out to 21/64 inch, and silver-soldered over the hole in the copper piece.

Connection between the top of the shield and the vaporizer outlet tube was effected by a specially formed Teflon sleeve. This thin-walled sleeve was one inch long and had an inside diameter of 1/2 inch in its upper half. The lower half had the same contour as the tapered outside surface of the vaporizer outlet tube. An epoxy-resin adhesive (Armstrong Products Company type C-1) was applied between the glass and the sleeve to make certain that any small irregularities in the glass or sleeve did not lead to leaks between the shield and the vaporizer. The strength of the bond with the Teflon sleeve need not be of concern here, because in the assembled calorimeter this bond was not under stress. It was observed, however, that the bond was of sufficient strength to support the weight of the glass unit. In its quite limited exposure the resin was adequately resistant to attack by the vapor. The top of the Teflon sleeve was secured tightly to the copper outlet tube by forcing it over the tube. In addition, a brass tubing clamp was installed to make certain of the seal.

In assembling the calorimeter the bottom of the shield was secured to the upright cylinder, and the vacuum-jacketed vaporizer, which was joined to the top of the shield by the Teflon sleeve, was carefully lowered into position inside the shield. The bottom of the vacuum jacket was cushioned on the copper support by a coil of 24-guage Teflong spaghetti. A check for perfect alignment of the parts, which

was necessary to prevent damage to the glass, was made before the top of the shield was secured to the cylinder. A specially constructed Teflon ring with a wedge-shaped cross section was forced over the outside of the inlet tube in a position such that it could make the seal between the tube and the modified fitting. A nylon nut, manufactured for connectors used in conjunction with 1/4-inch polyethylene tubing, was slipped over the inlet tube and tightened to complete the seal at the bottom.

The entire calorimeter was insulated on its outer surfaces with about one inch of Fiberglas and then covered with a cloth jacket. The exposed parts of the sight-glass fittings were covered with molded asbestos.

The calorimeter was supported on the underside of the top flange by Flexaframe rods, which facilitated adjustment of the elevation of the calorimeter during preliminary experiments.

Auxiliary Equipment

The auxiliary equipment consisted of all the apparatus associated with the calorimeter in the flow system, except the electrical equipment. It can be broken down into three main categories - the preheater, the flow lines, and the collection system.

Figure 8 on page 68 is a sketch of the preheater. It consisted primarily of a shell constructed from a modified stainless-steel beaker and a brass top fabricated to accommodate and support a variety of apparatus. The top of a 5800-ml, stainless-steel beaker was cut off at a height of 7-3/4 inches to form the shell. A brass flange was

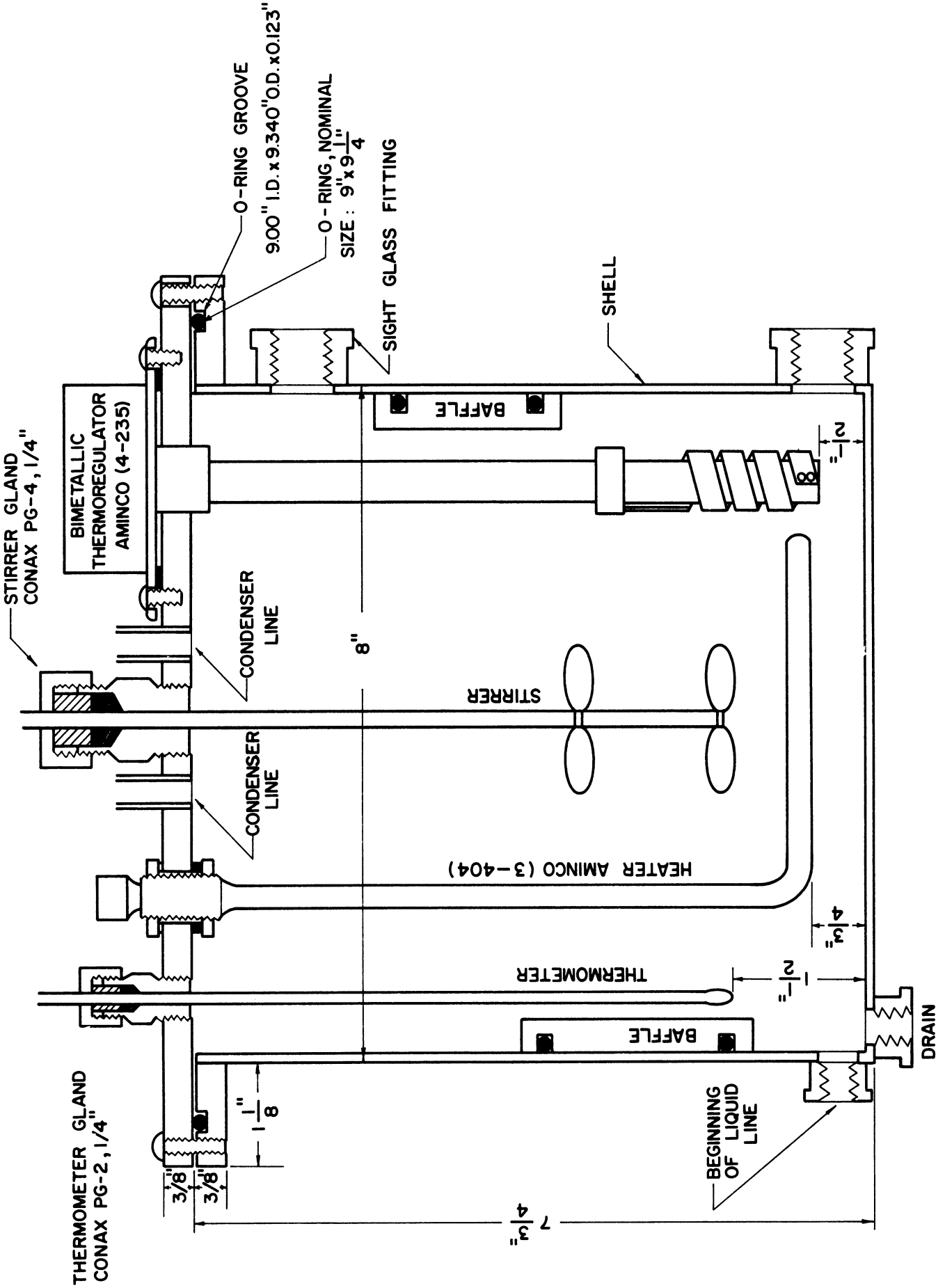

Figure 8. The Preheater.

silver-soldered to the top of the shell, and a groove was machined into the annulus to accommodate a Teflon O-ring which formed the seal between the flange and the top. The flange contained 12 tapped holes for the accommodation of the machine screws which secured the top. A sight glass similar to the one previously described for the calorimeter was installed on the shell. Thin, brass baffles, approximately one inch by two inches, were attached to small tabs, silver-soldered to the inside of the shell in an irregular configuration, in order to facilitate better mixing of the contents. The liquid outlet from the shell was located opposite the sight glass about 3/4 inch above the bottom. At this point a 1/4-inch, brass pipe fitting, milled to fit the wall curvature, was silver-soldered to the shell. This fitting accomodated the main, liquid-line valve (Hoke 306M). A drain valve was attached to the bottom of the shell in a similar manner.

The top of the preheater contained three lines from various condensers, a packing gland for the thermometer, two heater terminals, a thermoregulator, and the packing gland for the stirrer. The lines from the three condensers all terminated in short lengths of 3/8-inch copper tubing which were silver-soldered into holes in the top of the preheater. The thermometer (Cenco 19245-C), which was sealed in the top, had a range of 0 to 100°C with 0.1° subdivisios. Accurate readings were not required of this thermometer, hence its calibration was unnecessary. The active section of the copper-sheathed heater was bent into an almost circular shape with a diameter a little less than that of the shell. The "cold" section of the heater extended through the vapor space,

and the terminals were sealed in the top. These seals were effected by a Teflon gasket between the bottom nut of each of the electrically insulated terminals and the bottom of the plate. A Teflon gasket somewhat larger in inside diameter than the collar of the thermoregulator provided the seal between its flange and the top of the preheater.

The center of the top of the preheater was tapped to accomodate the packing gland for the stirrer. Teflon V-rings (nominal size: 1/4 inch by 5/8 inch) were used as packing. The stirrer was powered by a Sargent-Cone-Drive stirring motor adjusted for an operation that gave adequate agitation without excessive splashing. The 1/4-inch, stainless-steel shaft was equipped with two propellers approximately 1-1/2 inches long. The lower propeller was positioned 1-3/4 inches from the bottom of the shell, and the other was located 3-3/8 inches above the bottom.

The entire preheater was insulated on its outer surfaces in the same manner as the calorimeter. The preheater, like the calorimeter, was supported on the under side of the flange by Flexaframe rods which permitted adjustment of the liquid levels.

The liquid line, as shown in Figure 5 on page 52 , began at the main, liquid-line valve, which was attached to the preheater, and extended to the calorimeter where it divided into two branches. The lines consisted of 1/4-inch copper tubing and brass compression fittings. Because of their short lengths the lines seemed to be more fittings than tubing. At the point where the lines divided, the bottom port of the 1/4-inch brass cross was fitted with a valve (Hoke 306M) to which the

sampling apparatus was attached. The vaporizer branch contained a valve (Hoke 306M) and a 1/8-inch brass tee which accomodated a gland (Conax MTG-20-2S) used to seal the wires of thermocouple number 12. The end of the vaporizer line was joined to the glass inlet tube with a short length of thin-walled Teflon tubing which was forced over the glass and secured to the copper tubing by a tubing clamp. The shield branch contained only a valve (Hoke 304) and the necessary fittings. Teflon was used for the steam packing in all valves. All pipe threads were sealed with soft solder. The lines were wrapped with Fiberglas insulation to a diameter of about two inches and then enclosed in a cloth jacket.

The vapor lines, as shown in Figure 5 on page 52, extended from the calorimeter to the preheater. The lines were constructed of 10-mm, Pyrex glass tubing. They were joined to the short pieces of copper tubing, which protruded from both the calorimeter and the preheater, by short lengths of thin-walled Teflon tubing forced over the glass and secured to the copper tubing by tubing clamps. Three-way stopcocks with 4-mm bores were placed in the lines as shown. West-type, Pyrex glass condensers, 12 inches long with drip tips and 24/40-ground-glass joints, were installed in the vapor lines. Connections to the condensers were made with the aid of bushing-type adapters and necked-down 24/40-ground-glass joints. All ground-glass joints were lubricated with Dow Corning Silicone Lubricant. The lines were wrapped with heating tapes from the points of origin at the calorimeter to the tops of the condensers. One layer of Fiberglas insulation on top of the heaters helped to contain the heat and even-out the temperature distribution.

Two, Allihn-type condensers, each nine inches long and attached in series to the preheater, were open to the atmosphere and served to prevent liquid loss from the preheater, which subsequently would have changed the composition. In addition, the top condenser provided a convenient opening through which material was charged to the preheater without removing the top.

The collection system consisted of two condensers, two receivers, and a timer. The receivers were modified, 125-ml Erlenmeyer flasks with 24/40-ground-glass joints. They can be seen in the photograph on page 53 on top of the small platform below the condensers. During operation of the apparatus, each receiver rested in a beaker of crushed ice and was elevated so as to attach directly to the bottom 24/40-ground-glass joint of its condenser. No grease was used on this joint. In the attached position the modified flask was open to the atmosphere via a coil of 4-mm glass tubing. The passage through the coil began in the flask wall just below the ground-glass joint and extended externally almost to the bottom of the flask. At that point the coil turned upward in a straight tube which terminated in a small opening at a height approximately equivalent to the center of the ground-glass joint. This circuitous passage through the ice-filled beaker prevented losses by evaporation from the receiver. Light-weight tops from weighing bottles neatly stoppered the receivers when they were not attached to the condensers.

The length of time for which the condensate was collected was recorded on a stop watch which had 0.1-second divisions. The stop watch was checked several times with the Michigan Bell Telephone Company

time signal and with an electric timer over a 20-minute interval. The differences were never more than 0.2 second, and they were neither consistently fast nor consistently slow; consequently, the differences must be attributed to the operation of the stop-start button.

Heaters and Electrical Circuits

Four electrical heaters and the associated circuits constituted integral parts of the apparatus. They were (1) the vaporizer heater, (2) the shield heater, (3) the preheater heater, and (4) the vapor line heaters. In addition, the thermocouple and potentiometer circuits formed equally important components.

The vaporizer heater was constructed from 40 inches of 36-guage platinum wire. The wire was coiled on a 3/32-inch arbor, and for support in service it was slipped over a sealed, glass, melting-point tube formed into a helix of about 3/8-inch inside diameter. The room temperature resistance of the heater was approximately 8-1/2 ohms. Twenty-four-gauge copper leads were soldered to each end of the platinum. Approximately 1-1/2 inches above the heater coil, a position which corresponded approximately to the average liquid level in the vaporizer, potential leads of 24-gauge copper wire were soldered to the current leads. This arrangement permitted the very small potential drop in the leads to be included in the measurement of the potential drop across the heater. All leads were insulated with 24-gauge Teflon spaghetti. The four, relatively short leads were adequate support for the heater coil.

Figure 9 on page 75 shows the circuit for the vaporizer heater. The circuit consisted of two parts - the A.C. section which was used during the long cycling period in order to conserve the batteries, and the D.C. section which was used while the actual measurements were taken. The A.C. power was controlled by a variable transformer. The A.C. ammeter and voltmeter aided in the power adjustment. The D.C. power was supplied by three, 12-volt, lead storage batteries. These batteries were frequently recharged in order to keep the specific gravity in the range from about 1.225 to 1.235. Any one or any combination of the batteries could be switched into the circuit, as desired. The power consumed by the vaporizer heater was controlled by a combination of the number of batteries in the circuit and the adjustment of the water cooled, 35-ohm and 5-ohm variable resistors which were in series with the heater. The 35-ohm resistor afforded coarse control, and the 5-ohm resistor was used for fine control. The D.C. ammeter and voltmeter were used only for the adjustment of the power delivered to the heater; the voltmeter was switched out of the circuit after the adjustment had been made.

An accurate calculation of the power consumed by the heater was made from determinations of its current and potential drop. The potential drop was determined from the measurement of the potential across the 100-ohm standard resistor, which was part of the 100-ohm - 10,000-ohm combination connected in parallel with the heater. The current which passed through the heater was determined from the measurement of the potential across the 0.1-ohm standard resistor, which was in series with the heater. A correction was applied for the small

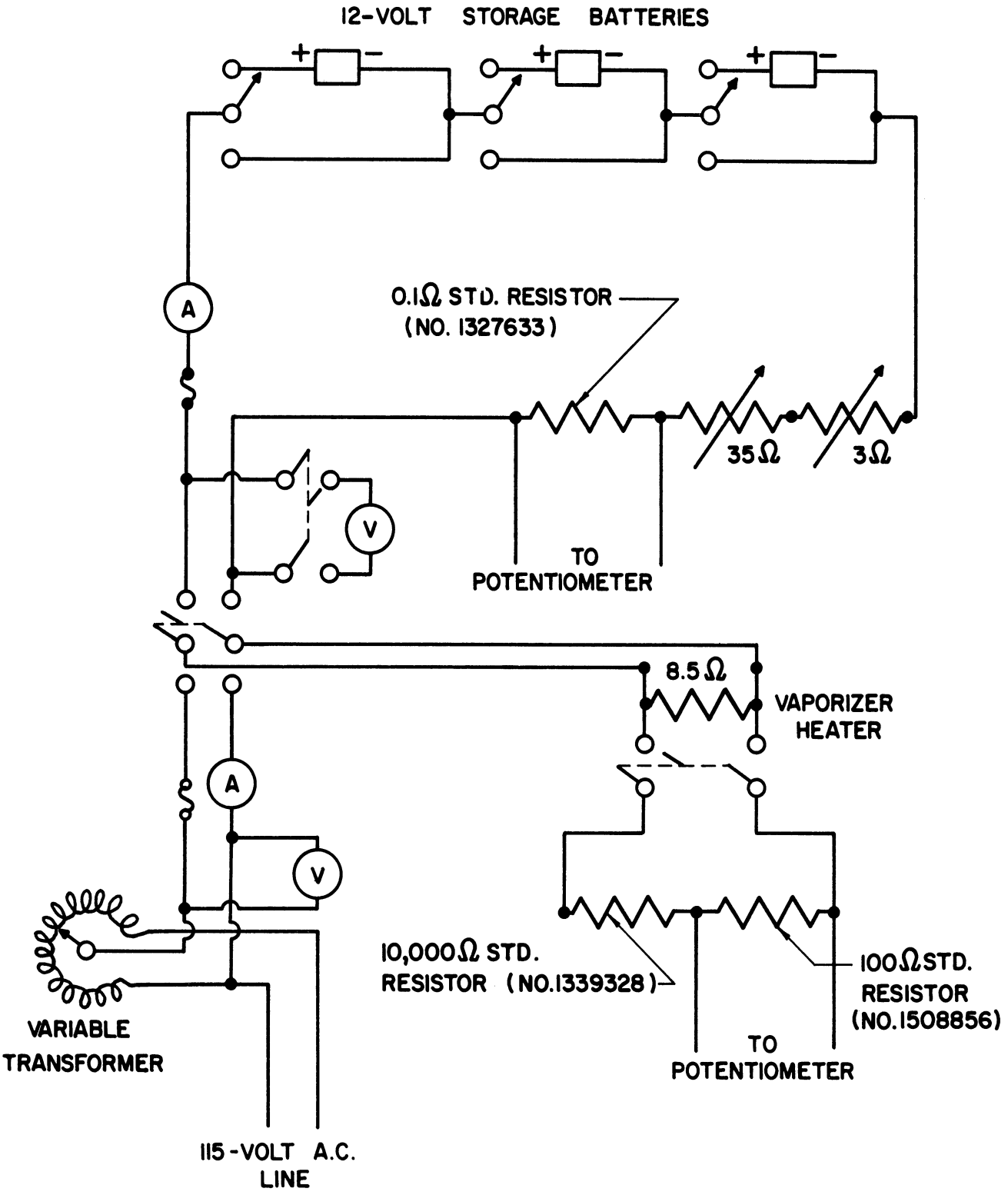

Figure 9. Circuit Diagram for the Vaporizer Heater.

amount of current which was shunted through the 100-ohm - 10,000-ohm circuit. The equation used to calculate the power from the two potential measurements is given in Appendix B.

The Leeds and Northrup, 100-ohm and 10,000-ohm standard resistors were of the National Bureau of Standards type and possessed recent certificates from the National Bureau of Standards which verified the actual resistances as 100.000 absolute ohms plus or minus 0.005 per cent and 10,000.5 absolute ohms plus or minus 0.005 per cent. The resistance of the leads and switch between these resistors and the heater was measured as approximately 0.2 ohm, which is less than the stated uncertainty in the 10,000-ohm resistor. The Leeds and Northrup, 0.1-ohm, standard resistor of the Reichsanstalt type also possessed a recent National Bureau of Standards certificate which verified its actual resistance as 0.099995 absolute ohm plus or minus 0.01 per cent. All three of the resistors were immersed in an oil bath to a level almost even with the top of the 0.1-ohm resistor.

The shield heater was constructed from approximately 7-1/2 feet of 28-gauge, Chromel-C wire. Its room temperature resistance was approximately 32 ohms. The wire was coiled on a 1/8-inch arbor. The strength of the wire coil made the support given it by the five Teflon tabs attached to the bottom of the shield more than adequate.

The circuit for the shield heater was quite simple. The heater was connected through a fuse and an ammeter to the output side of a variable transformer, which was used to control its power consumption.

The preheater circuit is shown in Figure 10 on page 78. The circuit provided a simple on-off control for the thermostated liquid bath. The temperature was quite easily controlled to within plus or minus 0.05°C. The full 500 watts of the heater were utilized during the early stages of an operation in order to rapidly bring the liquid contents of the preheater to the desired temperature. Once the operating temperature was reached, the variable transformer which controlled the voltage applied to the heater was adjusted so that the correct temperature could be maintained with only a minimum number of interruptions of the power supply by the control circuit. The presence of the variable transformer in the circuit required a modification of the Trimount Electronic Level Control, which had the function of connecting terminals 2 and 3 when heat was required, to prevent burning of its relay contacts. A 100-ohm resistor and a one-microfarad condenser connected in series between terminals number 2 and 3 served this purpose.

The four commercial heating tapes (60 ohms, two of 80 ohms, and 100 ohms) wrapped on the vapor lines were connected in parallel through a fuse and an ammeter to a variable transformer which was used to control their power consumption.

Copper-constantan thermocouples with bare junctions were used to measure temperatures at the points indicated on Figure 5 on page 52. The thermocouples were joined with soft solder, but not twisted, at the junctions. One thermocouple was used for the ice-point reference junction, and the remainder were soldered to the terminals inside the switch. This entire unit was then used in the calibration of the

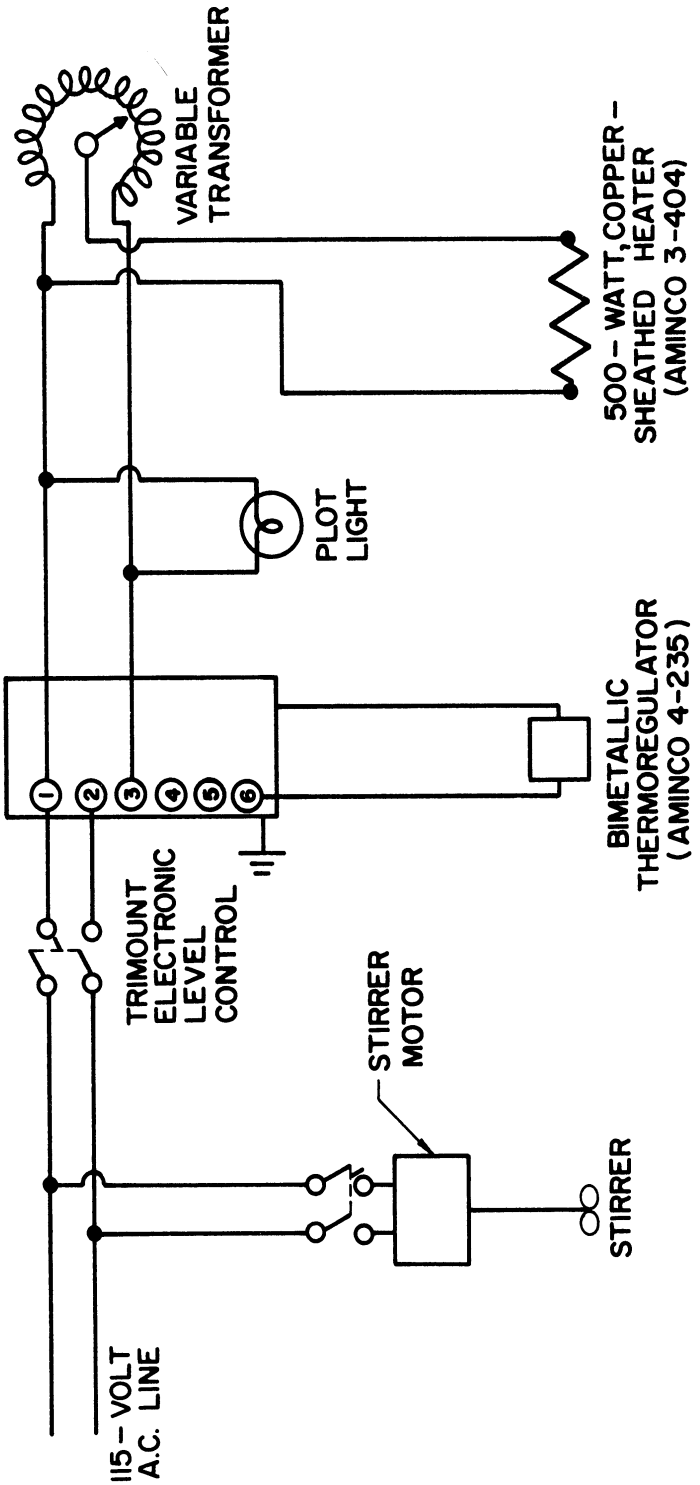

Figure 10. Circuit Diagram for the Preheater.

thermocouples in the controlled-temperature medium of a stirred-liquid bath. The calibration curves for the thermocouples used are given in Figure 37 of Appendix E. The wires were covered with a high temperature insulating enamel. In addition, ceramic insulators were used on numbers 16 and 17; the remainder were insulated with Teflon spaghetti.

Thermocouple number 12 was constructed from 30-gauge wires and was used to measure the liquid inlet temperature to the capillary. The junction was 1-mm in cross section and was located exactly at the entrance of the 1.3-mm capillary. Thus, the average inlet temperature was determined with one position of the thermocouple. Thermocouples number 13 and 14 were also constructed from 30-gauge wires and were located inside the vaporizer. Number 13 was submerged in the liquid about 1/2 inch above the heater. Number 14 was located in the vapor stream at the top of the vaporizer. Its size and environment were favorable for accurate temperature measurement. That is, it had a small junction, was located in the rapidly moving vapor stream, and "saw" silvered walls which were at the same temperature as the vapor itself. Numbers 13 and 14 were both attached to the insulated heater leads to insure their location at the desired position. Thermocouples number 16 and 17 were constructed from 24-gauge wires and were located inside the shield. Number 16 was located 1-5/8 inches below the top of the shield in the vapor space. Number 17 was used for measuring the liquid temperatures and was located 1-1/4 inches above the bottom of the shield. The ceramic insulators used on both 16 and 17 also served as support for the wires.

The potential-measuring circuit and the thermocouple connections are shown in Figure 11 on page 81. The potential measurements were made with a Leeds and Northrup, K-2-type potentiometer and suitable auxiliary equipment. Two Eppley standard cells (Nos. 132182 and 610144) were used during the work. At 25°C their emf's were 1.01867 and 1.01881 absolute volts, respectively, as determined with a Weston cell (No. 15559) of the unsaturated type which possessed a recent certificate from the National Bureau of Standards. A Leeds and Northrup, type-2500-C galvanometer was used to detect unbalances in the potentiometer circuit. A 330-ohm damping resistance was installed between the galvanometer and the potentiometer. The unbalances were indicated on the etched ground glass of a Leeds and Northrup, type-2100 lamp and scale located at a distance of one meter from the galvanometer mirror. Four, 1.5-volt dry cells in a series-parallel connection supplied the working current for the potentiometer.

A pinch-type, DPDT switch was the hub of the potentiometer circuit. Its center terminals were connected to both the emf terminals of the potentiometer and the inner contact rings of the multipoint thermocouple switch. With the thermocouple switch in an open position the potential across either the 100-ohm or the 0.1-ohm standard resistor could be applied to the emf terminals of the potentiometer by throwing the pinch switch. With the pinch switch in an open position any of the thermocouples could be connected directly to the potentiometer. The thermocouples were attached to the ten-point, double-pole switch as shown in the figure.

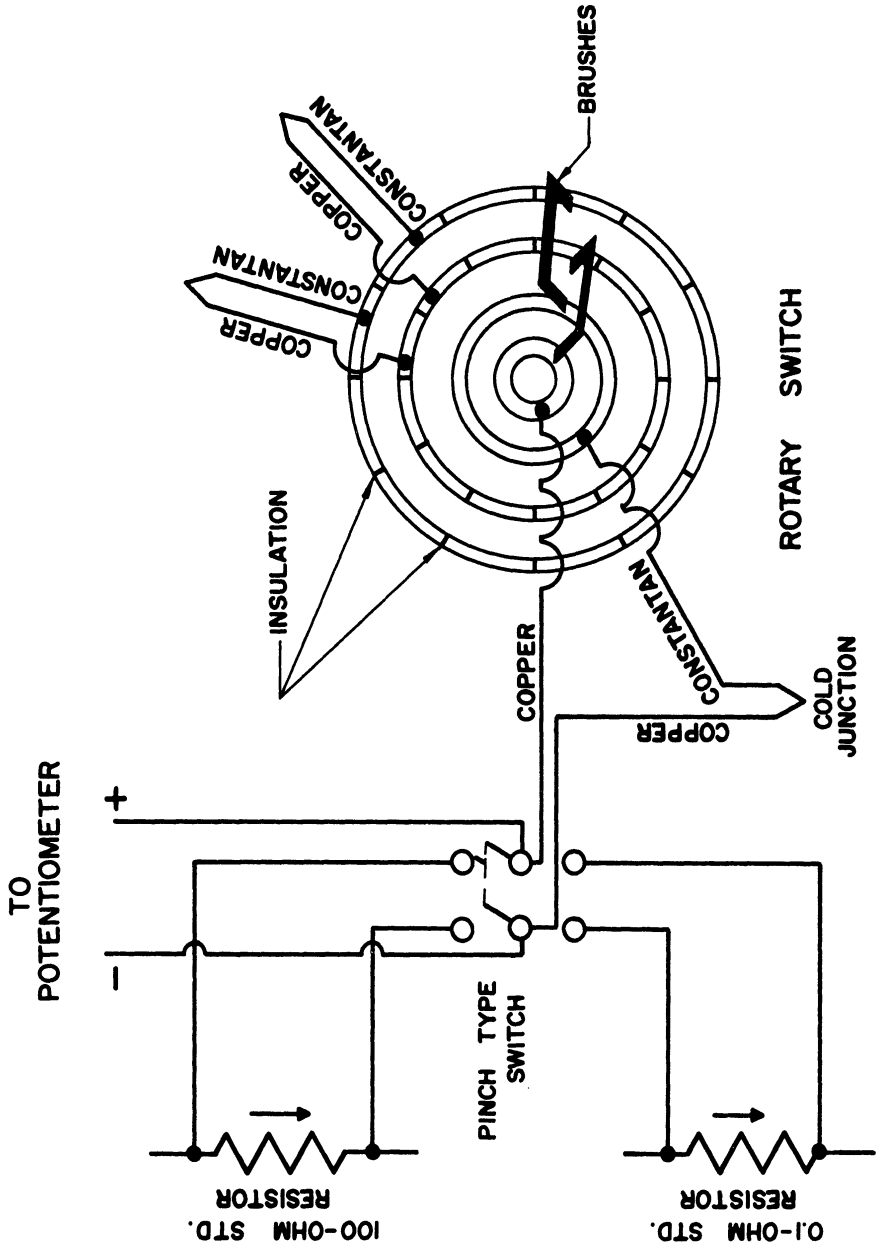

Figure 11. Potential-Measuring Circuit and Thermocouple Circuit.

Analytical Equipment

Analyses of the mixtures were determined from the measurements of the density of the liquids in calibrated pycnometers. Hot liquid samples were withdrawn from the system through the sampling valve, D, (Figure 5 on page 52) and were cooled in the detachable sample cooler before delivery to the pycnometers. The condensate samples were taken directly from the receivers.

The volumes of six pycnometers of various sizes (nominally: one 5-ml, four 10-ml, and one 25-ml) with ground-glass joints and caps, which contained capillary perforations, were determined by calibration. The calibrations were made at 25 °C and 35 °C with double-distilled water in the constant-temperature medium of a well agitated, thermostatically controlled water bath. The temperature, which was easily controlled to plus or minus 0.05 °C, was observed on a mercury-in-glass thermometer (Prince No. 460641) which possessed a recent certificate from the National Bureau of Standards. The pycnometers were submerged to a depth approximately 1/2 inch below the top of the caps by custom-fitted suspensions fashioned from 1/8-inch copper tubing and attached to the side of the bath. The weights of the pycnometers were determined quickly and easily on a Christian Becker Projectomatic Balance (Model AB-1).

The detachable sample cooler consisted primarily of a coil of 1/4-inch copper tubing soft-soldered into a number-2-1/2 tin can. In service the can contained crushed ice which surrouned the coil. Both ends of the coil protruded through the side of the can. A short length of polyethylene tubing was installed for flexibility between the top

of the protruding coil and the fittings used to attach the cooler to the sampling valve. The bottom end of the coil delivered the sample directly to the pycnometer.

Materials

Reagent-grade isopropyl alcohol of 99.91 per cent purity marketed by the J. T. Baker Chemical Company was used without further purification.

Reagent-grade acetone of 99.60 per cent purity marketed by Merk and Company, Inc. was used without further purification.

Double-distilled water from the University Chemistry Store was used for all dilutions and calibrations.

EXPERIMENTAL PROCEDURE

Summary

The culmination of the experimental procedure was reached during a timed interval in which the actual data used for the determination of the integral isobaric heat of vaporization were taken. During this interval measurements of mass, power, and temperature were made on the calorimeter. Less engaging, but of no less importance to the final results, were the prerequisite procedures of preparation for the run and of cycling the mixture in the apparatus. The post-requisites of sampling and analysis were likewise indispensable.

Preparation

The preparation period was considered to have begun with the routine laboratory tasks and to have extended to the time at which the first vapor escaped from the shield.

A liquid mixture approximately of the composition of interest was charged to the preheater through the opening in the top of the reflux condenser. The liquid was allowed to run into the shield and vaporizer until it reached a level of 3-1/2 inches from the bottom of the shield, as shown in the sight glass. At that time the valves in the shield and vaporizer branches of the liquid line were closed, and the liquid level in the preheater was brought to 4-1/2 inches from the bottom, as shown in its sight glass. Experience gained from preliminary experiments with various adjustments of the Flexaframe supports indicated that these levels were desirable and easily maintained.

The entire composition range was covered by beginning with a rich mixture of the more volatile component, either isopropyl alcohol or acetone. Thus, the more frequently used charging process consisted of the dilution of the rich mixture already in the preheater with double-distilled water. However, after a number of dilutions the preheater was drained and refilled with a completely fresh mixture as previously described.

After many runs, which began with the same liquid composition everywhere in the system, had been made with the observation that a steady state was attained as described in a previous section entitled "The Flow System," it was decided to shorten the lengthy cycling period by assisting in the approach to steady state. The final contents of the shield and vaporizer were always leaner in the more volatile component (isopropyl alcohol or acetone) than were the initial contents. (An exception to the foregoing statement occurred for compositions of the isopropyl alcohol-water binary between the minimum-boiling azeotrope and pure isopropyl alcohol; however, this case is not relevant to the discussion here because all runs in this composition range happened to have been made with the original procedure of beginning with the same composition throughout the apparatus.) Therefore, a mixture with a higher concentration of water than the mixture in the preheater was charged to the shield and vaporizer through the sampling valve. However, this special, shield-vaporizer charge always contained less water than the final contents of the shield and vaporizer in order to guarantee that steady state was at all times approached from the same direction.

That is to say, to guarantee that the concentration of water in the shield and vaporizer always increased with time and never decreased. In order to insure this condition for the vaporizer, it was necessary, because of the relative volumes of the apparatus involved, to drain from the vaporizer and its liquid line a volume of the special mixture equivalent to the line volume and to then allow the line to refill with the mixture from the preheater.

After the correct mixture was charged to the apparatus and a number of routine tasks, such as turning on cooling water, were completed, the preheater was readied. Stirring and heating were begun, and the thermoregulator was adjusted to control the temperature at approximately two centigrade degrees lower than the bubble point. As the temperature of the contents approached the control temperature, the voltage applied to the heater was reduced to a level, usually between 27 and 60 volts, which experience had shown was satisfactory for maintaining a constant temperature with a minimum of interruptions of the power by the controller.

Simultaneously with the preparation of the preheater a predetermined amount of power was supplied to the shield heater and the vapor-line heaters. Experience gained from preliminary experiments indicated that power at a level 2-1/2 times that consumed by the vaporizer heater should be supplied to the shield heater for smooth operation and a reasonable rate of cycling of material through the shield. Observations during preliminary experiments showed that, for the complete range of mixtures, from 72 to 118 watts were required by the vapor-line

heaters in order to prevent condensation in the lines. A period of approximately 1-1/2 hours was required to warm-up the apparatus and to get a significant flow of vapor from the shield. When a significant flow was established, the valve in the shield branch of the liquid line was opened and adjusted to maintain a liquid level of 3-1/2 to 3-5/8 inches in the shield. Operating conditions and the relative densities of the preheater and shield contents affected the levels; consequently, the operator's experience was valuable in the adjustment of the valve.

As the mixture began to cycle in the shield the valve in the vaporizer branch of the liquid line was opened, and alternating current was supplied to the vaporizer heater in an amount sufficient to establish the desired flow rate. Vaporization in this container began almost immediately because the surroundings had been conditioned by the shield; thus, all of the heat was immediately available to the liquid.

Cycling

The cycling period was considered to have begun with the mixture circulating through the apparatus and to have extended to the beginning of the actual determination.

The average cycling period lasted about 2-1/2 hours. During this time temperature readings were taken at intervals at all points. A number of consecutive, unvarying temperatures in the vaporizer and shield indicated that the apparatus had reached steady state. This period also provided time for necessary, routine tasks, such as attaching the receivers with their ice-filled beakers to the condensers and

insulating the liquid-line valve handles after the final adjustments had been made.

When temperature observations indicated that a steady state had been reached and about 20 minutes before the actual determination was begun, the vaporizer heater was switched from alternating current to direct current. Prior to the switch the sliding-contact, water-cooled resistors in the D.C. circuit were positioned so as to make the initial battery-supplied power approximately the same as the A.C. power. Experience in positioning the resistors made the instantaneous switch from A.C. power to battery power, and the subsequent fine adjustment of the current to the vaporizer heater, a process which required only a few seconds. After the final adjustment of power had been made, the D.C. voltmeter, which would have drawn a small amount of current, was switched out of the circuit.

The steady-state cycling was continued for about 20 minutes during which time the potentials across the standard resistors and the emf's of all the thermocouples were measured and recorded.

Measurements

Two successive determinations were always carried out on the same mixture, at the same flow rate; consequently, the measurement period extended from the start of the timer at the beginning of the first determination to the stop of the timer at the end of the second determination. The average length of the first determination was approximately 22 minutes; the second averaged approximately 17 minutes. Measurements were taken for each particular mixture at flow rates of

approximately 1-1/2 grams per minute and one gram per minute. Data were taken for each of the pure components at four flow rates between 0.703 and 1.733 grams per minute.

With the material cycling smoothly in the apparatus, a determination was begun by simultaneously starting the timer and turning stopcock number 2 to divert the vapor into its condenser and tared receiver. A 60-minute stop clock was then started in order to give the approximate time of the determination at a glance. Two sets of measurements of the potentials across the standard resistors were taken and recorded along with the time of each measurement. The emf's of thermocouple numbers 13, 14, 16 and 17 were measured twice and compared with the measurements obtained during the cycling period. If they were not in agreement the determination was halted and discarded, and the cycling period was continued. The emf of thermocouple number 12 was measured several times during the interval. This temperature was not perfectly constant with time; however, it rarely varied more than plus or minus 0.5 °C and usually varied considerably less. An arithmetic average of the readings taken was used for calculations. After the thermocouple emf's had been measured one more set of measurements of the potentials across the standard resistors was made. Stopcock number 2 was then turned to a straight-through position simultaneously with the stopping of the timer in order to end the determination. During the determination, readings of all the meters and gauges attached to the apparatus, as well as the barometric pressure and ambient temperature, were recorded.

Immediately after the end of the first determination, a second was begun using stopcock number 1 and its condenser and tared receiver. The procedure followed was identical to the one described in the previous paragraph, except that one of the two early sets of potential measurements was eliminated.

At this point in the procedure two alternatives were available. The vaporizer heater could be switched to A.C. power at a lower level in order to begin the cycling period for the determinations at a slower flow rate, or the sampling and analysis could be started immediately in which case the apparatus would be shut down and the slower-rate run made at a later date. The former procedure practically eliminated another preparation period and considerably shortened the cycling period. Usually, the slow-rate determination could be commenced as soon as the sampling and analysis which was associated with the faster rate and which could not be delayed had been completed. From these standpoints the former procedure was preferred; however, the time required for the single run was quite lengthy, and an increase of 1/3 to 1/2 was not always possible. In practice the runs were split approximately equally between the alternative procedures.

Sampling and Analysis

The period for sampling and analysis began immediately after the final determination. The amount of condensate in each receiver was determined, and samples of the condensate, preheater contents, vaporizer contents, and shield contents were analyzed by density measurements.

The receivers were detached from the condensers, stoppered, removed from the ice-filled beakers, and dried. The receivers, which had tares of approximately 105 grams, were then weighed on a three-kilogram, chain-type, Seko balance with weights calibrated with a set of class S weights which possessed a National Bureau of Standards Certificate verifying their accuracy.

In spite of the fact that the condensers were cleaned thoroughly with chromic-acid cleaning solution and rinsed with distilled water before use, a few, small droplets of condensate clung to the inside of the condenser tubes at the end of determinations on mixtures which contained high concentrations of water. The droplets which remained in the tubes and which could not be "coaxed" down the tubes into the receivers by gentle tapping were swabbed out quantitatively. Two identical swabs, approximately 3/4 inch by 1-1/2 inches, cut from the same piece of filter paper were used. One piece was attached to a wire and used to absorb the droplets on the inside of one of the condensers, after which it was put into a tared weighing bottle which was weighed on an analytical balance; the other piece was used as tare on the weight pan of the balance. The net weight of the additional material, thus collected and measured, was added to the weight of the receiver contents. The maximum amount of material recovered in this fashion was 0.078 gram, which is approximately 0.2 per cent of the average amount of condensate of 33 grams. The average difference in weight in ten preliminary attempts to cut identical swabs amounted to only 0.002 gram.

After the receivers had been weighed, they were returned to the ice-filled beakers to again cool the condensate. Samples of the cold condensate were then transferred directly from the receivers to the 10-ml pycnometers.

The apparatus had to be partially shut down prior to taking the liquid samples. The vaporizer heater was turned off simultaneously with the closing of the valve in the vaporizer branch of the liquid line, as were the shield heater and the valve in the shield branch. It was necessary to continue the power to the vapor-line heaters until after the samples were taken in order to prevent the rich vapor from condensing and falling back into the containers, and thereby changing the composition of the contents. The main liquid-line valve was then closed, and one of the ice-filled sample coolers was attached to the open sampling valve. About 25 mls of the preheater liquid were drained through the sample cooler before the actual sample was taken in the 25-ml pycnometer. This sample cooler was then removed, and the second was attached. About 20 mls of liquid were drained from the shield line and the shield through the cooler before the actual sample was taken in one of the 10-ml pycnometers. After the coil of the sample cooler was drained, a similar procedure was follwed in taking the vaporizer sample, except that only about 15 mls were wasted before two successive samples were transferred to 10-ml and the 5-ml pycnometers.

The full pycnometers were suspended in the constant-temperature medium of a well agitated-water bath for approximately seven minutes. It was found in preliminary tests with a pycnometer which contained a

thermometer that only about five minutes were required for the contents to attain the same temperature as the bath. The temperature in the water bath was always higher than ambient temperature and was easily controlled to plus or minus 0.05 °C. The thermometer could be read to plus or minus 0.02 °C with the aid of a magnifying reader. As the pycnometers were removed from the water bath, each was touched quickly in ice water to contract the liquid in the capillary-perforated top and then wiped dry with absorbent, lintless paper. The pycnometers were weighed rapidly on a projectomatic-type analytical balance. Evaporation losses were quite small because of the contraction of the liquid down the capillary and away from the atmosphere and because of the rapid handling which was greatly facilitated by the rapidity with which approximately known weights could be determined on the projectomatic-type balance.

Density of the isopropyl alcohol-water mixtures was measured at 35.00 °C. Analysis was effected by use of the precise density-composition data at 35.00 °C of Langdon and Keyes.[38] Preliminary measurements of the density of nine carefully prepared mixtures of known composition, which were randomly distributed over the entire composition range of 0 to 100 per cent, showed an average deviation without regard to sign of only 0.08 mass per cent from the smoothed data presented by Langdon and Keyes.

Density of the acetone-water mixtures was measured at 25.00 °C. Preliminary measurements of the density of carefully prepared mixtures of known composition at 25.00 °C did not produce agreement with any single set of published density-composition data[26,62,69] over the

entire range of composition. Agreement within 0.1 mass per cent with the data of Thomas and McAllister[69] was observed in the composition ranges of 0 to 52 and 92 to 100 mass per cent acetone. However, these investigators covered the entire range of composition with only seven density points, which made interpolation for accurate analytical purposes quite impractical and uncertain. No set of the aforementioned, published data agrees over the entire range of composition with any of the other sets to closer than plus or minus 0.5 mass per cent. Although the density-composition measurements taken in this investigation were not completely in agreement with any published set, they were quite self-consistent and reproducible to less than plus or minus 0.2 mass per cent. Therefore, a density-composition curve at 25.00°C was produced for analytical purposes by measuring the density of 24 carefully prepared mixtures of known composition over the entire range of 0 to 100 per cent. The smoothed values of density at even values of composition are shown in Table XIX of Appendix E.

CALCULATIONS

Summary

The essence of all the calculations is contained in the equation

$$\text{Integral Isobaric Heat of Vaporization} = \frac{(\text{Power})(\text{Time})}{(\text{Mass of Condensate})} - \text{Corrective Terms} \qquad (75)$$

The first term on the right-hand side is referred to as the uncorrected latent heat. Of a number of possible corrective terms only the sensible-heat correction was found to be significant, and it averaged only 1.5 per cent of the uncorrected latent heat. A sample calculation which demonstrates the use of Equation (75) is presented in Appendix B. Tabular values of the important measured quantities used in the calculations for each mixture are shown in Appendix F.

The vapor-liquid equilibrium data were obtained directly from the corrected temperature measurements and from density measurements used in conjunction with density-composition data.

Uncorrected Latent Heat

The calculation of the uncorrected latent heat, the first term on the right-hand side of Equation (75), was carried out in three distinct steps. Firstly, the measurements of potential across the standard resistors, taken at various times during the determination, were used to calculate the instantaneous power consumption of the vaporizer heater. Secondly, these values of power were plotted versus time and the area under the power-time curve was calculated to determine

the total heat evolved by the vaporizer heater. Sample calculations which illustrate the first two steps are shown in Appendix B. Thirdly, the total heat evolved was divided by the mass of condensate collected during the determination and was multiplied by the proper conversion factor to arrive at the desired set of units.

Corrections

Of a number of possible corrective terms only the correction for the small amount of sensible heat supplied to the liquid was significant. The others were either eliminated by the design of the apparatus or were insignificant from the beginning.

The sensible-heat correction was required because the liquid was not delivered to the vaporizer exactly at its bubble-point temperature, but usually a few degrees lower. The corrective term was calculated from the equation

$$\text{Sensible-Heat Correction} = 0.981\ \bar{C}^{l}_{P,m}(t_{BP} - t_{In}) \qquad (76)$$

The factor 0.981 is a constant; its significance and origin is explained in a subsequent paragraph. $\bar{C}^{l}_{P,m}$ is the average specific heat of the liquid mixture between the temperatures, t_{BP} and t_{In}. Data on the specific heats of liquid mixtures near their bubble points are scarce, and for the mixtures studied in this investigation these data are nonexistent. Consequently, the available data for acetone-water mixtures at 25 and 40°C[36] were adjusted for use in Equation (76) in accordance with the temperature variance of the specific heats of the pure components[33,46,64] and with the observed temperature dependence of the

mixtures in the 25-40°C interval; the available data for isopropyl alcohol-water mixtures[14,56] were treated similarly with the aid of the pure-component data.[24,46] Fortunately, the average corrective term amounted to only 1.5 per cent of the uncorrected latent heat, so that an error as large as five per cent in the estimation of the specific heat of the mixture would introduce an error of only 0.075 per cent in the integral isobaric heat of vaporization. In Equation (76) t_{BP} is the bubble-point temperature of the mixture. This temperature was read from the bubble-point line on a temperature-composition diagram, which was obtained from the vapor-liquid equilibrium data taken over the entire composition range during this investigation. The inlet temperature, t_{In}, is an experimental quantity which was measured during each determination.

During the timed interval of a determination, material was withdrawn from the system into a receiver, thus causing a drop in the liquid level of all containers. This drop in level was quite small because of the large surface area and volume of the preheater. During the average fast-rate determination 33 grams, or approximately 40-mls, of material were withdrawn. The resulting drop in level was approximately 0.11 cm. In spite of the small magnitude of the drop an investigation of its significance is in order.

The drop in level means that during the timed interval of a determination slightly less liquid flowed into the vaporizer than was collected as condensate in the receiver. Thus, the sensible-heat corrective term should include the ratio of the mass of liquid which

flowed into the vaporizer during the interval to the mass of condensate collected during that time, because the vaporizer heater was not required to make up the full amount of sensible heat. This ratio of masses is actually dependent only upon the relative cross-sectional areas of the apparatus and is independent of the amount of material collected in a receiver during a determination. The essential items for the calculation of this ratio are shown in Equation (77).

$$\frac{\text{Liquid Entering Vaporizer}}{\text{Mass of Condensate}} = 1 - \frac{\text{Area of Vaporizer}}{\text{Area of Entire Apparatus}}$$

$$= 1 - \frac{7.06\ \text{cm}^2}{366.7\text{cm}^2} = 0.981 \qquad (77)$$

This factor appears in the sensible-heat correction, Equation (76).

When the liquid level fell in the vaporizer this volume, previously occupied by liquid, was filled by material which was vaporized but which was not accounted for in the condensate at the end of the determination. This correction to the mass of condensate involves the ratio of the density of the vapor to the density of the liquid, as well as the relative cross-sectional areas of the apparatus. The proper combination of these factors leads to a corrective term, which indicates that the measured mass of condensate should be increased by approximately 0.001 per cent. This amount, of course, is insignificant.

It was also possible that a falling liquid level could upset the steady-state operating condition. However, the fall of level actually involved was too slight to produce any significant effects. The constancy of the composition of the condensate, collected during consecutive determinations, experimentally verified this conclusion.

Evaporation of material from the receivers prior to the time at which they were weighed could involve a correction of the measured mass of condensate. The design of the receivers cut this loss to an insignificant fraction. Preliminary tests with 30 grams of acetone in each stoppered receiver showed the evaporation rate to be approximately 0.004 gram per hour at room temperature over a period of approximately one day. In actual practice the receivers were set in ice-filled beakers which further reduced the evaporation rate. The receivers were always weighed within 15 minutes after the termination of a run. Thus, the correction involved was insignificant.

The experimental runs were not conducted at a controlled pressure, but were conducted at the ambient pressure on a given day. The barometer readings were recorded several times during each run. The ambient pressure encountered during the entire series of runs ranged from 723.9 to 745.0 mm of mercury with approximately 90 per cent of the runs falling between 733 and 743 mm of mercury. The pressure variation of the heat of vaporization over this range is less than the experimental accuracy; however, the measured temperatures used in the vapor-liquid equilibrium data had to be corrected for the pressure differences.

Interpolation of the precise data of the National Bureau of Standards on the heat of vaporization of water[46] at the pressures extremes of 723.9 and 745.0 mm of mercury shows a difference of only 0.499 calorie per gram, or approximately 0.09 per cent of the heat of vaporization. The difference between the heat of vaporization of water at 760 mm of mercury and at the average pressure of 736.7 mm of mercury

is 0.1 per cent, which indicates that the data presented herein can be used at a pressure of 760 mm of mercury within the experimental accuracy.

It was desirable to correct the measured temperatures used in the vapor-liquid equilibrium data to a common pressure. A linear relationship between the logarithm of the pressure and reciprocal temperature was assumed for the small pressure range involved. The required slope for each mixture was obtained from a molal average of the slopes for the pure components, which were taken to be -2200 for water, -2300 for isopropyl alcohol, and -1630 for acetone. The units used were mm of mercury and °K. All measured temperatures were corrected to a pressure of 760 mm of mercury. The average correction amounted to approximately 0.8°C.

Effects of Flow Rate

Operation of the apparatus at a number of flow rates aided in the evaluation of the effectiveness of the thermal shielding and of the design of the vaporizer and its heater.

The few, remaining, small heat leaks, which were not eliminated by design, were detected by a variation in flow rate. With a given material in the apparatus heat leaks would be essentially constant with time and roughly independent of flow rate. Therefore, approximately the same quantity of heat would be lost in any given time interval, regardless of the flow rate. As a result, the greater the through-put (or flow rate), the less effect these heat leaks would have on the magnitude of the resulting heat of vaporization. At an infinite flow rate the effect would be infinitesimal.

The heats of vaporization of the three pure components were measured over approximately a 2.5-fold range of flow rates, and the results were plotted as a function of reciprocal flow rate. The curve obtained for water is shown in Figure 12 on page 102. An extrapolation of the data to the ordinate, $1/F = 0$, which corresponds to an infinite flow rate, results in an answer which is devoid of heat leaks. The unguided extrapolation of a curve is dependent on judgement and prejudice; therefore, the latent heats were plotted as a function of reciprocal flow rate to the third power, as shown in Figure 13 on page 102, which permitted a straight-line extrapolation. The equation of the line was determined by a least-squares fit of the data. Similar graphs for isopropyl alcohol and acetone are shown in Appendix E.

The fact that the observed heats of vaporization should be higher than the extrapolated one is rather easy to explain qualitatively. Consider the first term on the right-hand side of Equation (75). "Power" and "Time" are measured quantities unaffected by heat leaks, so that attention must be focused on the "Mass of Condensate." If the direction of heat flow is from the calorimeter toward the surroundings, as was the case in this investigation because all the pure components and mixtures had boiling points above ambient temperatures, then any small amount of heat which leaks out is unavailable for vaporizing material. As a result, the condensate which is actually collected and weighed is less than the amount which would be observed in the perfectly adiabatic system. The "Mass of Condensate" appears in the denominator of the equation; therefore, this less-than-true-value quantity produces a high latent heat.

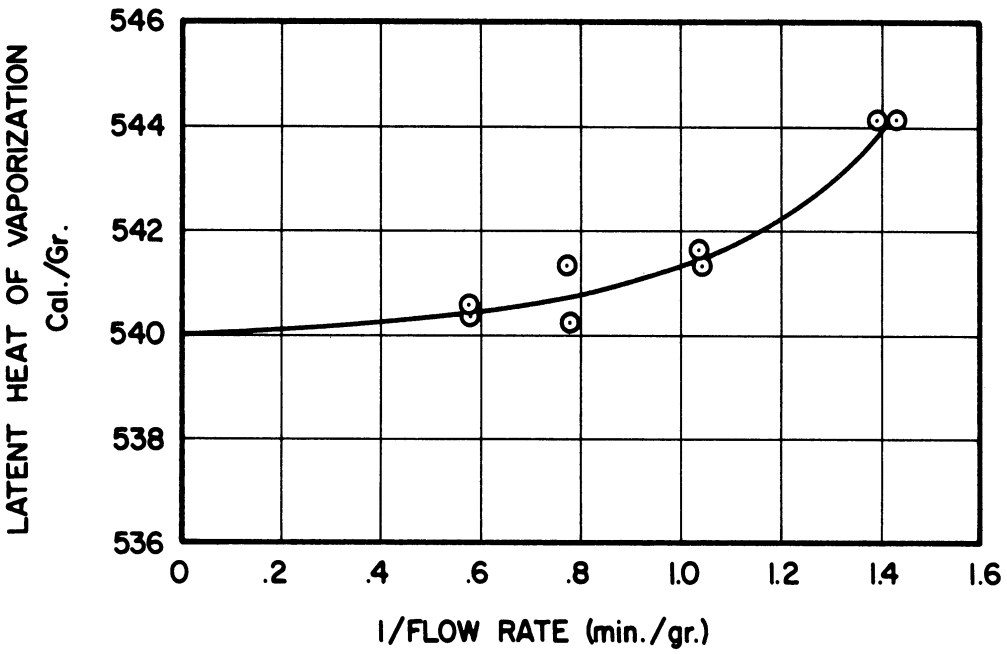

Figure 12. Heat of Vaporization of Water as a Function of the Reciprocal of the Flow Rate through the System.

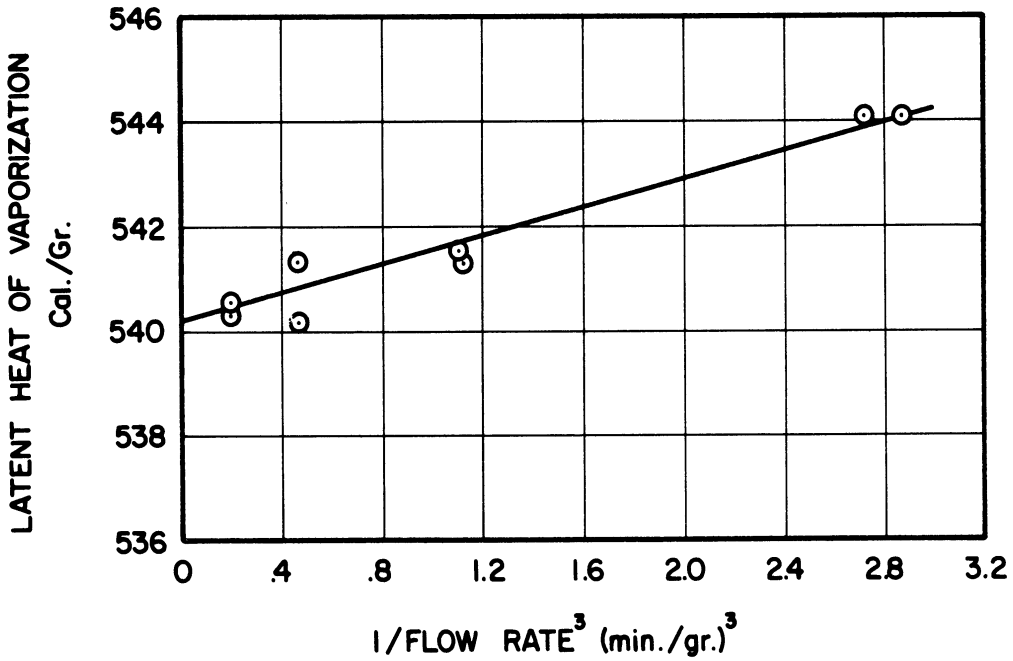

Figure 13. Heat of Vaporization of Water as a Function of the Reciprocal Flow Rate to the Third Power.

The foregoing discussions were developed on the basis that the heat leaks were constant with time and independent of flow rate. Actually, the design of the equipment was such that an even more favorable situation was encountered in practice; in that, one of the individual heat leaks was reduced by faster flow rates. The flow of the liquid through the capillary at the bottom of the vaporizer was in the opposite direction to the heat flow along the capillary. As a result the faster flow rates tended to lessen this individual heat leak, as well as reduce the overall effect of heat leaks.

The difference between the heat of vaporization at rates greater than 1.5 grams per minute and the extrapolated values was small enough so that data taken in the range of 1.5 grams per minute were adequate. It was, therefore, unnecessary to determine the entire curve for every composition; however, a run was made as a check at a slower rate, approximately 1.0 grams per minute, for nearly every composition. A flow rate of approximately 1.5 grams per minute happens to correspond to the 120-ml-per-hour rate recommended by Canjar and Lonergan[5] for use in obtaining vapor-liquid equilibria in circulating - type stills.

The variation in flow rate also helped establish the absence of entrainment or of mechanical ejection of liquid by any mode from the vaporizer. Observations during preliminary experiments with a number of vaporizer heaters, used under a variety of conditions, showed that the bare-wire heater of the design used in this investigation could be used to vaporize liquids at the contemplated power levels without ejecting any liquid from the vaporizer onto the externally heated vapor lines. These observations were borne out by the operation of the apparatus at

a number of flow rates. Any liquid thrown out of the vaporizer and subsequently vaporized by externally applied heat would have increased the observed mass of condensate over what it would have been under proper operating conditions. The mass of condensate appears in the denominator of Equation (75), and therefore the resulting latent heat would have been low. As the flow rate, which was controlled by the power supplied to the vaporizer heater, was increased the amount of liquid ejected from the vaporizer would have increased markedly, and the curve shown in Figure 12 on page 102 would have dropped off sharply with increasing flow rate, rather than level off and approach a nearly horizontal tangent as is actually shown.

Estimate of Accuracy

Estimates of the errors involved in the individual measurements and the results of the calibration data on pure components suggest that a conservative estimate of accuracy for the integral isobaric heat of vaporization is plus or minus 0.3 per cent. The compositions were measured to plus or minus 0.1 mass per cent for the isopropyl alcohol-water mixtures and to plus or minus 0.2 mass per cent for the acetone-water mixtures. The temperatures used in the vapor-liquid equilibrium data were measured to plus or minus 0.1 °C; the inlet temperature to the vaporizer was good to plus or minus 0.2 °C.

The errors associated with measurements involved in the integral isobaric heat of vaporization can be broken down into four groups - those associated with (1) power, (2) time, (3) mass of condensate, and (4) sensible-heat correction. The stated accuracy of the standard

resistors and the expected accuracy of the potentiometer measurements suggest that the power, including any uncertainties in the interpolations on the power-time curve, is correct to plus or minus 0.07 per cent. Errors in the time measurement, which include possible errors of approximately 0.2 second for starting and stopping the timer at the correct instant, totaled not more than 0.5 second, or about 0.04 per cent, for the average interval of 22 minutes. The mass of condensate was accurate to approximately plus or minus 0.04 gram, which amounts to about 0.12 per cent for the average collection of 33 grams. The specific-heat corrective term averaged only 1.5 per cent of the latent heat, so that errors as large as 7 per cent in the specific heat and the temperature difference would have caused only about 0.10 per cent error in the latent heat. If all of the errors affected a latent-heat determination at the same time and in the same direction, the magnitude of the total error would be approximately 0.33 per cent.

EXPERIMENTAL DATA AND RESULTS

Summary

Data in tabular and graphical form on both the integral isobaric heats of vaporization and vapor-liquid equilibria for atmospheric pressure are presented in this section for the isopropyl alcohol-water and acetone-water binaries. These data have been used to accurately derive enthalpy-concentration diagrams. Heats of mixing in the liquid phase and differential heats of condensation have also been calculated using these data as starting points.

A graph to facilitate the conversion between mass and mole per cent is shown in Appendix E on page 177 for convenience.

Calibration Data

The reliability of the apparatus, which, although designed specifically for use with mixtures, could be used successfully with pure materials, was checked by determining the heat of vaporization of the pure components of each mixture and comparing the values obtained with recent experimental data reported in the literature. The pure-component heats of vaporization were taken over a range of flow rates and extrapolated to infinite flow rate as indicated in the section entitled "Effects of Flow Rate." Table II on page 107 shows the data obtained and the comparison with recent experimental data reported in the literature.

TABLE II

HEAT OF VAPORIZATION OF THE PURE COMPONENTS

Component	Heat of Vap. (cal/g) this Investigation	Temp. (°C)	Heat of Vap. (cal/g) from Literature	Ref.
Acetone	119.9	55.2	120.0	(50)
Isopropanol	159.3	81.6	159.6	(79)
Water	540.2	99.3	540.13	(46)

Integral-Isobaric-Heat-of-Vaporization Data

The data for the isopropyl alcohol-water binary at atmospheric pressure are presented in Table III on page 112 and in Figures 14 and 15 on pages 108 and 109 in the form of integral isobaric heat of vaporization as a function of composition. Figure 14 shows the data on a mass basis. The curve on Figure 15, which is on a mole basis, was obtained simply by conversion of the units of the curve shown on Figure 14 from a mass basis to a mole basis. Smoothed values of heat of vaporization at even values of composition have been read from a large plot of Figure 14 and are presented in Appendix E in Table XV.

The data for the acetone-water binary are presented in the identical fashion as the isopropyl alochol-water data. Table IV on page 112 and Figures 16 and 17 on pages 110 and 111 show the heat of vaporization data. The smoothed values of heat of vaporization at even compositions are shown in Appendix E in Table XVI. Figures 15 and 17 have ordinates which are nearly ten times larger than those of Figures 14 and 16. Due to this magnification the exact inflections of the curves on Figures 15 and 17 are not to be taken too literally.

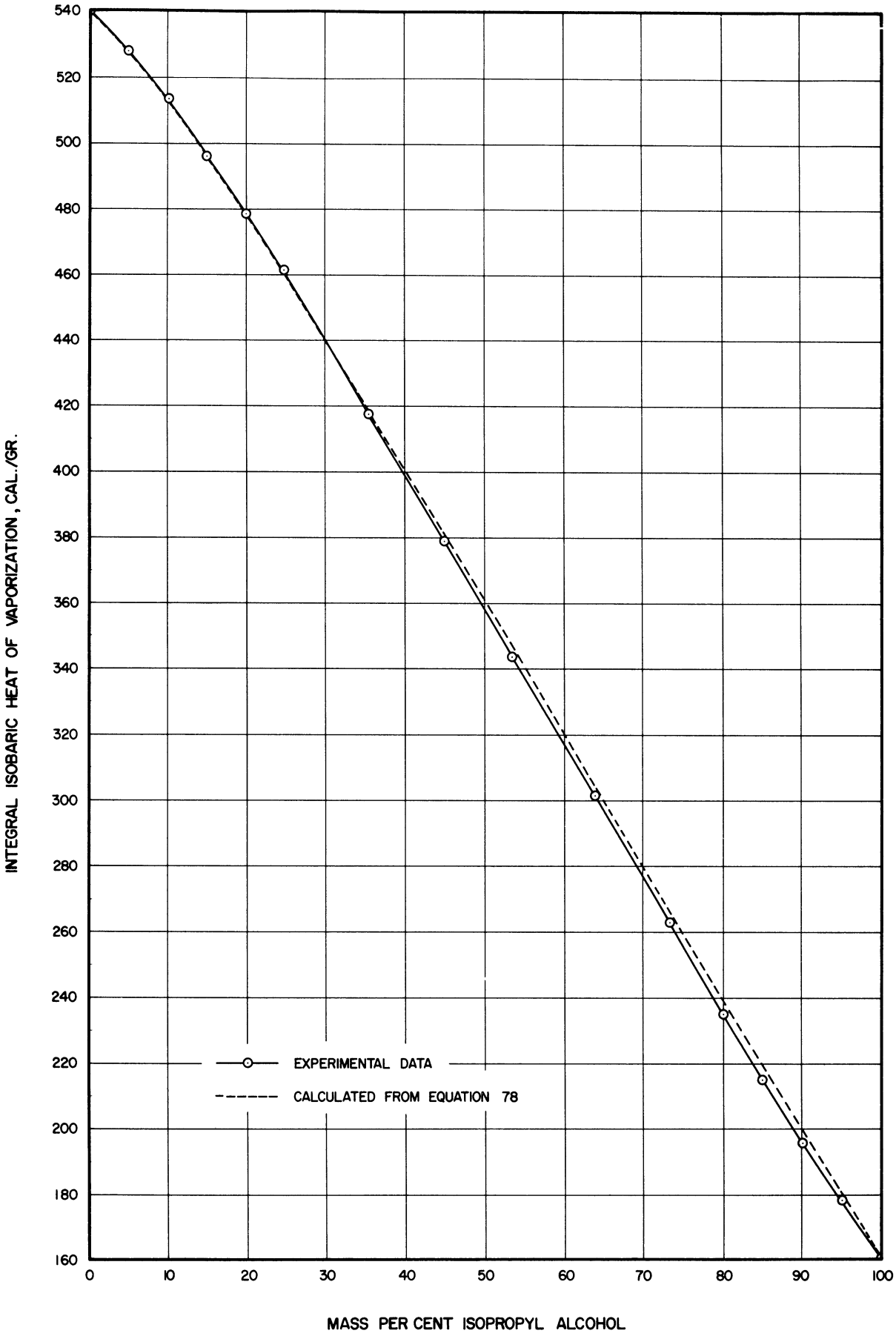

Figure 14. Integral Isobaric Heat of Vaporization of Isopropyl Alcohol-Water Mixtures on a Mass Basis. (Atmospheric Pressure)

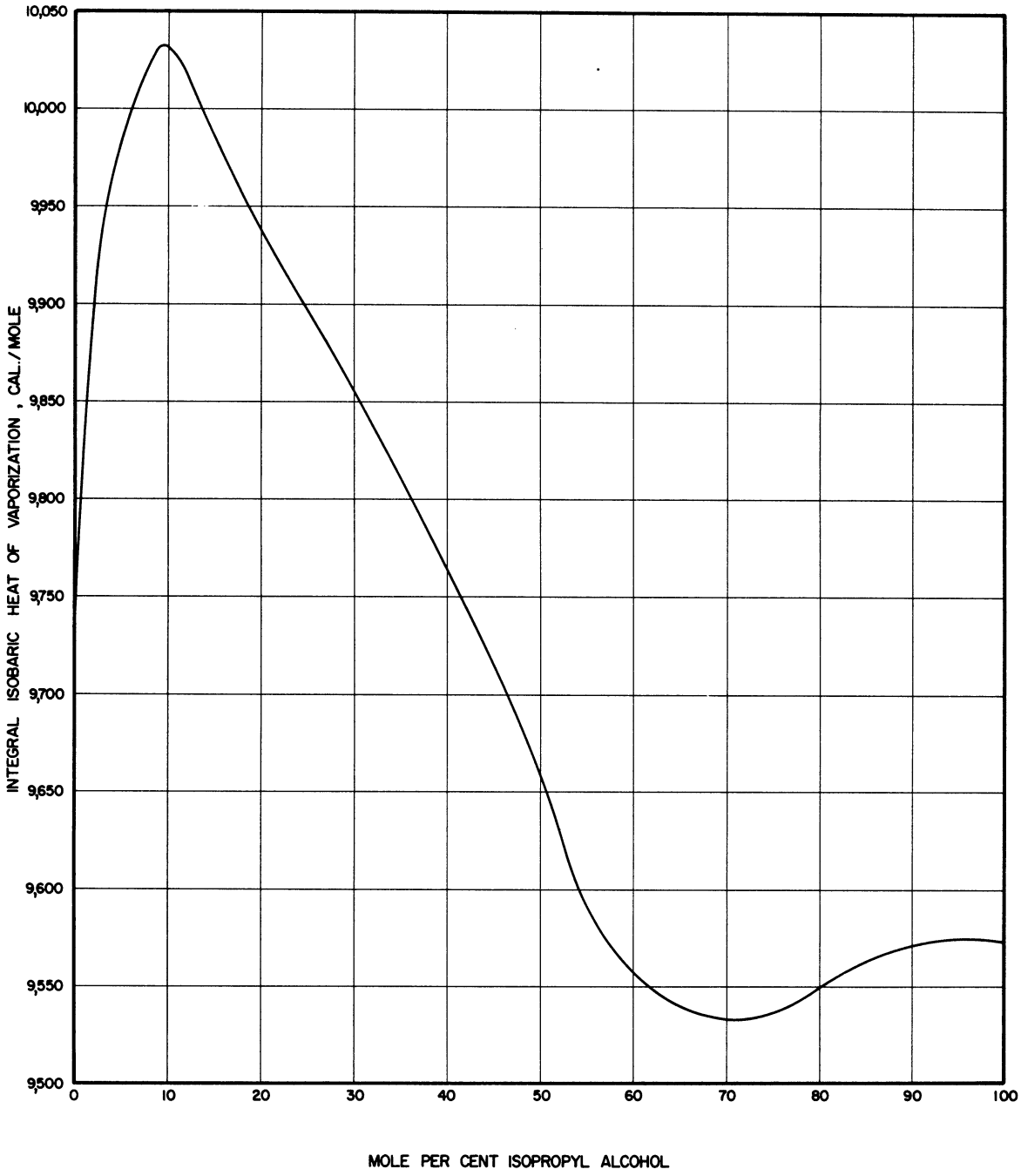

Figure 15. Integral Isobaric Heat of Vaporization of Isopropyl Alcohol-Water Mixtures on a Mole Basis. (Curve derived from Figure 14)(Atmospheric Pressure)

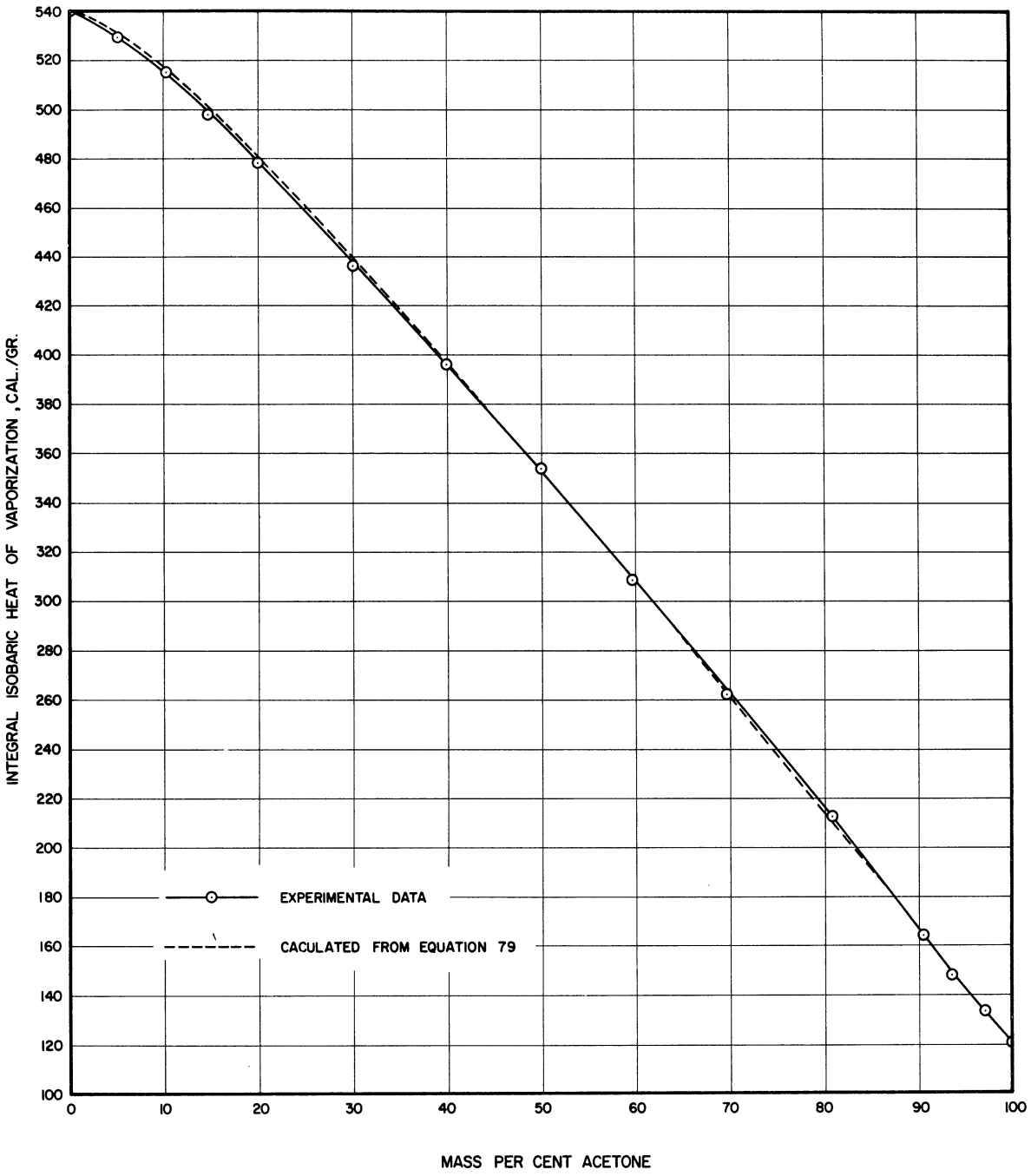

Figure 16. Integral Isobaric Heat of Vaporization of Acetone-Water Mixtures on a Mass Basis. (Atmospheric Pressure)

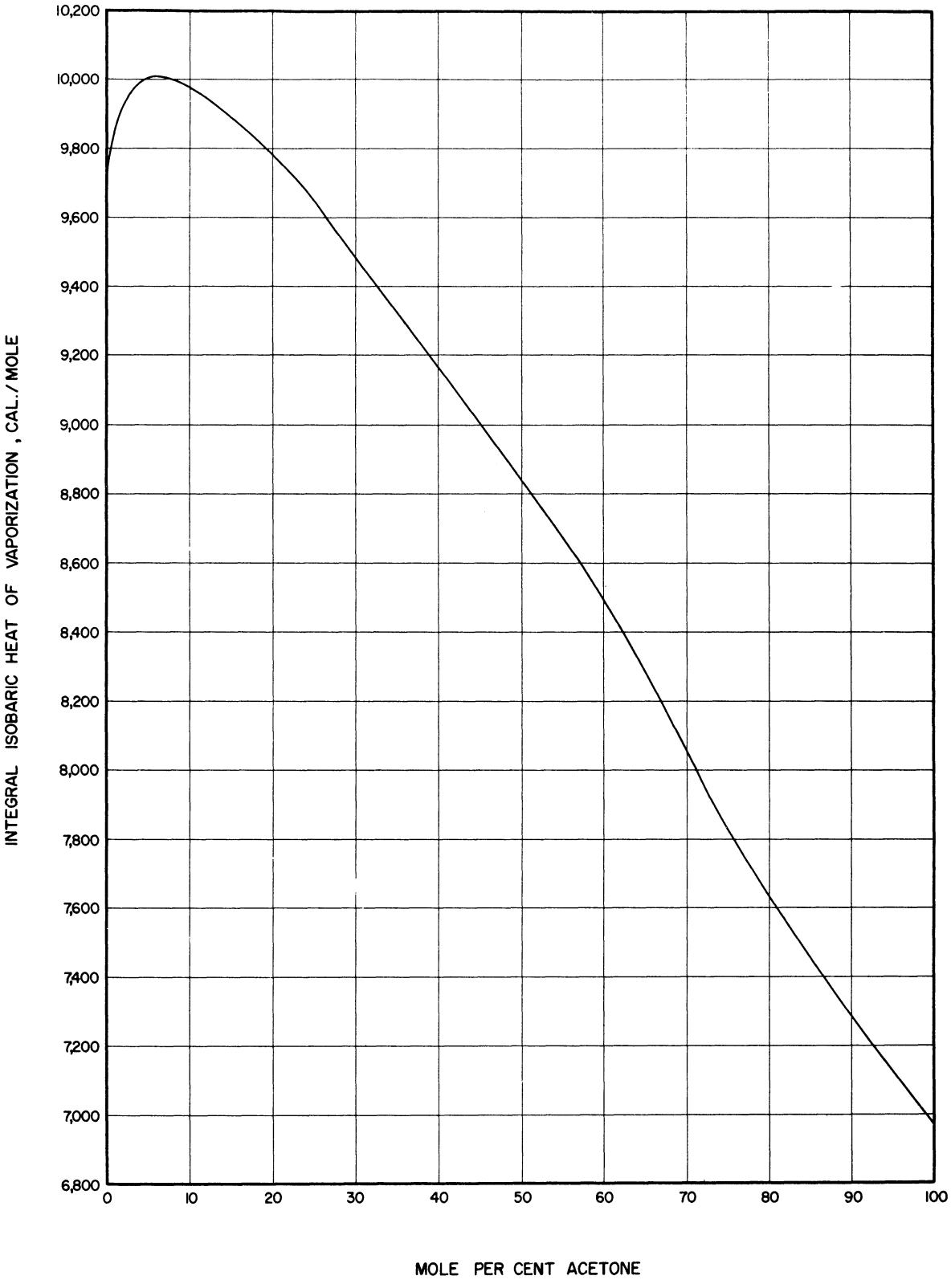

Figure 17. Integral Isobaric Heat of Vaporization of Acetone-Water Mixtures on a Mole Basis. (Curve derived from Figure 16) (Atmospheric Pressure)

TABLE III

INTEGRAL ISOBARIC HEAT OF VAPORIZATION - ISOPROPYL ALCOHOL-WATER

Atmospheric Pressure			
Mass Pct. Isopropanol	Mole Pct. Isopropanol	Heat of Vap. (cal/g)	Heat of Vap. (cal/mole)
0	0	540.2	9732
5.1	1.6	528.0	9869
10.2	3.3	513.5	9964
15.1	5.1	495.7	9982
19.9	6.9	478.3	9991
24.7	9.0	461.4	10054
35.4	14.1	417.2	9976
44.9	19.6	378.9	9953
53.4	25.6	343.4	9879
63.9	34.7	301.3	9828
73.3	45.2	262.9	9726
80.0	54.5	234.4	9607
85.0	62.9	214.6	9523
90.2	73.4	195.1	9527
94.9	84.8	178.2	9564
100.0	100.0	159.3	9573

TABLE IV

INTEGRAL ISOBARIC HEAT OF VAPORIZATION - ACETONE-WATER

Atmospheric Pressure			
Mass Pct. Acetone	Mole Pct. Acetone	Heat of Vap. (cal/g)	Heat of Vap. (cal/mole)
0	0	540.2	9732
5.2	1.7	529.1	9929
10.3	3.4	514.6	9982
14.9	5.2	498.1	9998
20.2	7.3	478.0	10005
30.2	11.8	436.2	9923
40.2	17.3	395.9	9873
50.1	23.8	353.9	9745
59.8	31.6	308.2	9449
69.7	41.6	262.1	9091
80.8	56.6	212.5	8653
90.5	74.7	164.4	7883
93.4	81.5	148.0	7496
97.0	90.9	132.9	7235
100.0	100.0	119.9	6964

The data for both binaries were correlated very well by the equation developed in a previous section entitled "The Enthalpy-Temperature-Diagram Approach."

$$\lambda_P = z_j L_{j,T_1} + z_k L_{k,T_1} + (z_j \overline{C}^{\circ}_{P,j} + z_k \overline{C}^{\circ}_{P,k})(T_2 - T_1) \qquad (34)$$

Neither Edmister's[16] equation nor the modification thereof which was suggested in the section entitled "Application of Equilibrium-K Values" were successful in correlating the integral-isobaric-heat-of-vaporization data. A sample calculation demonstrating the use of these equations is shown in Appendix D on page 167. For the isopropyl alcohol-water system Equation (34) in terms of temperatures in degrees centigrade and mass fractions becomes

$$\begin{aligned}\lambda_P = {} & Z_I[194.3 - 0.425t_1] + Z_W[599.8 - 0.600t_1] \\ & + \{Z_I[0.341 + 0.00100\,\tfrac{1}{2}(t_1 + t_2) - 0.000\,0006\,\tfrac{1}{4}(t_1 + t_2)^2] \\ & + Z_W[0.438 + 0.000125\,\tfrac{1}{2}(t_1 + t_2)]\}\{t_2 - t_1\} \qquad (78)\end{aligned}$$

For the acetone-water system it is

$$\begin{aligned}\lambda_P = {} & Z_A[134.4 - 0.262t_1] + Z_W[599.6 - 0.598t_1] \\ & + \{Z_A[0.283 + 0.00083\,\tfrac{1}{2}(t_1 + t_2) - 0.000\,0005\,\tfrac{1}{4}(t_1 + t_2)^2] \\ & + Z_W[0.438 + 0.000125\,\tfrac{1}{2}(t_1 + t_2)\}\{t_2 - t_1\} \qquad (79)\end{aligned}$$

The resulting integral isobaric heats of vaporization are in units of calories per gram.

The integral isobaric heats of vaporization calculated from Equations (78) and (79) at even values of composition are presented in Appendix E in Tables XV and XVI and are shown in this section by the dashed curves on Figures 14 and 16. The maximum deviation between the predicted and smoothed experimental values for the isopropyl alochol-water binary occurs at 85.0 mass per cent isopropyl alcohol and amounts to 2.0 per cent of the latent heat. The average deviation without regard to sign is 0.8 per cent. For acetone-water the maximum deviation occurs at 25.0 mass per cent acetone and amounts of 0.5 per cent of the latent heat. The average deviation disregarding sign is 0.3 per cent.

Whereas it would be desirable to write Equations (78) and (79) with only composition terms on the right-hand side, to do so would produce cumbersome expressions which would be difficult to handle. The bubble-point and dew-point temperatures in the equations would have to be replaced by the appropriate temperature-composition relationships, which in themselves are quite complex and which, in fact, do not usually lend themselves to explicit expressions of temperature as a function of composition. As a result, computations with the correlating equations were performed in conjunction with vapor-liquid equilibrium data in the form of temperature-composition diagrams. A sample calculation showing the steps required for the prediction of the integral isobaric heat of vaporization of an aqueous mixture of 50 mass per cent acetone is shown in Appendix C.

Vapor-Liquid Equilibrium Data

The vapor-liquid equilibrium data for the isopropyl alcohol-water binary at atmospheric pressure are shown in the form of a

temperature-composition diagram in Figure 18 on page 116 and in the form of a y - x diagram in Figure 19 on page 117. After smooth curves had been drawn on these figures for the data obtained in this investigation, two sets of experimental data recently reported in the literature[4,80] were plotted on the figures for comparative purposes. Smoothed values read from a large plot of Figure 18 at even values of composition are shown in Appendix E in Table XVII. The following tabular values supplement the data shown on the figures.

TABLE V

VAPOR-LIQUID EQUILIBRIUM DATA - ISOPROPYL ALCOHOL-WATER

Atmospheric Pressure

Isopropanol in Vapor		Isopropanol in Liquid		Temp.
Mass Pct.	Mole Pct.	Mass. Pct.	Mole Pct.	(°C)
0	0	0	0	100.0
5.1	1.6	0.2	0.06	99.8
10.2	3.3	0.6	0.18	99.3
15.1	5.1	0.8	0.24	98.8
19.9	6.9	1.1	0.3	98.3
24.7	9.0	1.4	0.4	97.7
35.4	14.1	2.6	0.8	96.2
44.9	19.6	3.8	1.2	94.3
53.4	25.6	5.4	1.7	92.3
63.9	34.7	8.0	2.5	89.1
73.3	45.2	14.0	4.7	85.3
80.0	54.5	48.0	21.7	81.5
85.0	62.9	81.1	56.3	80.7
90.2	73.4	91.2	75.7	80.6
94.9	84.8	96.0	87.8	81.2
100.0	100.0	100.0	100.0	82.4

The data for acetone-water are presented in identical fashion as the data for isopropyl alcohol-water. Table VI on page 120 and Figures 20 and 21 on pages 118 and 119 show the vapor-liquid equilibrium

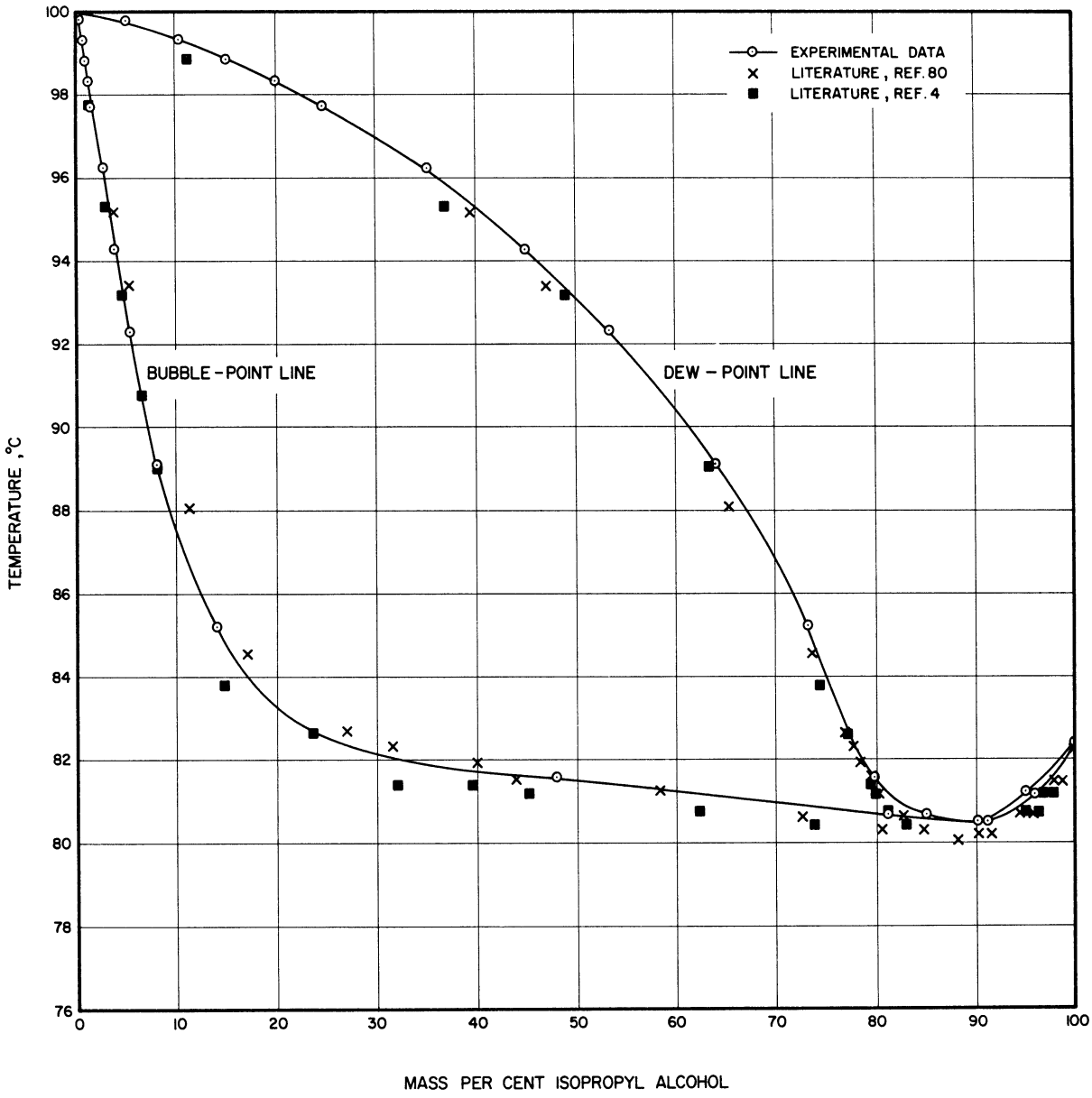

Figure 18. Temperature-Composition Diagram for Isopropyl Alcohol-Water. (Atmospheric Pressure)

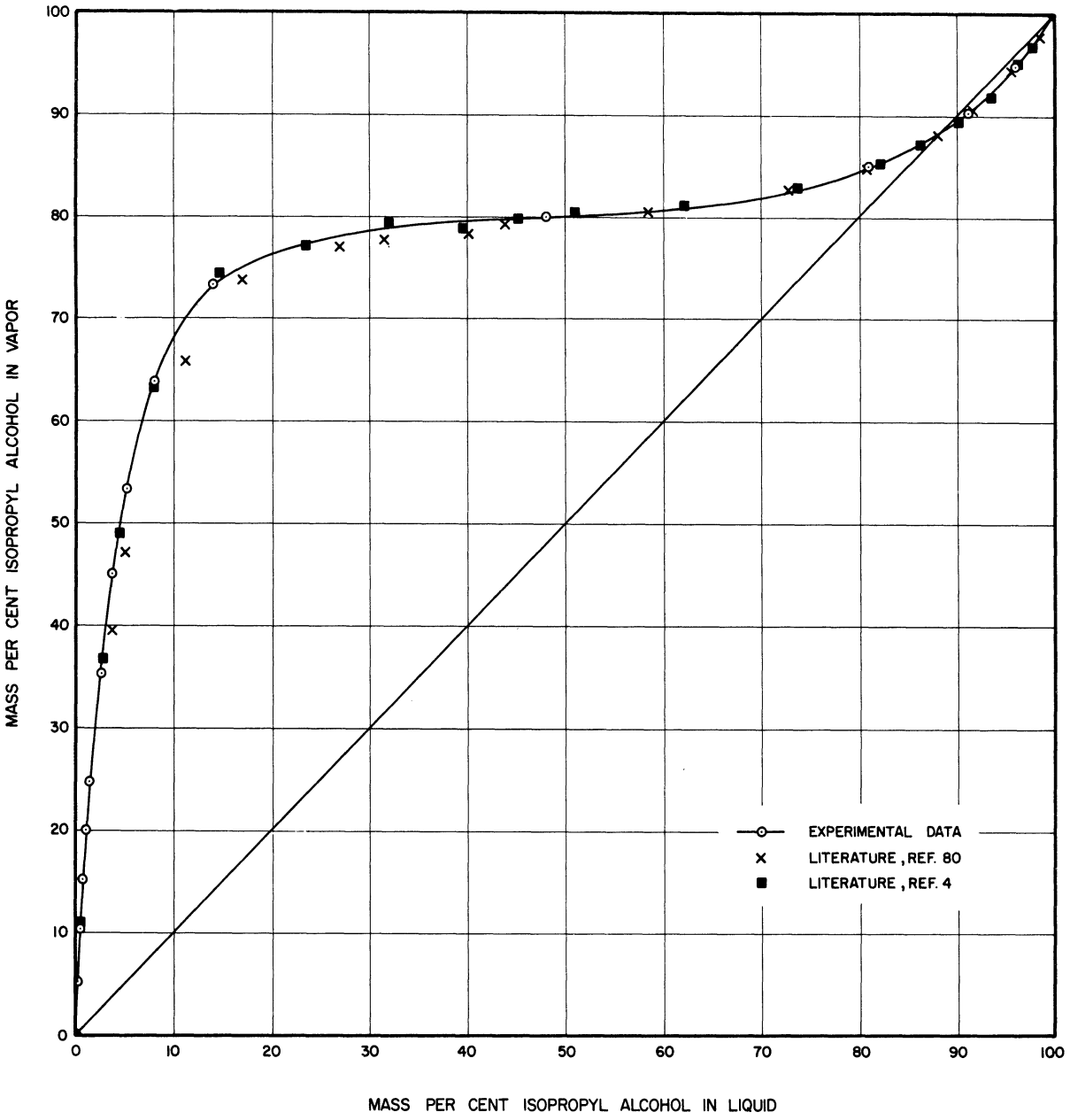

Figure 19. y - x Equilibrium Diagram for Isopropyl Alcohol-Water. (Atmospheric Pressure)

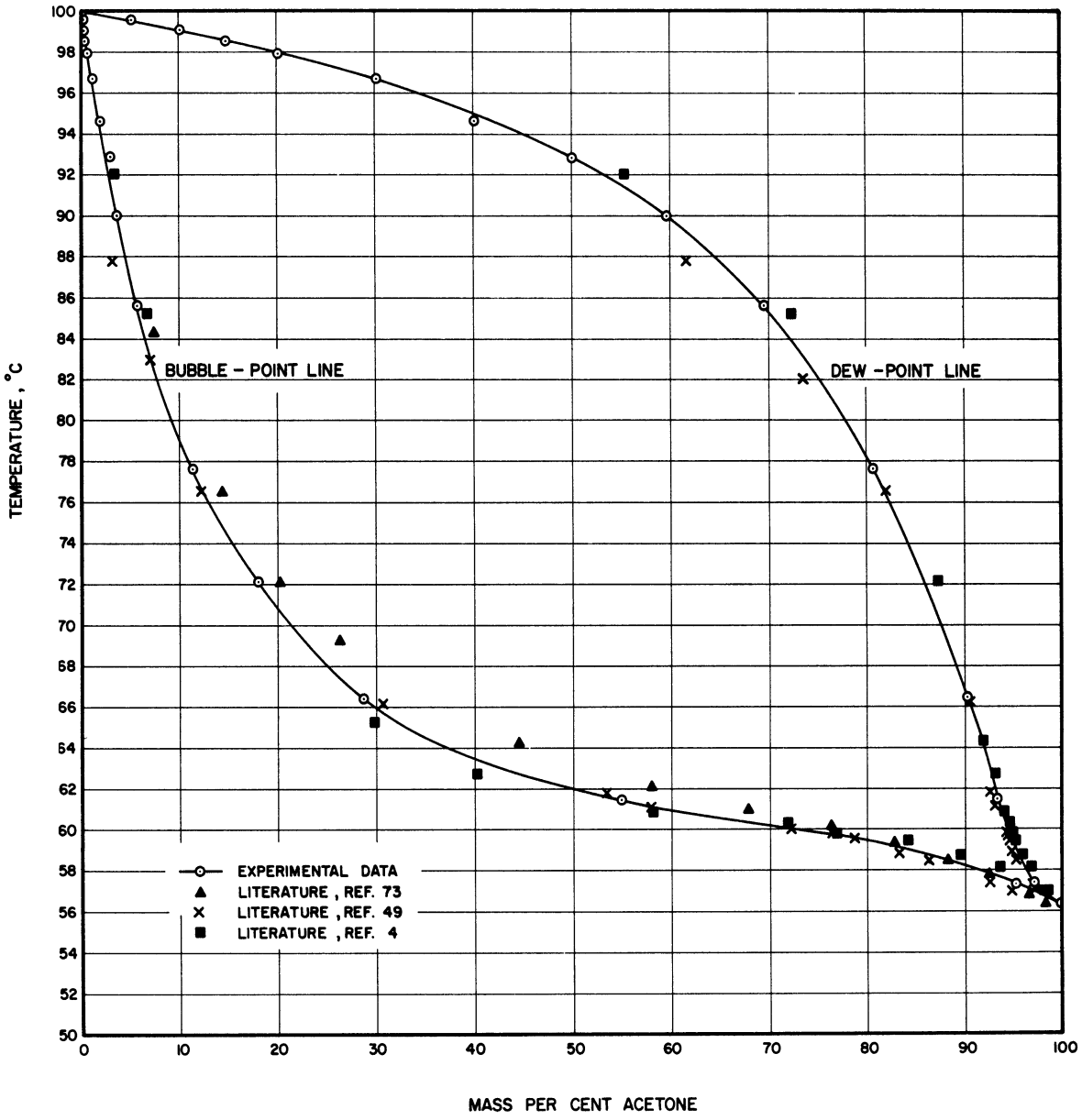

Figure 20. Temperature-Composition Diagram for Acetone-Water. (Atmospheric Pressure)

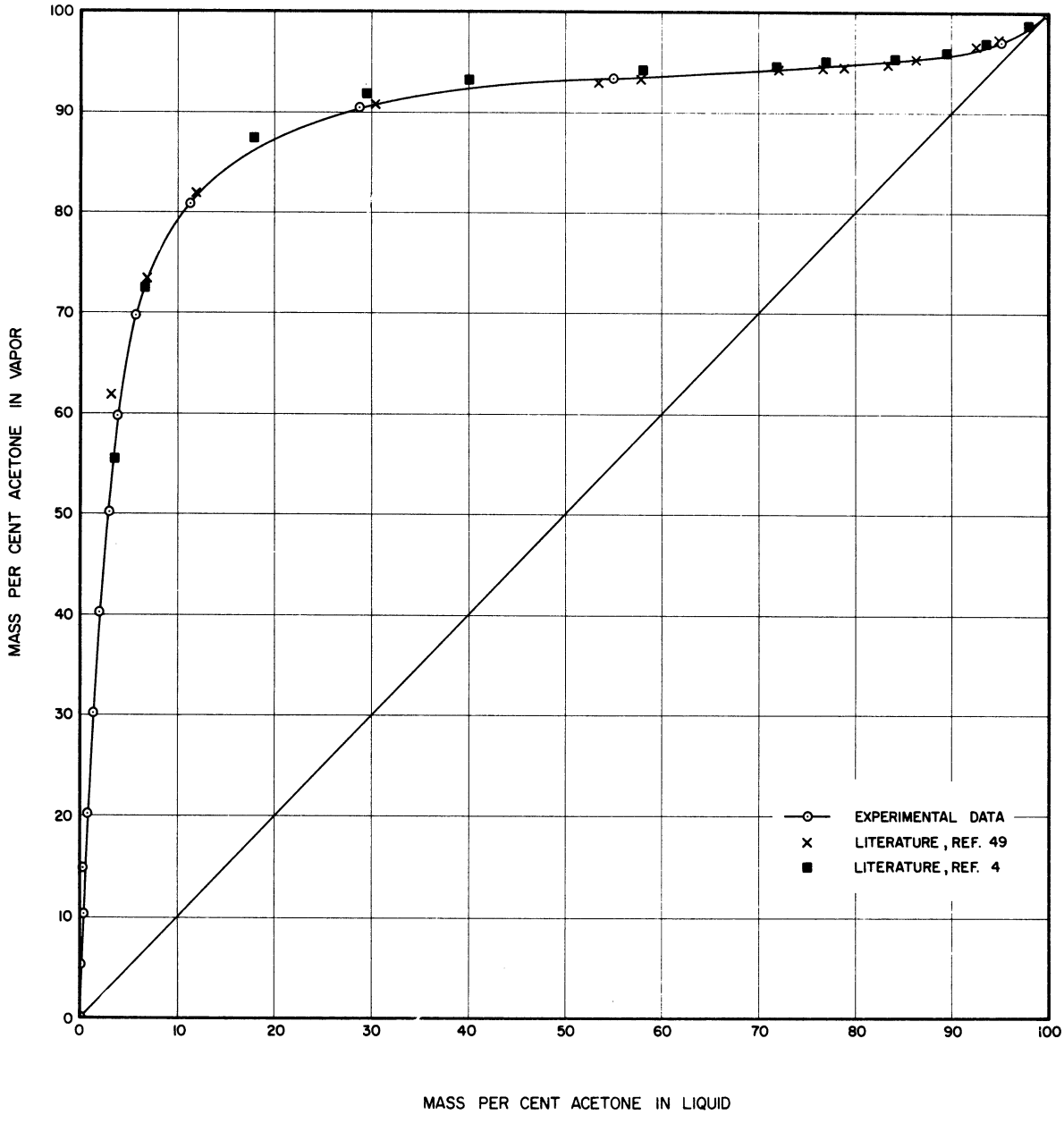

Figure 21. y - x Equilibrium Diagram for Acetone-Water. (Atmospheric Pressure)

data. Three sets of recent experimental data from the literature[4,49,73] have been plotted on these figures for comparative purposes. Smoothed values are shown in Appendix E in Table XVIII.

TABLE VI

VAPOR-LIQUID EQUILIBRIUM DATA - ACETONE-WATER

Atmosphere Pressure

Acetone in Vapor		Acetone in Liquid		Temp.
Mass Pct.	Mole Pct.	Mass Pct.	Mole Pct.	(°C)
0	0	0	0	100.0
5.2	1.7	0.1	0.03	99.5
10.3	3.4	0.3	0.09	99.0
14.9	5.2	0.3	0.09	98.5
20.2	7.3	0.7	0.2	97.9
30.2	11.8	1.4	0.4	96.6
40.2	17.3	2.0	0.6	94.6
50.1	23.8	3.1	1.0	92.8
59.8	31.6	3.8	1.2	90.0
69.7	41.6	5.8	1.9	85.5
80.8	56.6	11.4	3.8	77.6
90.5	74.7	28.9	11.2	66.4
93.4	81.5	55.1	27.6	61.4
97.0	90.9	95.3	86.3	57.1
100.0	100.0	100.0	100.0	56.2

The vapor-liquid equilibria were correlated by both the Redlich-Kister[55] equation, which is of the form

$$\log \frac{\gamma_j}{\gamma_k} = B(x_k - x_j) + C(6x_jx_k - 1) + D(x_k - x_j)(1 - 8x_jx_k) + \ldots \quad (80)$$

and by a modified version of the Redlich-Kister equation proposed by Chao[6], which is of the form

$$\log \frac{\gamma_j}{\gamma_k} = a + b(x_k - x_j) + c(6x_jx_k - 1) + d(x_k - x_j)(1 - 8x_jx_k) + \ldots \quad (81)$$

where γ_j and γ_k are the activity coefficients in the liquid phase of components j and k, respectively; x_j and x_k are mole fractions in the liquid phase of components j and k, respectively; and letters a and b through d in both upper case and lower case are constants used to fit the data. The Redlich-Kister equation embodies the Duhem relationship[15] and inherently forces the data, when plotted on a graph of log γ_j/γ_k versus the mole fraction of j in the liquid, to fit a curve which bounds with the ordinates, $x_j = 0$ and $x_j = 1$, areas of equal magnitude above and below the abscissa, log $\gamma_j/\gamma_k = 0$. However, many experimental vapor-liquid equilibrium data do not in fact fall in such a pattern. Chao used this observation as a basis to modify the Redlich-Kister equation. The modified equation includes an additional term, "a", which is a constant and has a magnitude equal to the net area; that is, the area above the abscissa, log $\gamma_j/\gamma_k = 0$, minus the area below. As a result, the modified equation is more complex than the Redlich-Kister equation. The acceptability of this added complexity must be judged for each system on the basis of the improvement in the correlation.

Graphs of log γ_I/γ_W versus the mole fraction of isopropyl alcohol in the liquid for the isopropyl alcohol-water binary are shown in Figure 22 on page 124. A similar graph for the acetone-water system is shown in Figure 24 on page 126. Because of the primary objective of this investigation, which was to obtain integral-isobaric-heat-of-vaporization data, it was necessary to evenly distribute the vapor compositions of the runs over the entire range of concentrations. Therefore, due to the relative volatilities many of these runs involved quite low concentrations of the more volatile component in the equilibrium

liquid. As a result, much of the vapor-liquid equilibrium data, when plotted as a function of mole fraction of the more volatile component in the liquid, appears, as in Figures 22 and 24, near the left-hand ordinate.

The data for both binaries were fit to the correlating equations by the method of least squares. Only a few of the points at very low concentrations of the more volatile component were used in the correlations in order to avoid weighting the results excessively in favor of the low concentrations. The curves representing both equations are shown on each graph. For the isopropyl alcohol-water system the Redlich-Kister equation is

$$\log \gamma_I/\gamma_W = 0.661(x_W-x_I) - 0.323(6x_Ix_W-1) + 0.114(x_W-x_I)(1-8x_Ix_W)$$

$$= 1.098 - 4.400\ x_I + 4.674\ x_I^2 - 1.824\ x_I^3 \qquad (82)$$

and the modified equation is

$$\log \gamma_I/\gamma_W = 0.019 + 0.669(x_W-x_I) - 0.305(6x_Ix_W-1)$$
$$+ 0.103(x_W-x_I)(1-8x_Ix_W)$$
$$= 1.096 - 4.198\ x_I + 4.302\ x_I^2 - 1.648\ x_I^3 \qquad (83)$$

For the acetone-water system the Redlich-Kister equation is

$$\log \gamma_A/\gamma_W = 0.825(x_W - x_A) - 0.127(6x_Ax_W - 1)$$

$$= 0.952 - 2.410\ x_A + 0.760\ x_A^2 \qquad (84)$$

and the modified equation is

$$\log \gamma_A/\gamma_W = - 0.046 + 0.840(x_W - x_A) - 0.173(6x_Ax_W - 1)$$

$$= 0.966 - 2.716\ x_A + 1.036\ x_A^2 \qquad (85)$$

The average deviations, without regard to sign, between the values of the term $\log \gamma_I/\gamma_W$ calculated from Equations (82) and (83) and those obtained directly from experimental data were 0.020 for the Redlich-Kister equation and 0.021 for the modified equation. For the acetone-water system these deviations amounted to 0.033 for Equation (84) and 0.023 for Equation (85). The small differences in the average deviations leave little to choose between the correlations on that basis; the Redlich-Kister equations are, on the whole, simpler. The shortage of the data at high concentrations of the more volatile component, however, reduces the rigidity of the evaluation of the two correlations.

Figures 23 and 25 on pages 125 and 127 show the individual γ's - γ_I, γ_A, and γ_W - plotted as a function of the mole fraction of the more volatile component in the liquid for the isopropyl alcohol-water system and the acetone-water system, respectively. The curves drawn on these figures represent the equations for the individual γ's which can be developed by combining the relationship

$$x_j \log \gamma_j + x_k \log \gamma_k = x_jx_k[B + C(x_j-x_k) + D(x_j-x_k)^2 + \ldots] \qquad (86)$$

with either the Redlich-Kister equation or Chao's modified version. Equation (86) was developed during the derivation of the Redlich-Kister equation.(55) The individual γ's are, therefore, consistent

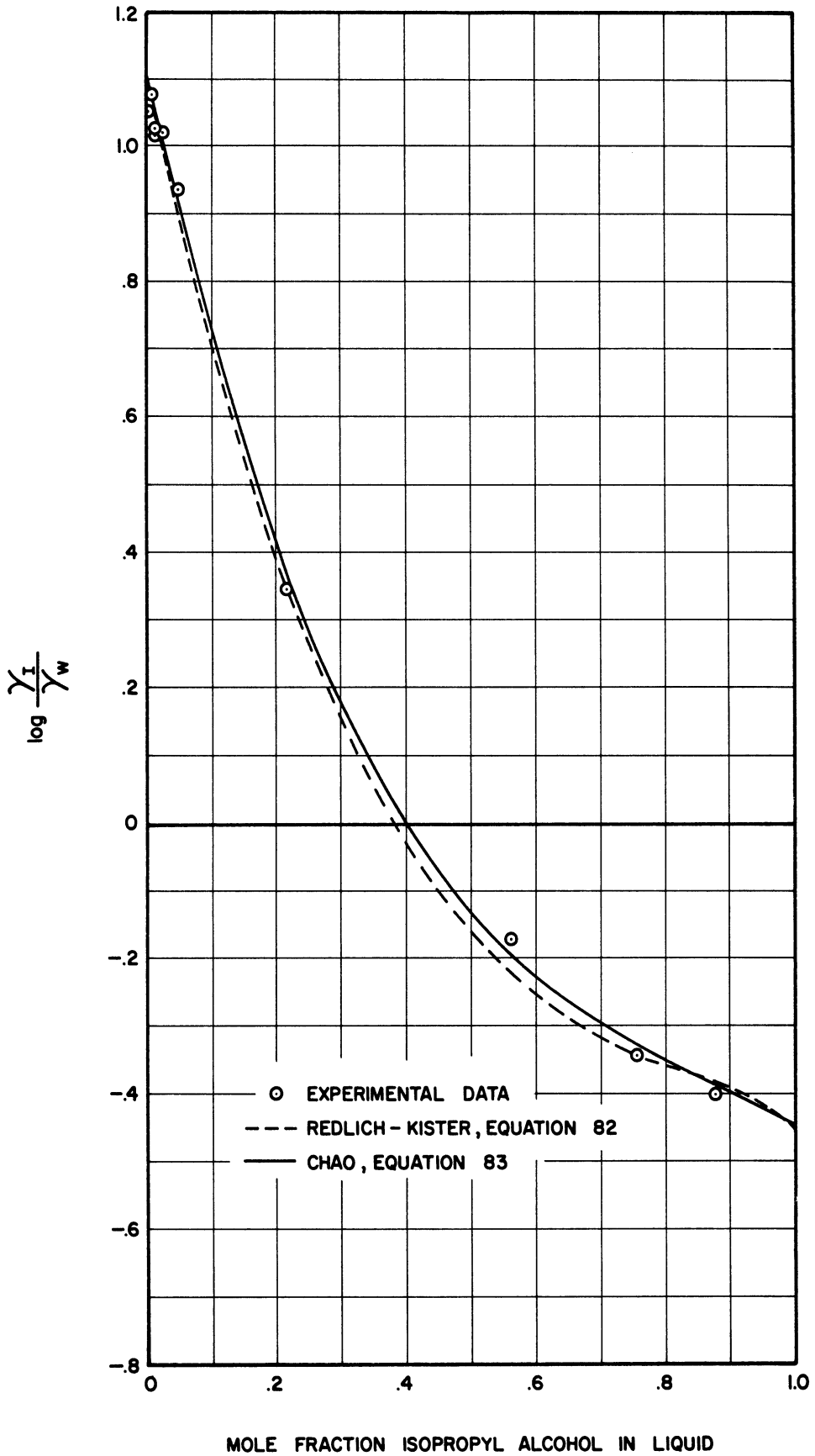

Figure 22. Log of the Ratio of Activity Coefficients Versus Concentration for Isopropyl Alcohol-Water.

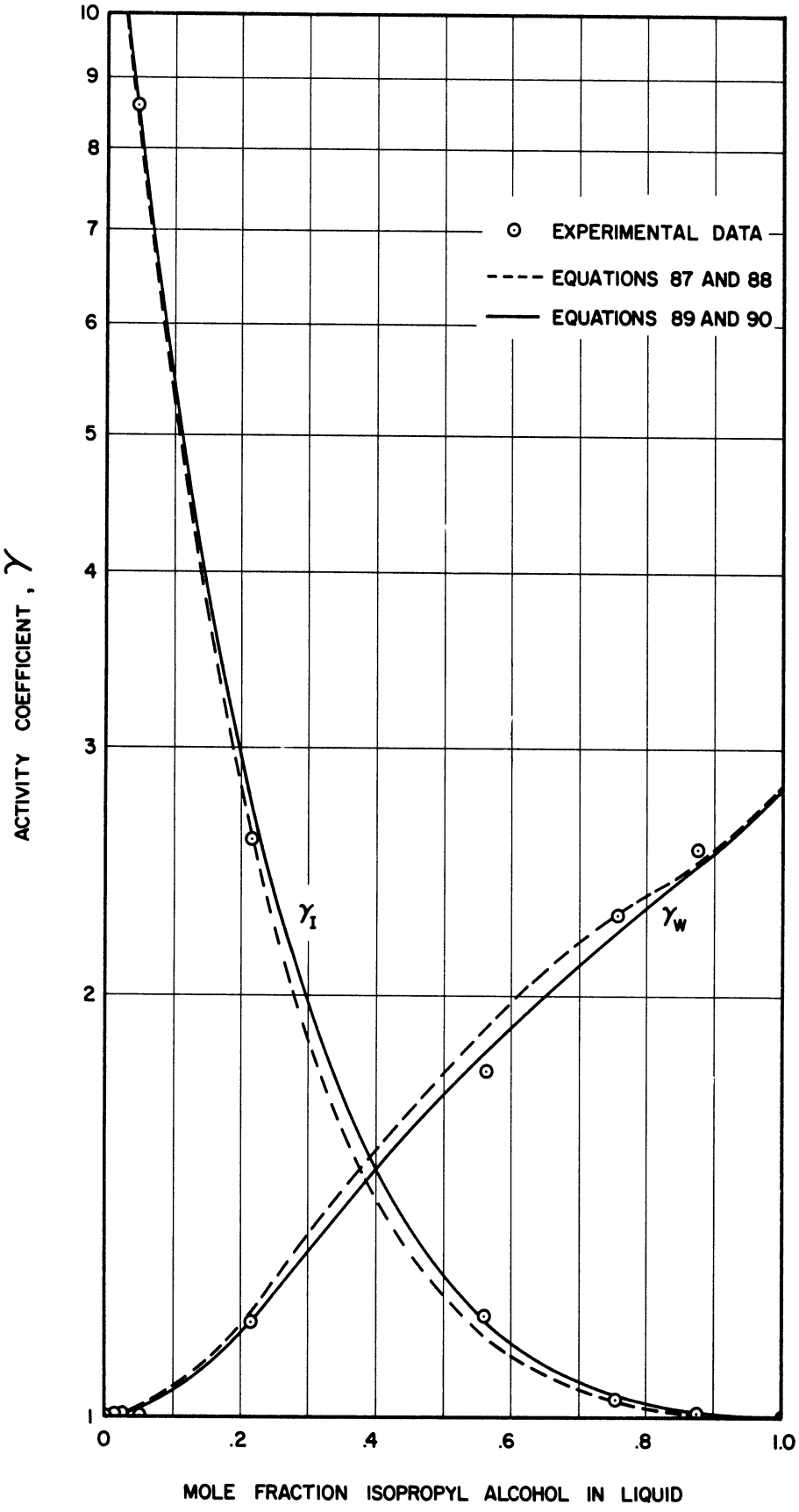

Figure 23. Individual Activity Coefficients Versus Concentration for Isopropyl Alcohol-Water.

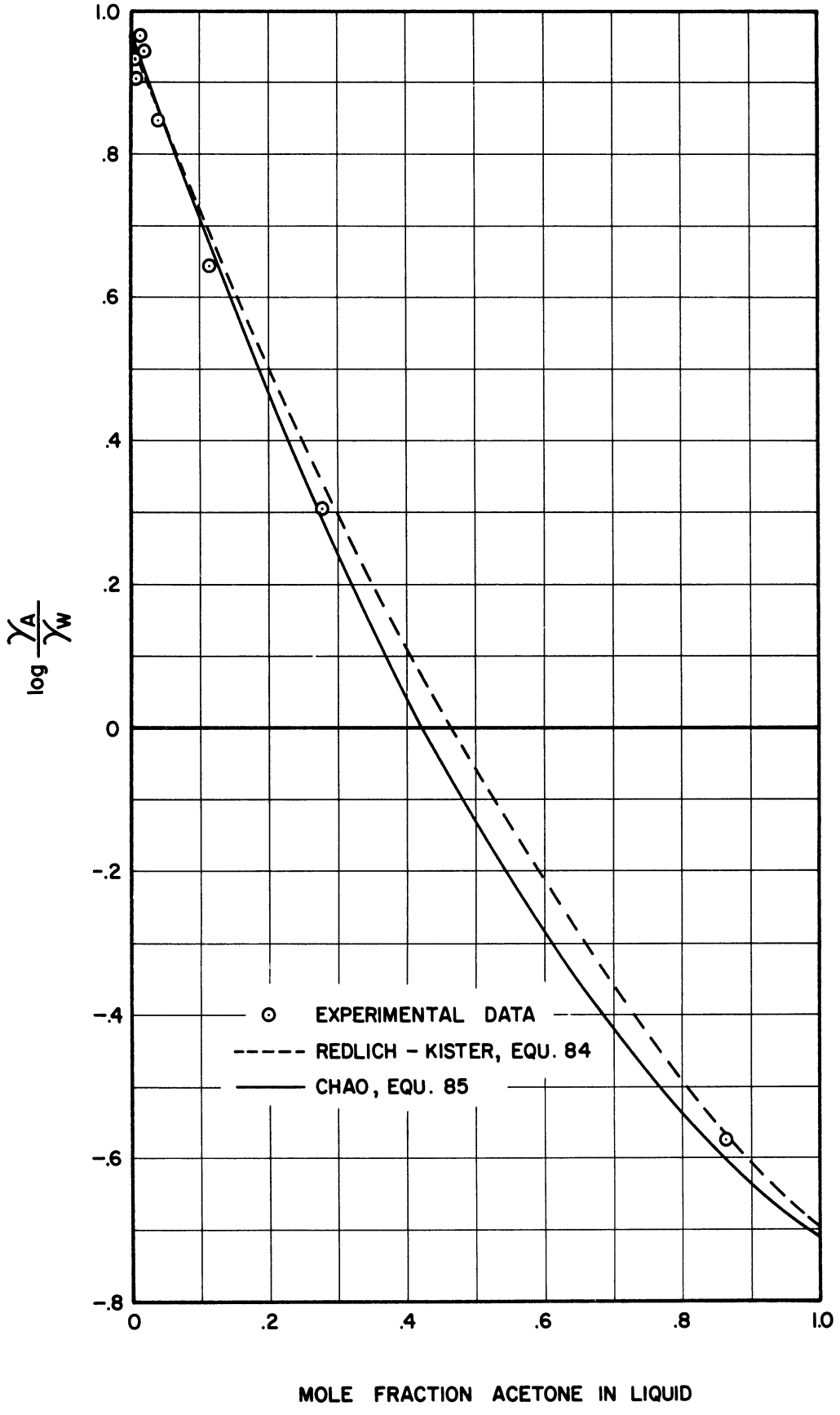

Figure 24. Log of the Ratio of Activity Coefficients Versus Concentration for Acetone-Water.

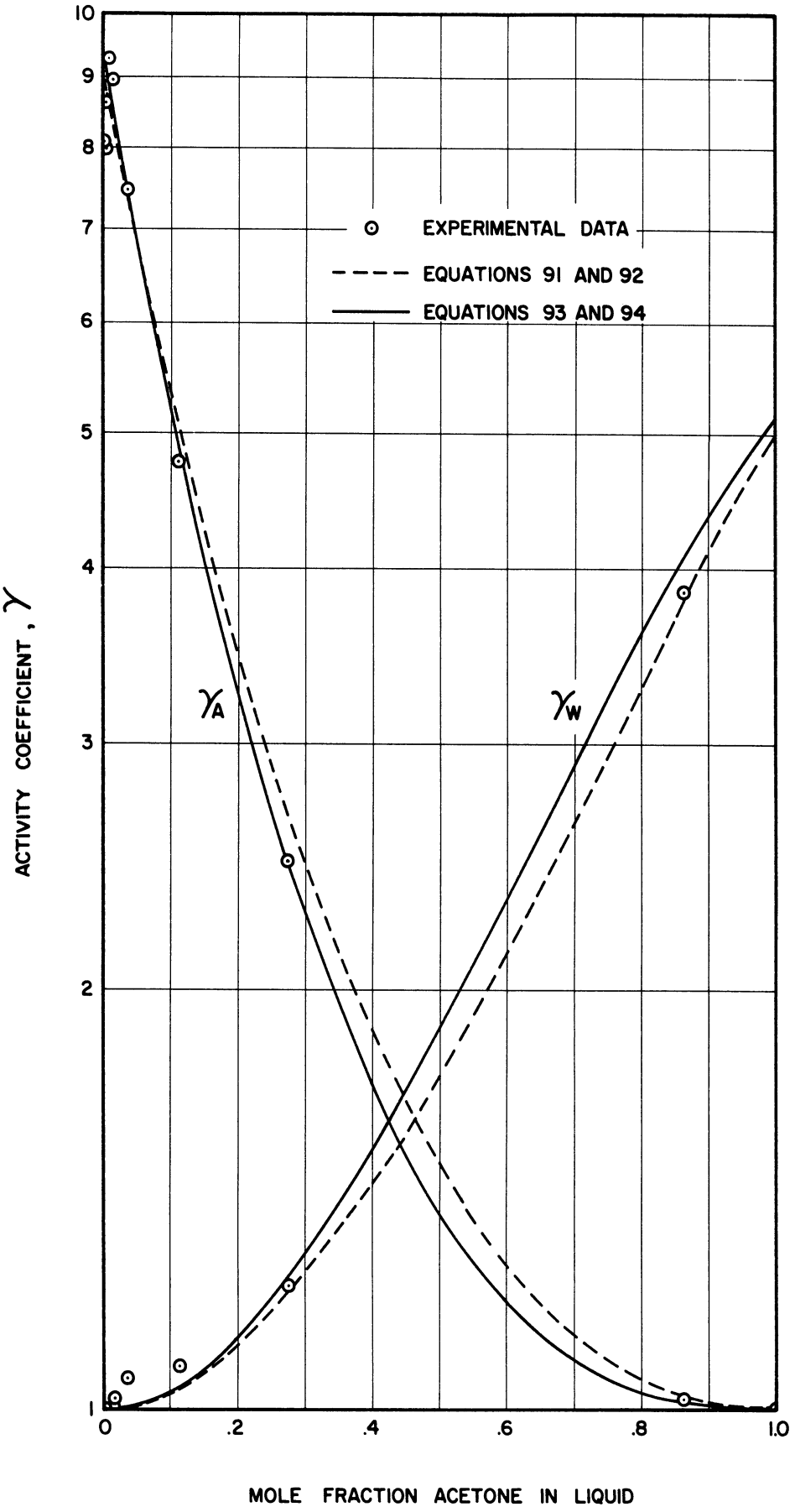

Figure 25. Individual Activity Coefficients Versus Concentration for Acetone-Water.

with the correlating equations. For the isopropyl alcohol-water system the individual γ's as obtained from the Redlich-Kister equation are

$$\log \gamma_I = x_W^2[0.661 + 0.323(1 - 4x_I) - 0.114(x_I - x_W)(1 - 6x_I)]$$

$$= 1.098 - 4.400\, x_I + 6.874\, x_I^2 - 4.940\, x_I^3 + 1.368\, x_I^4 \qquad (87)$$

$$\log \gamma_W = x_I^2[0.661 - 0.323(1 - 4x_W) + 0.114(x_I - x_W)(1 - 6x_W)]$$

$$= 2.200\, x_I^2 - 3.116\, x_I^3 + 1.368\, x_I^4 \qquad (88)$$

and as given by the modified equation are

$$\log \gamma_I = x_I x_W[0.661 - 0.323(x_I - x_W) + 0.114(x_I - x_W)^2] + x_W[0.019$$

$$+ 0.669(x_W - x_I) - 0.305(6x_I x_W - 1) + 0.103(x_W - x_I)(1 - 8x_I x_W)]$$

$$= 1.096 - 4.196\, x_I + 6.300\, x_I^2 - 4.392\, x_I^3 + 1.192\, x_I^4 \qquad (89)$$

$$\log \gamma_W = x_I x_W[0.661 - 0.323(x_I - x_W) + 0.114(x_I - x_W)^2] - x_I[0.019$$

$$+ 0.669(x_W - x_I) - 0.305(6x_I x_W - 1) + 0.103(x_W - x_I)(1 - 8x_I x_W)]$$

$$= 0.002\, x_I + 1.998\, x_I^2 - 2.744\, x_I^3 + 1.192\, x_I^4 \qquad (90)$$

For the acetone-water system the individual γ's as obtained from the Redlich-Kister equation are

$$\log \gamma_A = x_W^2[0.825 + 0.127(1 - 4x_A)]$$

$$= 0.952 - 2.412\, x_A + 1.968\, x_A^2 - 0.508\, x_A^3 \qquad (91)$$

$$\log \gamma_W = x_A^2[0.825 - 0.127(1 - 4x_W)]$$

$$= 1.206\ x_A^2 - 0.508\ x_A^3 \qquad (92)$$

and as given by the modified equation are

$$\log \gamma_A = x_A x_W[0.825 - 0.127(x_A - x_W)] + x_W[-0.046 + 0.840(x_W - x_A)$$

$$- 0.173(6x_A x_W - 1)]$$

$$= 0.967 - 2.733\ x_A + 2.550\ x_A^2 - 0.784\ x_A^3 \qquad (93)$$

$$\log \gamma_W = x_A x_W[0.825 - 0.127(x_A - x_W)] - x_A[-0.046 + 0.840(x_W - x_A)$$

$$- 0.173(6x_A x_W - 1)]$$

$$= -0.015\ x_A + 1.512\ x_A^2 - 0.784\ x_A^3 \qquad (94)$$

Enthalpy-Concentration Diagrams

The integral-isobaric-heat-of-vaporization data have been used for the accurate construction of enthalpy-concentration diagrams for the two systems studied in this investigation. The diagrams are for atmospheric pressure, and the reference points for the enthalpies ($\underline{H}$=0) were taken to be the pure liquids at 0°C under atmospheric pressure. Tabular values of the saturated-vapor and saturated-liquid enthalpies, as well as a few values in the superheated-vapor and subcooled-liquid regions, support the graphs presented herein.

The first step in the construction of the diagrams required the enthalpy-temperature relationships for both pure components. For

the liquid phase the equation

$$\underline{H}_i^l = \int_0^{t_{bp}} C_{P,i}^l \, dt \qquad (95)$$

was evaluated for a number of temperatures up to the boiling point of the pure component. The specific-heat data required by Equation (95) were taken from the literature.[24,33,46,64] The experimentally determined heat of vaporization of the pure component was added to the enthalpy of the liquid at the boiling point to obtain the enthalpy of the vapor at the boiling point. For the vapor phase the equation

$$\underline{H}_i^v = \underline{H}_i^{sat.v.} + \int_{t_{bp}}^{t} C_{P,i}^v \, dt \qquad (96)$$

was evaluated for a number of temperatures above the boiling point. The specific-heat data required by Equation (96) for the pure components at atmospheric pressure were taken from the literature.[34,50,60] For water and isopropyl alcohol it was also necessary to evaluate Equation (96) at temperatures below the boiling point. A completely rigorous treatment would require the evaluation of the enthalpy change which would accompany an isothermal expansion of the saturated vapor to a pressure sufficiently low so that the temperature (below the normal boiling point) at which the enthalpy was being evaluated would be the saturation temperature. Near atmospheric pressure and over the small pressure ranges involved the pressure effect on enthalpy can be neglected safely. Thus, Equation (96) was used for the evaluation of enthalpies with a temperature either above or below the normal boiling point, as desired, for the upper limit on the integral.

The enthalpy of a given mixture in its saturated-vapor state was evaluated by (1) determining its dew-point temperature from the experimental vapor-liquid equilibrium data, (2) determining the enthalpies at that temperature of both pure components from the enthalpy-temperature relationships in the vapor state, and (3) combining the pure component enthalpies according to the proportions of each component in the mixture. The final step involves an assumption of zero heat of mixing in the vapor phase, which is a satisfactory assumption at atmospheric pressure. A series of such calculations for a number of concentrations established the curve of saturated-vapor enthalpy versus concentration.

The enthalpies of the mixtures in the superheated-vapor range were obtained by combining the pure-component enthalpies at the temperature of interest according to the concentration of each component in the mixture.

The saturated-liquid enthalpy of a given mixture was calculated by subtracting the experimental integral isobaric heat of vaporization from the enthalpy of the saturated vapor for that mixture. A series of such calculations established the curve of saturated-liquid enthalpy versus concentration.

The enthalpies in the subcooled-liquid region were calculated by application of the equation

$$\underline{H}^{l} = \underline{H}^{sat.l.} + \int_{t_{BP}}^{t} C_{P,m}^{l}\, dt \qquad (97)$$

where $C_{P,m}^{l}$ is the specific heat of the liquid mixture in question. No specific-heat data near the bubble points are available in the literature

for the mixtures studied in this investigation. Consequently, the available data for acetone-water mixtures[36] and isopropyl alcohol-water mixtures[14,56] at lower temperatures were adjusted for use at the higher temperatures, pursuant to the observed temperature variation of the mixtures over lower temperature intervals and the temperature variation of the pure-component specific heats.[24,33,46,64] These estimates are, therefore, reflected directly in the enthalpies given for the subcooled-liquid region.

The enthalpy-concentration diagram on a mole basis for the isopropyl alcohol-water binary at atmospheric pressure is shown in Figure 26 on page 133. Note the interruption of the ordinate. The experimental vapor-liquid equilibrium data were added to the diagram in the form of constant-temperature tie lines, which connect points on the saturated-liquid line with corresponding equilibrium points on the saturated-vapor line. Values of the enthalpy of saturated vapor and saturated liquid and a few values in the superheated-vapor and subcooled-liquid regions are listed for even values of concentration in Table VII on page 135.

Similar information for the acetone-water binary are shown in identical fashion in Figure 27 on page 134 and in Table VIII on page 135.

The integral heat of mixing for a given mixture in the liquid phase at its bubble point temperature can be determined by subtracting from the saturated-liquid enthalpy, the molal-average enthalpy of the pure components at that temperature. The accuracy of the heat of mixing derived by this procedure suffers from the fact that a small answer

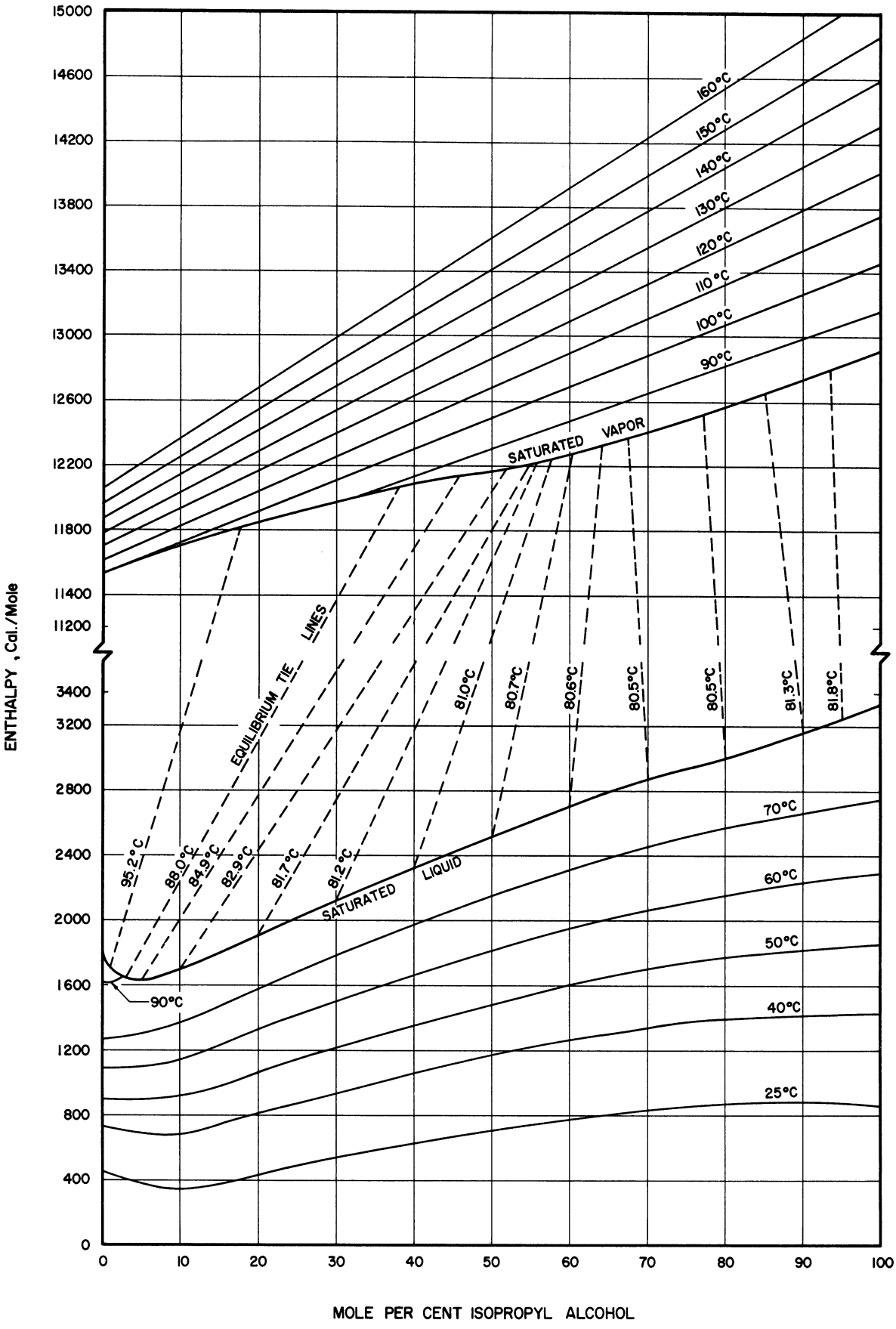

Figure 26. Enthalpy-Concentration Diagram for Isopropyl Alcohol-Water (Atmospheric Pressure)($\underline{H}$ = 0 for pure liquids at 0°C)

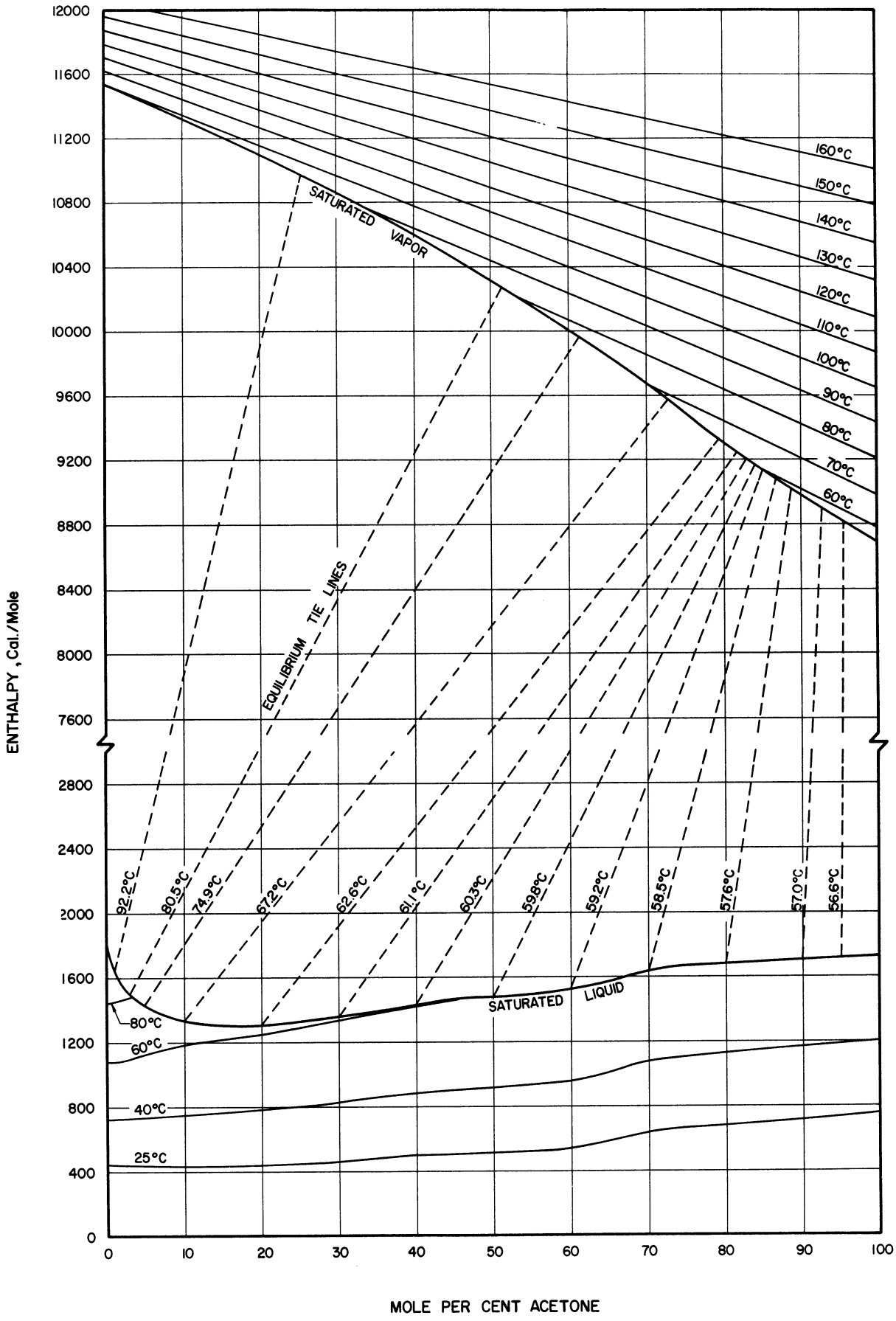

Figure 27. Enthalpy-Concentration Diagram for Acetone-Water. (Atmospheric Pressure)($\underline{H}$ = 0 for pure liquids at 0°C)

TABLE VII

ENTHALPY OF ISOPROPYL ALCOHOL-WATER MIXTURES

Atmospheric Pressure * Calories per mole

Mole Pct. Isopropanol	Subcooled Liq. 25°C	70°C	Sat. Liq.	Sat. Vap.	Superheated Vap. 90°C	120°C
0	450	1260	1800	11,540	-	11,710
5	380	1320	1640	11,620	-	11,820
10	340	1370	1670	11,700	-	11,940
15	400	1490	1790	11,780	-	12,050
20	440	1590	1900	11,840	-	12,160
30	540	1790	2120	11,970	-	12,400
40	630	1970	2320	12,080	12,130	12,630
50	710	2140	2510	12,170	12,300	12,860
60	780	2310	2700	12,260	12,470	13,090
70	840	2460	2870	12,400	12,640	13,320
80	870	2570	3010	12,560	12,820	13,550
90	870	2660	3160	12,730	12,990	13,780
95	870	2710	3250	12,820	13,070	13,900
100	860	2750	3340	12,910	13,160	14,010

TABLE VIII

ENTHALPY OF ACETONE-WATER MIXTURES

Atmospheric Pressure * Calories per mole

Mole Pct. Acetone	Subcooled Liq. 25°C	60°C	Sat. Liq.	Sat. Vap.	Superheated Vap. 80°C	110°C
0	450	1080	1800	11,540	-	11,620
5	430	1130	1430	11,430	-	11,530
10	430	1190	1340	11,320	-	11,440
15	430	1220	1310	11,210	-	11,350
20	430	1250	1310	11,100	-	11,270
30	460	1330	1360	10,850	-	11,090
40	500	1410	1420	10,590	-	10,920
50	510	-	1460	10,310	-	10,740
60	540	-	1500	9,990	10,070	10,570
70	650	-	1620	9,680	9,860	10,390
80	710	-	1670	9,300	9,640	10,220
90	710	-	1690	8,970	9,430	10,040
95	730	-	1710	8,830	9,320	9,950
100	760	-	1730	8,690	9,210	9,870

is obtained by subtracting two numbers of nearly equal magnitude. Table IX on this page shows some heats of mixing for the bubble point temperature which were calculated by the above procedure. The heats of mixing are, of course, not at a common temperature because each mixture has a different bubble point.

A similar procedure was adopted to calculate the heats of mixing at a single temperature, 25 °C. These values, however, reflect the errors introduced into the subcooled-liquid enthalpies by the estimations of the specific heats of the liquid mixtures, and they suffer from the aforementioned subtraction of numbers of similar magnitude. Thus, some of the heats of mixing calculated in the above fashion even have the wrong sign when compared to experimentally determined values.[10,36] Table IX on this page shows some calculated heats of mixing for both binaries compared to the experimentally determined values.

TABLE IX

CALCULATED HEATS OF MIXING COMPARED TO EXPERIMENTAL VALUES

	Isopropyl Alcohol			Acetone		
Mole Pct. Isopropanol or Acetone	Heat of Mixing (cal/mole) Bubble Pt.	25 °C	25 °C, Lit. Value[10]	Heat of Mixing (cal/mole) Bubble Pt.	25 °C	25 °C, Lit. Value[36]
0	0	0	0	0	0	0
10	-10	-150	-142	40	-40	-128
20	70	-90	-118	20	-80	-145
30	100	-40	-68	20	-80	-120
40	140	10	-21	20	-80	-72
50	160	60	16	0	-90	-23
60	160	80	35	-20	-100	17
70	160	100	43	50	-20	51
80	130	90	31	50	10	70
90	60	40	17	0	-10	65
100	0	0	0	0	0	0

Differential Heat of Condensation

The relationship between the integral isobaric heat of vaporization and the differential heat of condensation is given by Equation (9).

$$\Lambda_{T,P} = - \Delta\bar{H}^{V}_{M} + \Delta\bar{H}^{V}_{heat} - \lambda_{P} \qquad (9)$$

The working form of this equation was established by neglecting the heat of mixing in the vapor phase, which would be insignificant at atmospheric pressure, and by assuming that the specific heat of the vapor mixture would be equivalent to a mass average of the pure-component specific heats at the average temperature between the bubble point and the dew point. Thus, the working equation for a binary becomes

$$\Lambda_{T,P} = -\lambda_{P} + (x_{j}\,\bar{C}^{V}_{P,j} + x_{k}\,\bar{C}^{V}_{P,k})(t_{2} - t_{1}) \qquad (98)$$

Differential heats of condensation for isopropyl alcohol-water mixtures and acetone-water mixtures at atmospheric pressure have been calculated by Equation (98) from smoothed values of the integral isobaric heat of vaporization taken at even values of composition. Table X on page 138 shows the values for isopropyl alcohol-water mixtures, and Table XI on page 138 gives the values for acetone-water mixtures. The equilibrium-liquid values given in these tables are essential data required by the definition of the differential heat of condensation.

TABLE X

DIFFERENTIAL HEAT OF CONDENSATION - ISOPROPYL ALCOHOL-WATER

Atmospheric Pressure

Mass Pct. Isopropanol Vapor	Mass Pct. Isopropanol Equil. Liquid	Differential Heat of Condensation (cal/g)
0	0	-540.2
10	0.5	-538.9
20	1.1	-537.1
30	2.0	-534.4
40	3.0	-531.4
50	4.5	-526.7
60	6.7	-519.2
70	11.1	-503.5
75	17.0	-481.7
80	47.5	-361.7
85	81.3	-228.7
90	89.4	-199.5
95	93.8	-182.0
100	100.0	-159.3

TABLE XI

DIFFERENTIAL HEAT OF CONDENSATION - ACETONE-WATER

Atmospheric Pressure

Mass Pct. Acetone Vapor	Mass Pct. Acetone Equil. Liquid	Differential Heat of Condensation (cal/g)
0	0	-540.2
10	0.5	-539.1
20	0.8	-537.9
30	1.3	-536.3
40	2.0	-534.1
50	2.9	-531.3
60	4.0	-527.9
70	5.9	-521.8
80	10.8	-504.8
85	16.0	-484.6
90	27.7	-436.2
93	50.5	-338.7
95	84.3	-189.4
100	100.0	-119.9

CORRELATION OF OTHER INTEGRAL-ISOBARIC-HEAT-OF-VAPORIZATION DATA

The success of the correlations given in the previous section for the integral isobaric heat of vaporization of the isopropyl alcohol-water system and the acetone-water system warrant application of the correlating equation to other systems for which experimental data are available. The values obtained from the general correlating equation,

$$\lambda_P = z_j L_{j,T_1} + z_k L_{k,T_1} + (z_j \overline{C}^{\circ}_{P,j} + z_k \overline{C}^{\circ}_{P,k})(T_2 - T_1) \quad (34)$$

are compared to experimental data on Figures 28 through 33 on pages 140 through 145 for most of the binaries listed in Table I on page 49. The bases for the graphs, either mass or mole, are consistent with manner in which the original experimental data were presented. The graphs are supplemented by Table XII on page 147 which summarizes the deviations between calculated and experimental values, as well as the references to the data used to make the calculations.

All except three of the systems listed in Table I on page 49 for which experimental integral-isobaric-heat-of-vaporization data are available have been included in this section. Those not included are the water-formic acid, the water-acetic acid, and the acetone-chloroform binaries. The data for the first two can be adequately represented by a molal average of the heats of vaporization of the pure components taken at their normal boiling points; Equation (34) will yield a comparable correlation, but the molal-average method is much simpler. Calculations for the third were restricted by lack of heat-of-vaporization data as a function of temperature for chloroform.

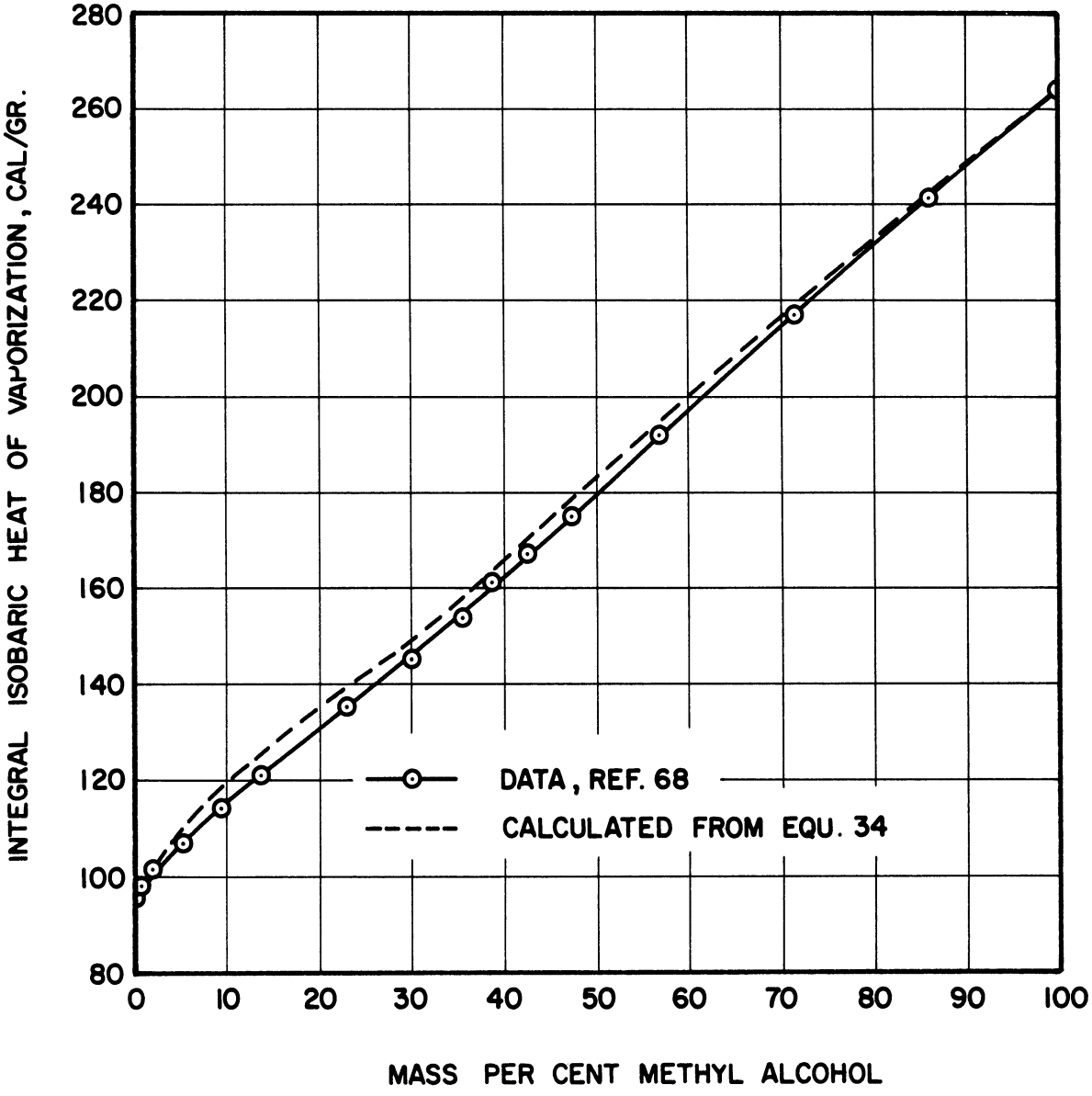

Figure 28. Calculated and Experimental Integral Isobaric Heat of Vaporization for Methyl Alcohol-Benzene Mixtures.

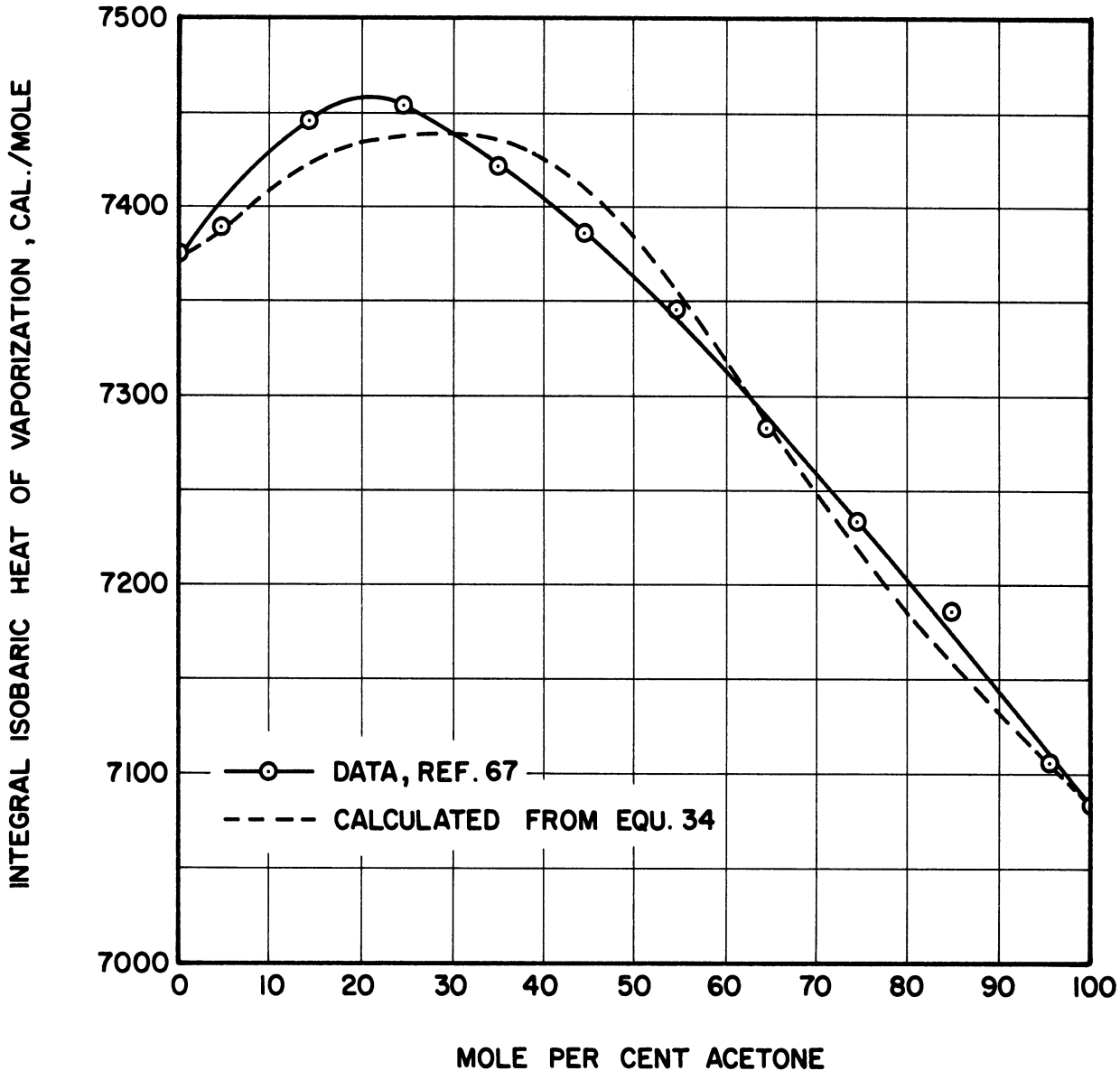

Figure 29. Calculated and Experimental Integral Isobaric Heat of Vaporization for Acetone-Benzene Mixtures.

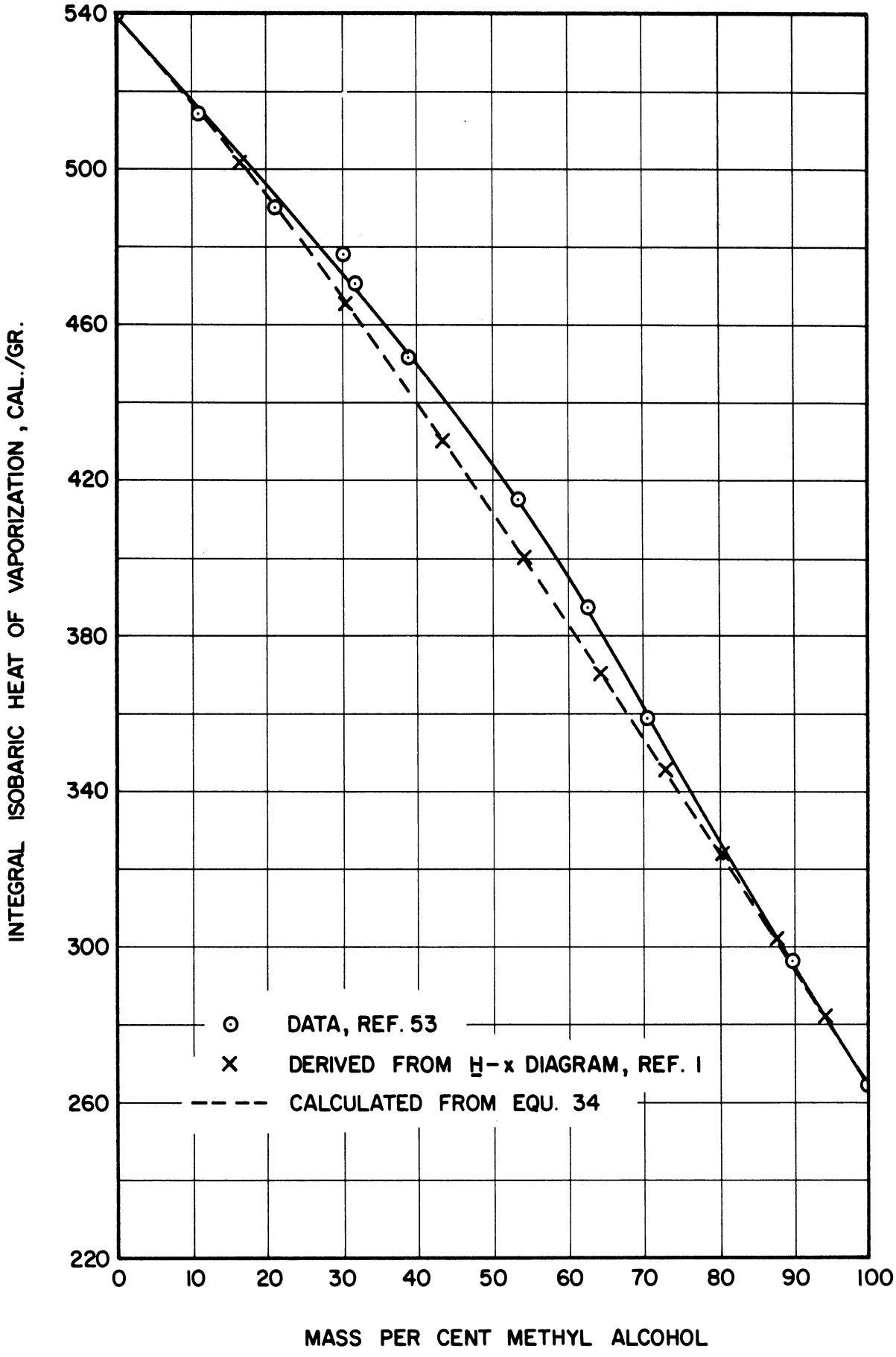

Figure 30. Calculated and Experimental Integral Isobaric Heat of Vaporization for Methyl Alcohol-Water Mixtures.

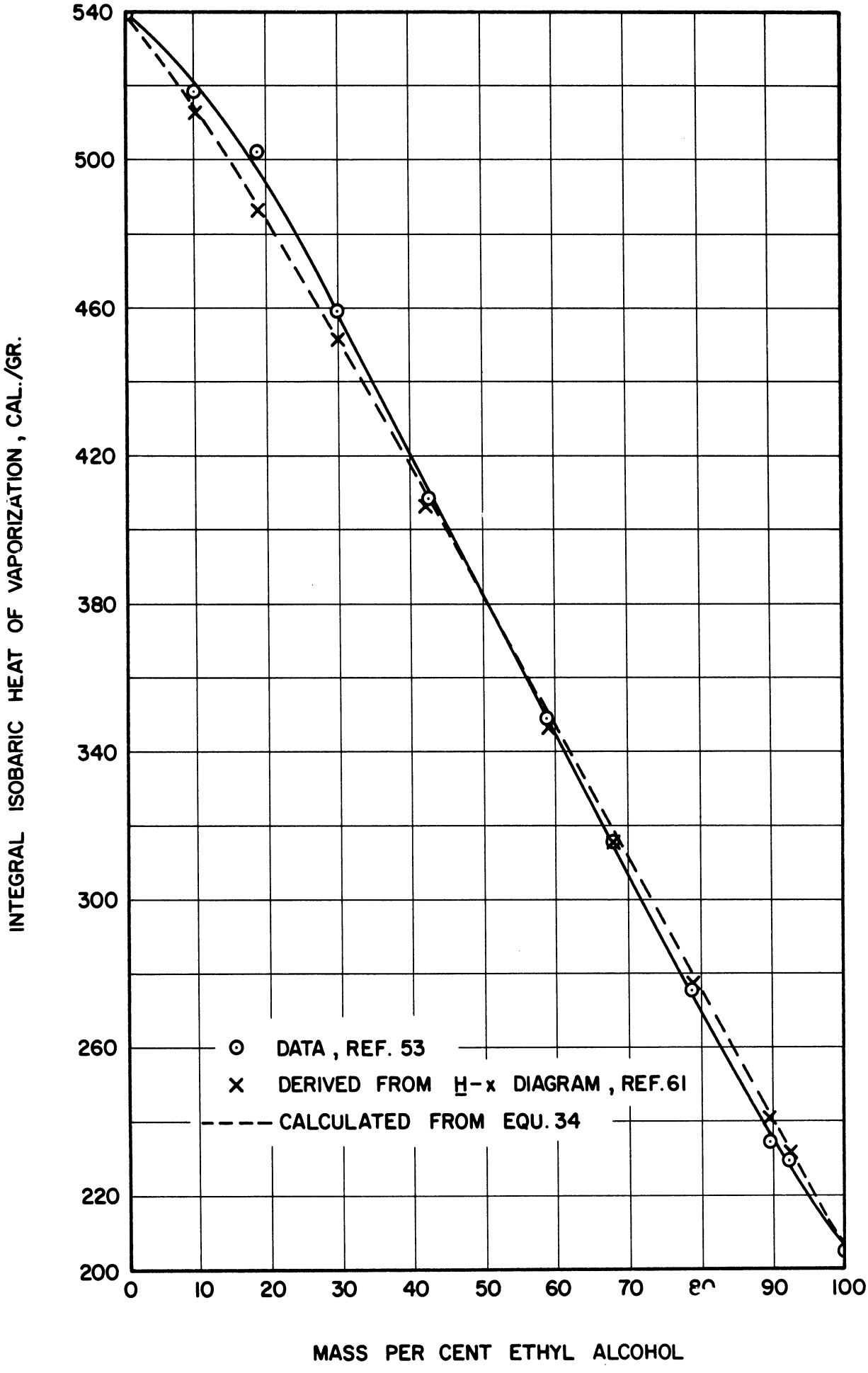

Figure 31. Calculated and Experimental Integral Isobaric Heat of Vaporization for Ethyl Alcohol-Water Mixtures.

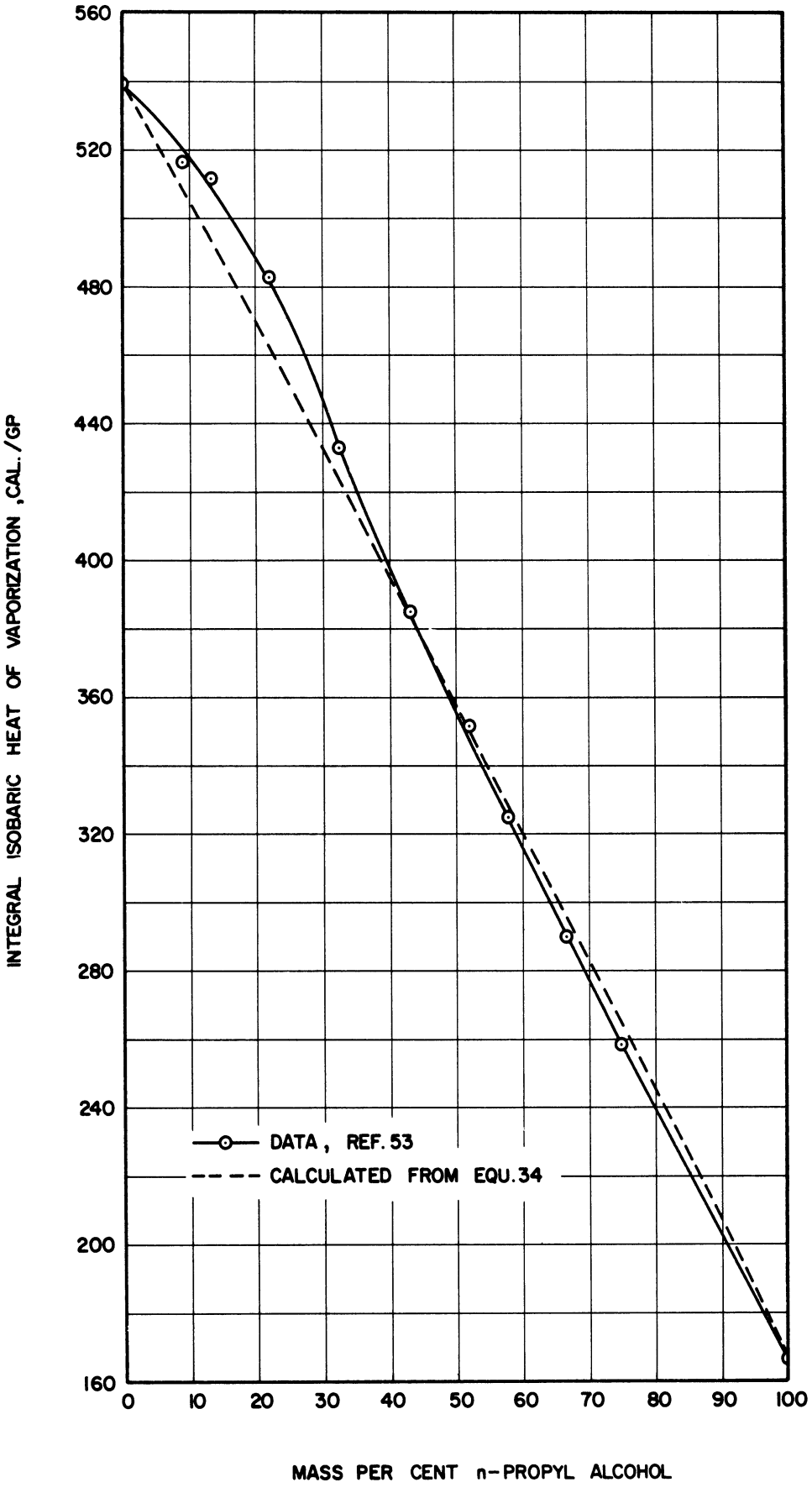

Figure 32. Calculated and Experimental Integral Isobaric Heat of Vaporization for n-Propyl Alcohol-Water Mixtures.

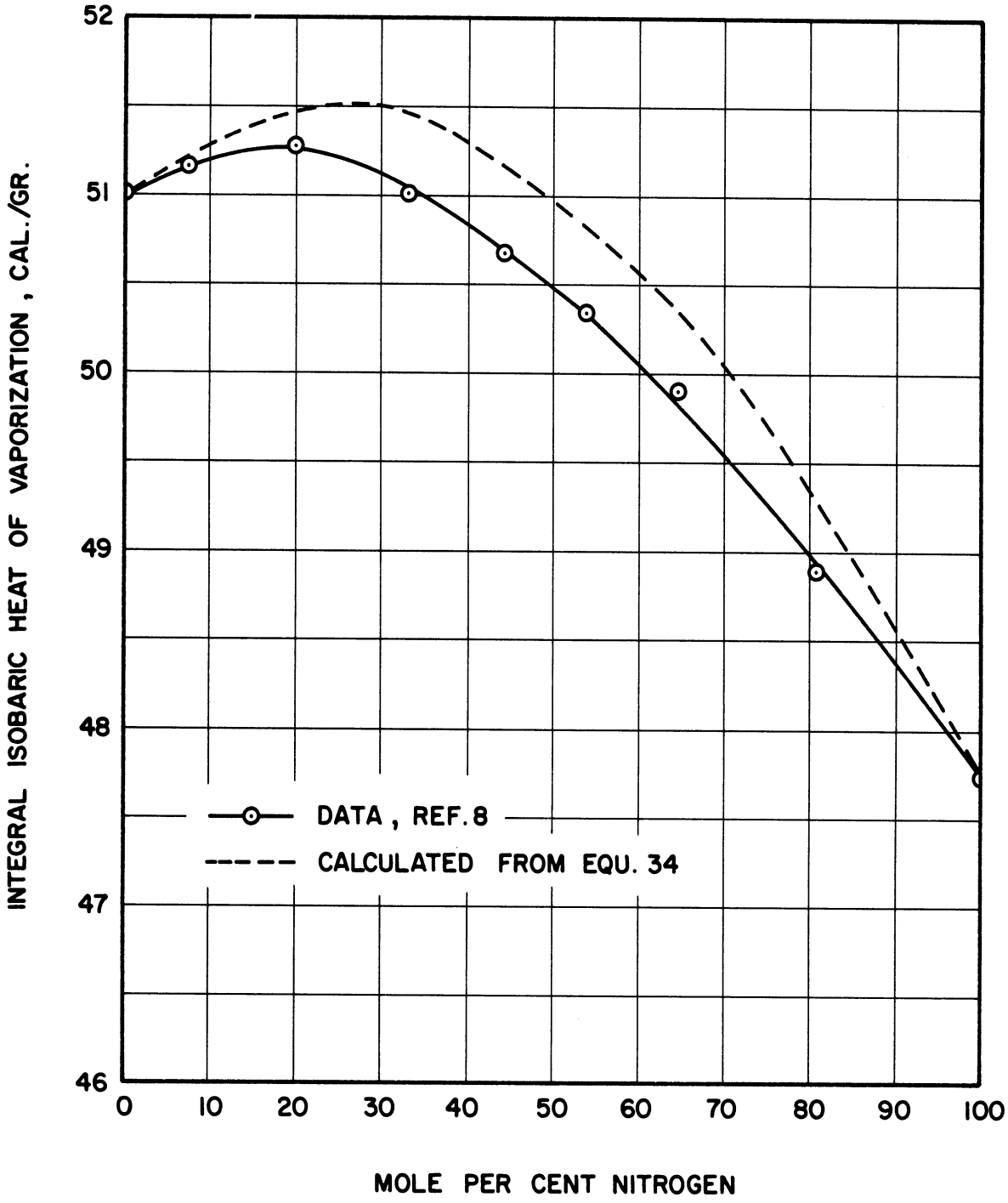

Figure 33. Calculated and Experimental Integral Isobaric Heat of Vaporization for Nitrogen-Oxygen Mixtures.

The enthalpy-concentration diagrams of Ansell et al.[1] and Smith et al.[61] for methyl alcohol-water and ethyl alcohol-water, respectively, provide additional comparative information for these systems. Their diagrams were derived in a manner similar to that outlined in the section entitled "The Enthalpy-Concentration-Diagram Approach" without the aid of any integral-isobaric-heat-of-vaporization data. The integral isobaric heats of vaporization obtained from these diagrams agree, as shown in Figures 30 and 31 on pages 142 and 143, almost identically with those predicted by Equation (34). The simplicity and ease with which Equation (34) may be used in comparison to the tediousness of constructing an enthalpy-concentration diagram is again pointed out. Or, in lieu of the construction of the diagram, the comparative cumbersomeness of Equations (62), (63) and (64) on page 36 , which are tantamount to constructing the diagram is also noted.

In the subsequent table, which supplements the graphs shown in this section, the first three columns following the list of systems give references to the data which were used to make the calculations. For cases in which the heat of vaporization of the pure components which made up the mixtures did not agree with the data taken from the literature, the latter had to be adjusted. For, if there is no agreement between the experimental values and the values used for calculations at the end points, $x = 0$ and $x = 1$, of a composition versus integral-isobaric-heat-of-vaporization curve, then any agreement between calculated and experimental values at intermediate compositions is merely fortuitous. In these cases the adjustment of the literature data was simply a constant displacement of the heat-of-vaporization

versus temperature curve, for the pure component in question at all temperatures, by the difference in the stated heats of vaporization at the normal boiling point. The heading "Avg. Diff." in the table is the arithmetic average of the percentage difference, without regard to sign, between the experimental curve and the predicted curve at the nine concentrations which are multiples of ten in the range between 10 per cent and 90 per cent.

TABLE XII

SUMMARY OF THE COMPARISON BETWEEN EXPERIMENTAL AND CALCULATED INTEGRAL ISOBARIC HEATS OF VAPORIZATION

System	Vap.-Liq. Equilibria	Heats of Vap.	Ideal-Gas Sp. Heats	Avg. Diff.	Max. Diff.
Methanol-Benzene	(68)	(21)(79)	(77) (57)	1.8%	3.4%
Acetone-Benzene	(48)	(50)(79)	(50) (57)	0.2%	0.4%
Methanol-Water	(25)	(21)(46)	(77) (34)	1.5%	3.1%
Ethanol-Water	(51)	(21)(46)	(37) (34)	1.3%	2.2%
n-Propanol-Water	(18)	(79)(46)	(37) (34)	2.1%	4.0%
Nitrogen-Oxygen	(11)	(23)	(27)	0.6%	1.0%

CONCLUSIONS

1. The apparatus designed, constructed, and operated for this investigation can be used for the precise measurement of the integral isobaric heat of vaporization with practically no heat leaks, even with mixtures which have a large temperature difference between the bubble point and the dew point. In particular, the integral isobaric heat of vaporization of the isopropyl alcohol-water system and the acetone-water system were measured at atmospheric pressure with an accuracy of plus or minus 0.3 per cent.

2. Reliable vapor-liquid equilibrium data can be obtained simultaneously with the heat-of-vaporization data and in the same apparatus, as evidenced by the agreement between such data taken in this investigation for the isopropyl alcohol-water system and the acetone-water system and similar data which have been reported in the literature.

3. The experimental integral-isobaric-heat-of-vaporization data for both binaries studied in this investigation are correlated by the equation

$$\lambda_P = z_j L_{j,T_1} + z_k L_{k,T_1} + (z_j \overline{C}^{\circ}_{P,j} + z_k \overline{C}^{\circ}_{P,k})(T_2 - T_1) \qquad (34)$$

This equation is relatively simple to apply. The average difference, without regard to sign, between experimental and calculated results is 0.8 per cent for the isoproyl alcohol-water system and 0.3 per cent for the acetone-water system.

4. The equation given under 3 above is also very successful in correlating the data taken by other investigators for the methyl alcohol-benzene, acetone-benzene, methyl alocohol-water, ethyl alcohol-water, n-propyl alcohol-water, and nitrogen-oxygen systems.

5. Neither the equation relating the equilibrium - K values to the integral isobaric heat of vaporization, which was proposed by Edmister,[16] nor the modification of that equation, which was suggested hereinbefore, is successful in correlating the data for the systems studied in this investigation.

6. Both the Redlich-Kister[35] equation and a modification of that equation suggested by Chao[6] are successful in correlating the vapor-liquid equilibrium data for both binaries studied in this investigation. The improvement of the correlation by the modified equation is not sufficient to justify its added complexity. However, it must be pointed out that the preponderance of the vapor-liquid equilibrium data taken during this investigation were at low concentrations of the more volatile component in the liquid phase - a condition which reduces the rigor of the comparison.

NOMENCLATURE, UNITS, AND CONVERSION FACTORS

Nomenclature

Superscripts

l	liquid phase
o	ideal-gas state
sat.l.	saturated-liquid condition
sat.v.	saturated-vapor condition
v	vapor phase
*	equilibrium composition

Subscripts

A	acetone
B.P.	bubble point
Com	compression
Cool	cooling
D.P.	dew point
Exp	expansion
H	heavy (less volatile) component
I	isopropyl alcohol
In	inlet to the vaporizer
L	light (more volatile) component
P	constant pressure
T	constant absolute temperature
T_l	bubble point temperature (absolute)
W	water

b.p.	normal boiling point of a pure material
heat	heating
i,j,k	pure components i, j, and k which make up a mixture
leads	heater leads
m	mixture
x	mole fraction in liquid phase
y	mole fraction in vapor phase
1,2,3,4	reference to points or some diagram
100; 10,000; 0.1	nominal size of standard resistors
735.7, 760	pressures in mm of mercury

Latin Symbols

B,C,D	arbitrary constants
B.P.	bubble-point conditions
C_P	specific heat at constant pressure
$\overline{C}^{o \text{ or } v}_{P,i}$	ideal-gas or vapor-phase specific heat of i at average temperature between bubble point and dew point
$\overline{C}^{l}_{P,i}$	partial-molal specific heat of i in the liquid phase, except where it is noted to be the specific heat of i at some average temperature
D.P.	dew-point conditions
E	potential drop
F	flow rate
$\underline{H}$	enthalpy, intensive property
$\underline{H}^{o}_{i,2}$	ideal-gas enthalpy of i at temperature T_2
$\overline{H}^{v \text{ or } l}_{i,2}$	partial molal enthalpy of i in either vapor or liquid phase at point 2 on some diagram

$\Delta\bar{H}^{v}_{i,2}$	$\bar{H}^{o}_{i,2} - \bar{H}^{v}_{i,2}$
$\Delta\bar{H}^{l}_{i,1}$	$\bar{H}^{o}_{i,1} - \bar{H}^{l}_{i,1}$
$\Delta\underline{H}^{o}_{i}$	$\underline{H}^{o}_{i,2} - \underline{H}^{o}_{i,1}$
$\Delta\underline{H}_{M}^{v \text{ or } l}$	integral heat of mixing in either the vapor or liquid phase
I	current
K_i	equilibrium ratio, y_i/x_i
L_{j,T_1}	heat of vaporization of pure j at temperature T_1
$L_{j,P}$	heat of vaporization of pure j at pressure P
M	moles of liquid holdup in vaporizer
N	constant total composition
P	pressure
$\bar{P}$	power
R	gas constant
$\underline{S}$	entropy, intensive property
T	absolute temperature
T_1	bubble-point temperature (absolute)
T_2	dew-point temperature (absolute)
V	voltage drop
$\underline{V}$	volume, intensive property
Z	mass fraction in any phase
a,b,c,d	arbitrary constants
d	differential operator
$\bar{f}_i^{v \text{ or } l}$	fugacity of component i in a mixture in either the vapor or liquid phase

h	heat released by vaporizer heater
i	current
log	logarithm to the base 10
ln	logarithm to the base e
p_i	vapor pressure of pure i
t	temperature, °C
t_1	bubble-point temperature, °C
t_2	dew-point temperature, °C
x	mole fraction in liquid phase
y	mole fraction in vapor phase
z	mole fraction in any phase

Greek Symbols

Δ	difference operator
$\Lambda_{T,P}$	differential heat of condensation
Σ	summation over i
γ_i	activity coefficient of component i in the liquid phase, $y_i P/x_i p_i$
∂	partial differential operator
λ_P	integral isobaric heat of vaporization
λ_T	integral isothermal heat of vaporization
$\lambda_{T,P}$	differential heat of vaporization
θ	time
φ	functional relationship

Units and Conversion Factors

1 calorie = 4.1840 absolute joules

1 absolute watt-minute = 14.3403 calories

Gas constant, R = 1.9872 calories per gram mole-°K

0°C = 273.16°K

Molecular weight of acetone = 58.078

Molecular weight of isopropyl alcohol = 60.094

Molecular weight of water = 18.016

APPENDIX A

UNSTEADY STATE OPERATING PERIOD OF THE VAPORIZER

An intuitive example is useful to illustrate the approach of the vaporizer to steady-state operation. Consider a binary mixture of L, the more volatile or light component, and H, the less volatile or heavy component. Assume that the liquid holdup in the vaporizer amounts to ten grams and that the feed preheater is stocked with an infinite supply of a 50.0 per cent mixture. Table XIII on page 156 is a running inventory of the vaporizer contents and of the vapor composition. Vaporization is assumed to occur in one-gram increments. In each of the increments 1, 2, 3, ..., n the following order of events is assumed: (1) one gram of vapor in equilibrium with the liquid contents is evolved, and (2) one gram of feed, immediately thereafter, enters the vaporizer and mixes perfectly with its contents. For the purposes of this example the relationship, $Y_L = \frac{1.5X_L}{1 + 0.5X_L}$, is taken as a representation of the vapor-liquid equilibria for the hypothetical L-H system. Prior to any vaporization (Increment 0) the 50.0 per cent mixture pervades the entire apparatus. For increment 1 the composition of the vapor, as calculated from the equilibrium relationship and shown in the table, is 60.0 per cent L. At the n-th increment the vapor will have reached a composition of 50.0 per cent L, and the vaporizer contents will have reached 40.0 per cent L.

A more sophisticated view point is the consideration of a time-varying material balance around the vaporizer. For the same, hypothetical L-H binary this material balance is

$$F(X_L)_o - FY_L = \frac{M dX_L}{d\theta} \qquad (99)$$

where

F = flow rate (constant) in moles per unit time

$(X_L)_o$ = mole fraction (constant) of L in liquid feed

Y_L = mole fraction of L in vapor at any time

M = moles (constant) of liquid holdup in vaporizer

X_L = mole fraction of L in liquid holdup at any time

Θ = time

TABLE XIII

INVENTORY OF VAPORIZER CONTENTS

	Vapor Leaving		Liquid Entering (50% Mixture)		Vaproizer Contents (10g)		
Increment	L(g)	H(g)	L(g)	H(g)	L(g)	H(g)	
0					5.000	5.000	50.0%L
1	0.600	0.400			-0.600	-0.400	
					4.400	4.600	
			0.500	0.500	+0.500	+0.500	
					4.900	5.100	49.0%L
2	0.590	0.410			-0.590	-0.410	
					4.310	4.690	
			0.500	0.500	+0.500	+0.500	
					4.810	5.190	48.1%L
3	0.581	0.419			-0.581	-0.419	
					4.229	4.771	
			0.500	0.500	+0.500	+0.500	
					4.729	5.271	47.3%L
...	...	...	...	...	...	...	
...	...	...	...	...	...	...	
...	...	...	...	...	4.000	6.000	
n	0.500	0.500			-0.500	-0.500	
					3.500	5.500	
			0.500	0.500	+0.500	+0.500	
					4.000	6.000	40.0%L

The vapor composition is related to the liquid composition by some function

$$Y_L = \varphi(X_L) \tag{100}$$

For the purpose of expediting a solution to the equations an equilibrium relationship of

$$Y_L = mX_L \tag{101}$$

will be considered valid over the composition range of interest.

Differentiation of Equation (101) and substitution into Equation (99) for dX_L yields

$$F[(X_L)_o - Y_L] = \frac{M}{m}\frac{dY_L}{d\Theta} \tag{102}$$

Separating variables, integrating between limits, and collecting terms results in

$$\frac{Fm}{M}\int_{\Theta=0}^{\Theta=\Theta} d\Theta = \int_{(Y_L)_o = m(X_L)_o}^{Y_L = Y_L} \frac{dY_L}{[(X_L)_o - Y_L]} \tag{103}$$

$$\frac{Fm}{M}\Theta = -\ln[(X_L)_o - Y_L] + \ln[(X_L)_o - m(X_L)_o] \tag{104}$$

$$\frac{-Fm}{M}\Theta = \ln\frac{(X_L)_o - Y_L}{(X_L)_o(1-m)} \tag{105}$$

$$\exp[\frac{-Fm}{M}\Theta] = \frac{(X_L)_o - Y_L}{(X_L)_o(1-m)} \tag{106}$$

As Θ becomes large the term on the right of Equation (106) must approach zero. Therefore,

$$Y_L \rightarrow (X_L)_o$$

as Θ becomes large. The case of m=1 is of no interest because m would equal one only for pure materials and azeotropic mixtures, and in those cases no steady-state problems are involved.

Equation (99) can also be solved with the use of the more realistic vapor-liquid-equilibrium relationship

$$Y_L = \frac{\beta X_L}{1 + (\beta-1)X_L} \tag{107}$$

in the place of Equation (101). The result is, of course, the same, but the solution is much more tedious.

The fact that in the actual apparatus the vapor was condensed and recycled to the preheater has been ignored in this analysis. In the apparatus the mass of the preheater contents was so large in comparison to the amount of material recycled that the composition of the original condensate had a negligible effect on the composition of the preheater contents. However, if the condensate had had an appreciable effect on the preheater contents, it would have been in a direction so as to hasten the attainment of the steady state, rather than delay it.

APPENDIX B

I. SAMPLE CALCULATION OF ENERGY CONSUMPTION IN THE VAPORIZER

The power consumed by the vaporizer heater was determined by the product of its voltage drop and current.

$$\overline{P} = EI \tag{108}$$

Neither E nor I was measured directly.

From the circuit diagram, Figure 9 on page 75 , it can be seen that

$$E = V_{100} + V_{10,000} + V_{leads} \tag{109}$$

where V_{100} is the voltage drop across the 100-ohm resistor, and similarly for the 10,000-ohm resistor and the leads. The use of Ohm's law and actual values of the resistances yields

$$E = i_{100}(100.000 + 10,000.5 + 0.2) \tag{110}$$

Ohm's law can be used to express the current, i_{100}, carried in this segment of the circuit in terms of the measured quantity, V_{100}, and the actual value of the 100-ohm standard resistor. Thus,

$$E = \frac{V_{100}}{100.000}(100.000 + 10,000.5 + 0.2) = 101.007\ V_{100} \tag{111}$$

The current, as measured in the 0.1-ohm standard resistor, was corrected for the small amount which passed through the 100-ohm - 10,000-ohm circuit. Application of Kirchoff's law yields

$$I = i_{0.1} - i_{100} \tag{112}$$

where $i_{0.1}$ is the current in the 0.1-ohm resistor. The application of Ohm's law and actual values of the resistances yields

$$I = \frac{V_{0.1}}{0.099995} - \frac{V_{100}}{100.000} \qquad (113)$$

Combination of Equations (111) and (113) in the manner indicated by Equation (108) produces the final equation for the vaporizer-heater power, $\overline{P}$, in terms of the measured quantities, V_{100} and $V_{0.1}$.

$$\overline{P} = 101.007\ V_{100} \left(\frac{V_{0.1}}{0.099995} - \frac{V_{100}}{100.000}\right)$$

$$= 1010.12\ V_{100}\ V_{0.1} - 1.01007\ V_{100}^2 \qquad (114)$$

Potential measurements of V_{100} and $V_{0.1}$ were made at intervals during the course of a determination. The measurements taken during Run No. A26-0 are shown in Table XIV along with the power, as calculated from Equation (114), for each pair of potentials. The second term in Equation (114) amounts to only 0.1 per cent of the first.

TABLE XIV

SAMPLE POTENTIAL MEASUREMENTS AND CALCULATED POWERS

Run No. A26-0 — Approx. Starting Time - 1:44 PM
Time of Run - 19.582 min. — Approx. Ending Time - 2:04 PM

Time	V_{100} (Volts)	Time	$V_{0.1}$ (Volts)	Power (Watts)
1:41	0.25565	1:42	0.22619	58.345
1:46	0.25549	1:47	0.22623	58.318
1:48	0.25549	1:49	0.22608	58.280
2:01	0.25536	2.02	0.22585	58.191
2:03	0.25526	2:04	0.22583	58.163

Figure 34 on page 162 shows the values of power as a function of elapsed time. The fall off in power with time, as in this example, usually amounted to about 0.3 per cent for a single run. The area under the curve between time-zero and time-19.582 minutes, which is the energy consumed by the heater in that time, amounts to 1140.68 watt-minutes. Errors introduced by interpolation of the power are less than the uncertainties of the individual power terms.

II. SAMPLE CALCULATION OF INTEGRAL ISOBARIC HEAT OF VAPORIZATION FROM MEASURED QUANTITIES

A calculation of the integral isobaric heat of vaporization from measurements obtained during a determination proceeded in two steps. The energy consumption of the vaporizer heater was determined first, as shown in the previous section, after which the basic equation

$$\text{Integral Isobaric Heat of Vaporization} = \frac{(\text{Energy Consumption})}{(\text{Mass of Condensate})} - 0.981\bar{C}_P^{l}(T_{BP}-T_{In}) \quad (115)$$

was applied. The following sample calculation is executed with the measurements obtained during Run No. A26-0.

The energy consumption, as shown in the calculation in the previous section, amounted to 1140.68 watt-minutes. The net mass of condensate was 31.464 grams, which was calculated from a gross of 134.625 grams and a tare of 103.161 grams. The uncorrected latent heat, the first term on the right-hand side of Equation (115), becomes

$$\text{Uncorrected Latent Heat} = \frac{(1140.68 \text{ watt-min})}{(31.464 \text{ g})} (14.3403 \text{ cal/watt-min}) \quad (116)$$

$$= 519.88 \text{ cal/g}$$

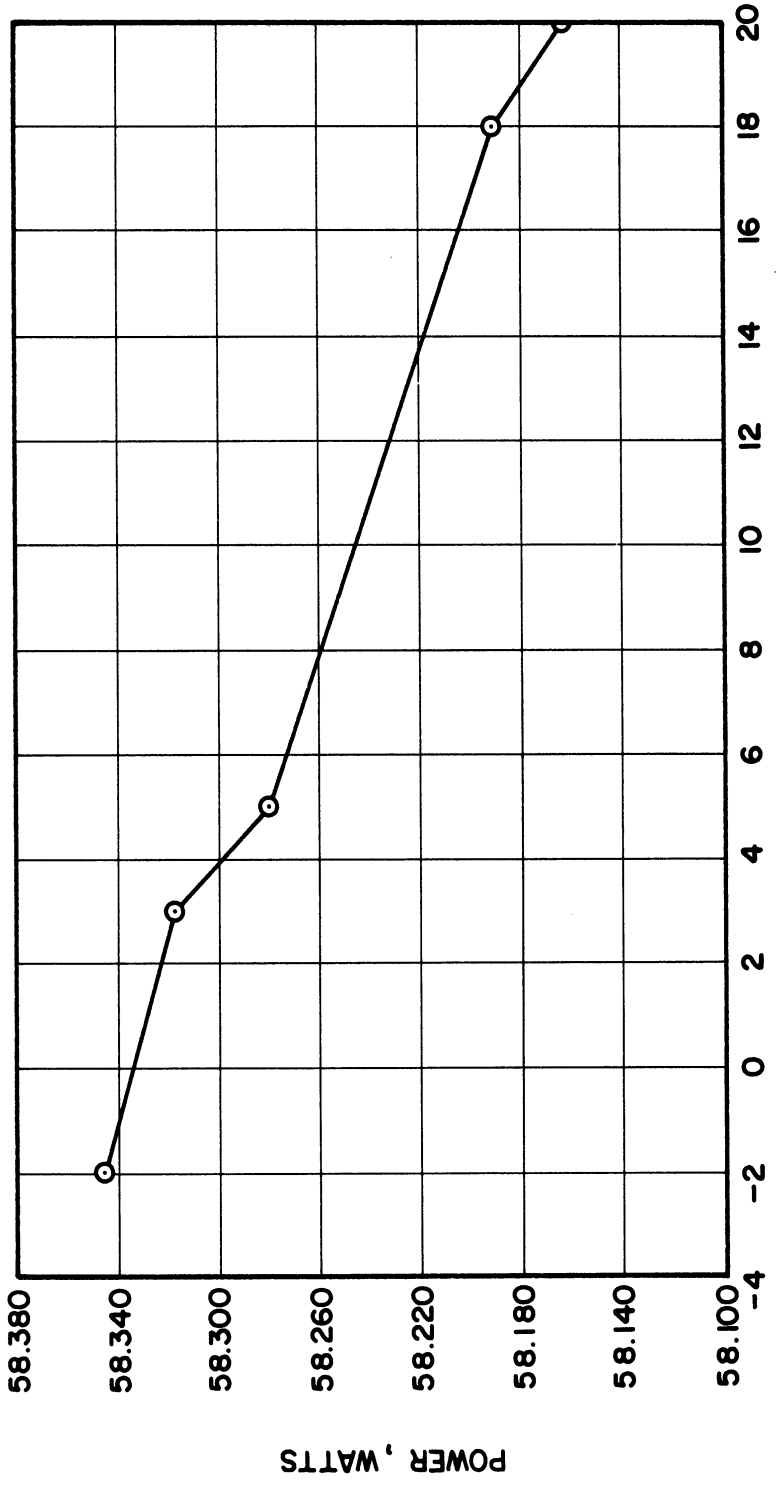

Figure 34. Sample Power-Time Curve (Run No. A 26-0)

Before the sensible-heat corrective term could be computed, it was necessary to know the exact composition of the mixture. Densities of 0.9832 and 0.9830 grams per ml from two trials with the condensate and of 0.9830 and 0.9829 grams per ml from two trials with the preheater liquid established the composition of the mixture at 10.3 mass per cent acetone. The bubble point temperature, T_{BP}, for this composition was read from the temperature-composition diagram which was produced from the vapor-liquid equilibrium data obtained for the entire range of composition. After making the small correction for pressure to 735.7 mm of mercury, the pressure at which the vaporization proceeded, T_{BP} was determined to be 77.8°C. T_{In}, the only directly determined experimental quantity which appears in the sensible-heat correction, was 72.7°C. $\overline{C}_P^l$ for 10.3 mass per cent acetone at the average temperature of 75.2°C was estimated to be 0.996 cal/g°C. The value of the corrective term is calculated, as follows, to be

$$\begin{aligned} \text{Sensible Heat Correction} &= (0.981)(0.996 \text{ cal/g°C})(77.8 - 72.7) \\ &= 4.98 \text{ cal/g} \end{aligned} \qquad (117)$$

The actual latent heat is the difference between the uncorrected latent heat and the sensible-heat correction. Thus, the integral isobaric heat of vaporization for an aqueous mixture of 10.3 mass per cent acetone has been determined to be 514.9 calories per gram.

For this particular mixture the composition of the vaporizer contents was determined from density measurements to be 0.3 mass per cent acetone. The temperature of the contents at 735.7 mm of mercury was found to be 98.0°C. This temperature was corrected for pressure

to 760 mm of mercury by a simplified version of the equation

$$\frac{\Delta \log P}{\Delta 1/T} = \text{Slope} \tag{118}$$

which expresses a linear relationship between log P and 1/T. The simplified equation actually used, along with its application to this example, is

$$\begin{aligned} \text{Temp. Correction} &= T_{760} - T_P \cong \frac{-T_P^2}{\text{Slope}} \log \frac{760}{P} \\ &= T_{760} - T_{735.7} = \frac{-(371.16°K)^2}{-2140°K} \log \frac{760}{735.7} = 0.9°K \end{aligned} \tag{119}$$

The slope, -2140°K, is the mass average of the pure-component slopes of -1630(°K) for acetone and -2200(°K) for water. The corrected temperature is 98.9°C. Thus, at 98.9°C on the temperature-composition diagram points of 10.3 mass per cent acetone on the dew-point line and 0.3 mass per cent acetone on the bubble-point line have been established.

APPENDIX C

SAMPLE CALCULATION OF INTEGRAL ISOBARIC HEAT OF VAPORIZATION FROM DATA AVAILABLE IN THE LITERATURE

The general equation developed in the section entitled "Enthalpy-Temperature-Diagram Approach" for the calculation of integral isobaric heats of vaporization is

$$\lambda_P = z_j L_{j,T_1} + z_k L_{k,T_1} + (z_j \overline{C}^{\circ}_{P,j} + z_k \overline{C}^{\circ}_{P,k})(T_2 - T_1) \qquad (34)$$

For acetone-water mixtures at atmospheric pressure this equation in terms of temperatures in degrees centigrade and mass fractions becomes

$$\lambda_P = Z_A[134.4 - 0.262t_1] + Z_W[599.6 - 0.598t_1] + \{Z_A[0.283 + 0.00083(\frac{t_1+t_2}{2}) - 0.000\ 0005(\frac{t_1+t_2}{2})^2] + Z_W[0.438 + 0.000125(\frac{t_1+t_2}{2})]\}\{t_2 - t_1\} \qquad (79)$$

The units of λ_P in Equation (79) are calories per gram. The following example shows the calculation of the integral isobaric heat of vaporization of an aqueous mixture of 50.0 mass per cent acetone.

The first step is to find the bubble-point and dew-point temperatures from vapor-liquid equilibrium data. For a 50.0 mass per cent mixture of acetone and water at atmospheric pressure the bubble point, t_1, is 61.9°C and the dew point, t_2, is 92.8°C. The mass fractions have, of course, been set by the statement of the problem at $Z_A = Z_W = 0.500$. If one desires to use Equation (34) directly, the heat of vaporization at 61.9°C of both pure water and pure acetone

would have to be determined from either graphs or tables which give the heat-of-vaporization - temperature relationships. The ideal-gas heat capacities of the pure components at the average temperature of 77.3°C would have to be determined similarly. However, the temperature variance of each of these properties has already been incorporated in Equation (79), so that insertion of the numbers $t_1 = 61.9$, $t_2 = 92.8$, $\frac{1}{2}(t_1+t_2) = 77.3$, and $Z_A = Z_W = 0.500$ yields the desired answer immediately.

$$\begin{aligned}\lambda_P &= 0.500[134.4 - (0.262)(61.9)] + 0.500[599.6 - (0.598)(61.9)] \\ &\quad + \{0.500[0.283 + (0.00083)(77.3) - (0.000\ 0005)(77.3)^2] \\ &\quad + 0.500[0.483 + (0.000125)(77.3)]\}\ \{92.8 - 61.9\} \\ &= (0.500)(118.2) + (0.500)(562.6) + [(0.500)(0.344) \\ &\quad + (0.500)(0.448)][30.9] \\ &= 59.1 + 281.3 + 12.3 = 352.7\ \text{cal/g}\end{aligned} \tag{120}$$

Equation (34) can be used to make the calculation on a mole basis if the z's are mole fractions and the units of the L's and the $\overline{C}_P^{\circ}$'s are calories per mole and calories per mole - °C, respectively. The resulting λ_P would be in the units of calories per mole.

APPENDIX D

SAMPLE CALCULATION OF INTEGRAL ISOBARIC HEAT OF VAPORIZATION USING THE EQUILIBRIUM-K-VALUE EQUATIONS

The equation given in the section entitled "Application of Equilibrium-K Values" for the calculation of integral isobaric heats of vaporization is

$$\lambda_P = \frac{RT_1T_2}{T_2-T_1} \sum_i z_i \ln \frac{K_{i,2}}{K_{i,1}} + \sum_i z_i \Delta H_i^o + \left[\frac{T_1T_2}{T_2 - T_1} \ln \frac{T_2}{T_1} - T_1\right] \sum_i z_i (\bar{C}_{P,i}^l - C_{P,i}^o) \qquad (61)$$

The following example shows the calculation of the integral isobaric heat of vaporization of an aqueous mixture of 50.0 mass per cent acetone. The calculation is in three steps - one for each of the terms in Equation (61).

The first term, when written out for an acetone-water binary, becomes

$$\frac{RT_1T_2}{T_2-T_1} \left[z_A \ln \frac{K_{A,2}}{K_{A,1}} + z_W \ln \frac{K_{W,2}}{K_{W,1}}\right] \qquad (121)$$

The z's here refer to mole fractions. The mixture corresponding to 0.500 mass fraction acetone contains 0.2368 mole fraction acetone. From vapor-liquid equilibrium data the bubble-point temperature, T_1, is found to be 335.1°K (61.9°C), and the dew-point temperature, T_2, is found to be 366.0°K (92.8°C). Vapor-liquid equilibria also contribute the y - x values for calculating the K's. The definition of $K_{A,2}$ is

$y_{A,2}/x^*_{A,2}$. The value of $y_{A,2}$ is, of course, 0.2368, and the composition of the equilibrium liquid, $x^*_{A,2}$, at the dew-point temperature, T_2, is 0.00918. Similarly, the definition of $K_{A,1}$ is $y^*_{A,1}/x_{A,1}$. The values of the equilibrium-vapor $y^*_{A,1}$ and the liquid are 0.803 and 0.2368, respectively. Substitution of these values into Statement (121) yields

$$\frac{RT_1T_2}{T_2-T_1} \sum_i z_i \ln \frac{K_{i,2}}{K_{i,1}}$$

$$= \frac{(1.987)(335.1)(366.0)}{(366.0 - 335.1)} [0.2368 \ln \frac{0.2368/0.00918}{0.803/0.2368}$$

$$+ 0.7632 \ln \frac{0.7632/0.99082}{0.197/0.7632}]$$

$$= 7890(0.481 + 0.834) = 10,390 \text{ cal/mole} \qquad (122)$$

The second term in Equation (61) is evaluated from the following expression

$$(z_A \bar{C}^\circ_{P,A} + z_W \bar{C}^\circ_{P,W})(T_2 - T_1) \qquad (123)$$

The z's and T's have been given in the previous paragraph. $\bar{C}^\circ_{P,A}$ and $\bar{C}^\circ_{P,W}$ are 19.97 cal/mole-°C and 8.07 cal/mole-°C, respectively. Applying these values to Statement (123) yields

$$\sum_i z_i \Delta\bar{H}^\circ_i = [(0.2368)(19.97) + (0.7632)(8.07)][366.0 - 335.1]$$

$$= (10.87)(30.9) = 366 \text{ cal/mole} \qquad (124)$$

The third term in Equation (61), when written out for an acetone-water binary, becomes

$$[\frac{T_1T_2}{T_2-T_1} \ln \frac{T_2}{T_1} - T_1][z_A(\bar{C}^l_{P,A} - C^\circ_{P,A}) + z_W(\bar{C}^l_{P,W} - C^\circ_{P,W})] \qquad (125)$$

The z's, T's, and C_P^o's have been given previously. The partial molal specific heats in the liquid phase were evaluated from specific-heat data for acetone-water mixtures. $\bar{C}^l_{P,A}$ is 36.7 cal/mole-°C, and $\bar{C}^l_{P,W}$ is 20.5 cal/mole-°C. Substitution of these values into Statement (125) yields

$$\left[\frac{T_1T_2}{T_2-T_1} \ln \frac{T_2}{T_1} - T_1\right] \sum_i z_i \left(\bar{C}^l_{P,i} - C^o_{P,i}\right)$$

$$= \left[\frac{(335.1)(366.0)}{(366.0 - 335.1)} \ln \frac{366.0}{335.1} - 335.1\right][0.2368(36.7 - 19.97) + 0.7632(20.5 - 8.07)]$$

$$= (15.9)(13.4) = 213 \text{ cal/mole} \qquad (126)$$

The sum of the first two terms of Equation (61), which constitute the Edmister equation, is 10,726 calories per mole, while the total of the three terms is 10,939 calories per mole. The smoothed experimental value for an aqueous mixture containing 23.68 mole per cent acetone is 9699 calories per mole.

The results for another typical mixture of 80 mass per cent acetone (55.37 mole per cent) show that the integral isobaric heat of vaporization as calculated from Equation (61) is 17,893 calories per mole. The corresponding experimental value is 8662 calories per mole.

Some of the reasons for the inability of Equation (61) to predict the experimental results can be seen by referring to the first term on the right-hand side. In this example this term is written out in Equation (122), where the value of 0.00918 (or 0.918 per cent) is entered for $x^*_{A,2}$. If the equilibrium compositions are known to, say, plus or minus 0.2 per cent, then an error of approximately 20 per cent could be

introduced into $K_{A,2}$ which is not compensated elsewhere. This error would, of course, be reflected severely in the final answer because the first term is much larger than either of the other two. In addition, it should be observed that the term $(T_2 - T_1)$ appears in the denominator of the first term on the right-hand side of Equation (61). Thus, for any mixture which has a small temperature difference between the bubble point and dew point, and in particular for mixtures which have a high concentration of either component, the first term in Equation (61) will become quite sensitive to any small error introduced in the estimation of the dew-point - bubble-point temperature difference.

APPENDIX E

SMOOTHED DATA

CALIBRATIONS

TABLE XV

SMOOTHED INTEGRAL ISOBARIC HEATS OF VAPORIZATION
AT EVEN COMPOSITIONS - ISOPROPYL ALCOHOL-WATER

Atmospheric Pressure		
Mass Pct. Isopropanol	Experimental Heat of Vap. (cal/gram)	Calculated (Eq. 78) Heat of Vap. (cal/gram)
0	540.2	539.8
5.0	528.3	527.6
10.0	513.8	513.9
15.0	496.0	496.5
20.0	477.8	477.7
25.0	459.4	458.6
30.0	439.5	439.2
40.0	398.3	399.9
50.0	357.6	360.4
60.0	316.9	320.3
70.0	276.0	279.9
75.0	255.4	259.2
80.0	234.3	238.6
85.0	214.5	218.7
90.0	195.7	199.3
95.0	177.7	179.5
100.0	159.3	159.3

TABLE XVI

SMOOTHED INTEGRAL ISOBARIC HEATS OF VAPORIZATION
AT EVEN COMPOSITIONS - ACETONE-WATER

Atmospheric Pressure		
Mass Pct. Acetone	Experimental Heat of Vap. (cal/gram)	Calculated (Eq. 79) Heat of Vap. (cal/gram)
0	540.2	539.8
5.0	529.7	531.5
10.0	515.5	517.3
15.0	498.1	499.8
20.0	478.6	480.7
25.0	458.6	460.9
30.0	438.3	440.0
40.0	396.3	397.0
50.0	352.6	352.6
60.0	307.1	307.3
70.0	261.3	261.5
75.0	238.4	238.2
80.0	215.5	214.5
85.0	191.5	190.8
90.0	166.1	166.7
95.0	142.2	142.3
100.0	119.9	119.7

TABLE XVII

SMOOTHED VAPOR-LIQUID EQUILIBRIA AT EVEN COMPOSITIONS - ISOPROPYL ALCOHOL-WATER

Atmospheric Pressure

Mass Pct. Isopropanol in Vapor	Mass Pct. Isopropanol in Liquid	Temperature (°C)
0	0	100.0
10.0	0.5	99.4
20.0	1.1	98.3
30.0	1.9	97.0
40.0	3.0	95.3
50.0	4.5	93.1
60.0	6.7	90.5
68.2	10.0	87.5
70.0	11.1	86.9
76.3	20.0	83.3
78.6	30.0	82.0
79.6	40.0	81.6
80.0	47.5	81.5
80.1	50.0	81.5
80.7	60.0	81.3
81.9	70.0	81.0
84.5	80.0	80.7
89.4	90.0	80.5
90.0	90.7	80.5
95.0	96.1	81.2
100.0	100.0	82.4

TABLE XVIII

SMOOTHED VAPOR-LIQUID EQUILIBRIA AT EVEN COMPOSITIONS - ACETONE-WATER

Atmospheric Pressure

Mass. Pct. Acetone in Vapor	Mass Pct. Acetone in Liquid	Temperature (°C)
0	0	100.0
10.0	0.2	99.1
20.0	0.6	98.0
30.0	1.3	96.7
40.0	2.0	94.9
50.0	2.9	92.8
60.0	3.9	89.8
70.0	5.9	85.3
79.0	10.0	79.1
80.0	10.8	78.2
87.1	20.0	70.6
90.0	27.7	66.8
90.5	30.0	66.3
92.3	40.0	63.4
92.9	50.0	62.3
93.6	60.0	61.0
94.1	70.0	60.3
94.7	80.0	59.4
95.0	84.5	59.1
95.7	90.0	58.4
100.0	100.0	56.2

TABLE XIX

SMOOTHED DENSITY-COMPOSITION DATA
AT 25 °C FOR ACETONE-WATER MIXTURES

Mass Pct. Acetone	Density (g/cc)
0	0.9971
5.0	0.9904
10.0	0.9836
15.0	0.9765
20.0	0.9693
25.0	0.9618
30.0	0.9539
35.0	0.9454
40.0	0.9365
45.0	0.9265
50.0	0.9160
55.0	0.9051
60.0	0.8940
65.0	0.8824
70.0	0.8700
75.0	0.8569
80.0	0.8434
85.0	0.8294
90.0	0.8153
95.0	0.7999
100.0	0.7846

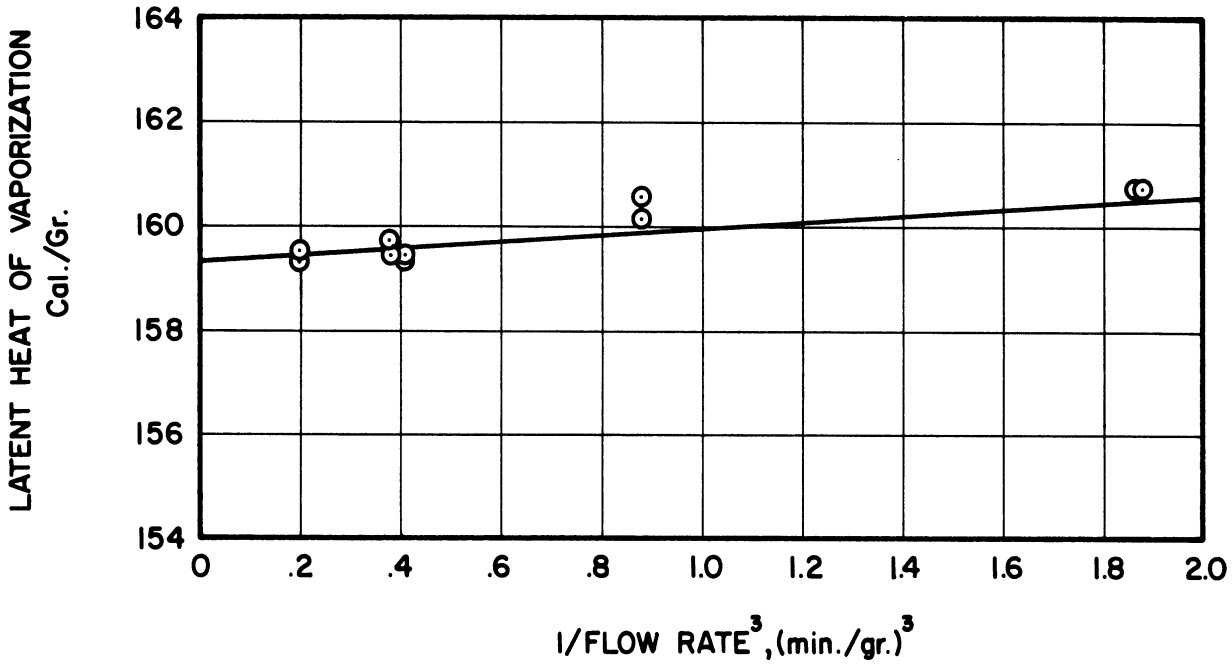

Figure 35. Heat of Vaporization of Isopropyl Alcohol as a Function of the Reciprocal Flow Rate to the Third Power.

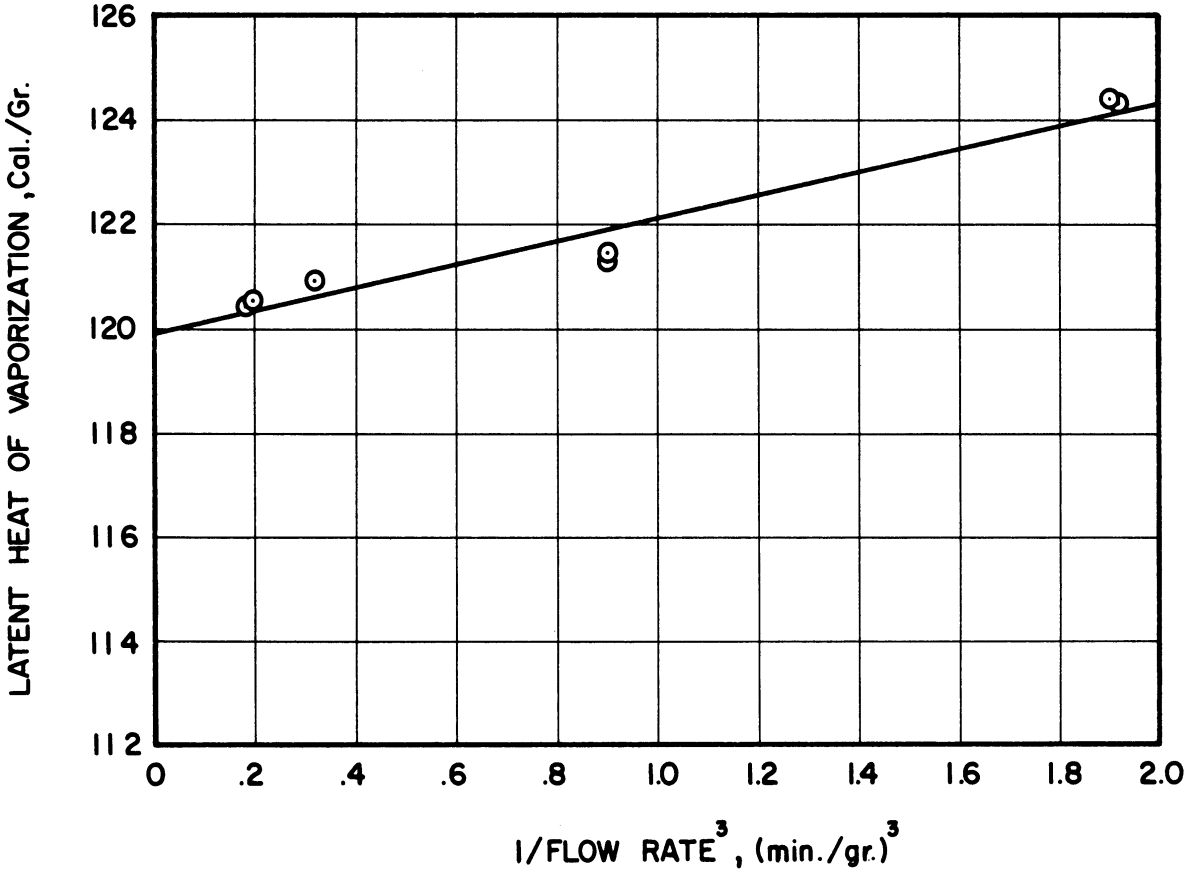

Figure 36. Heat of Vaporization of Acetone as a Function of the Reciprocal Flow Rate to the Third Power.

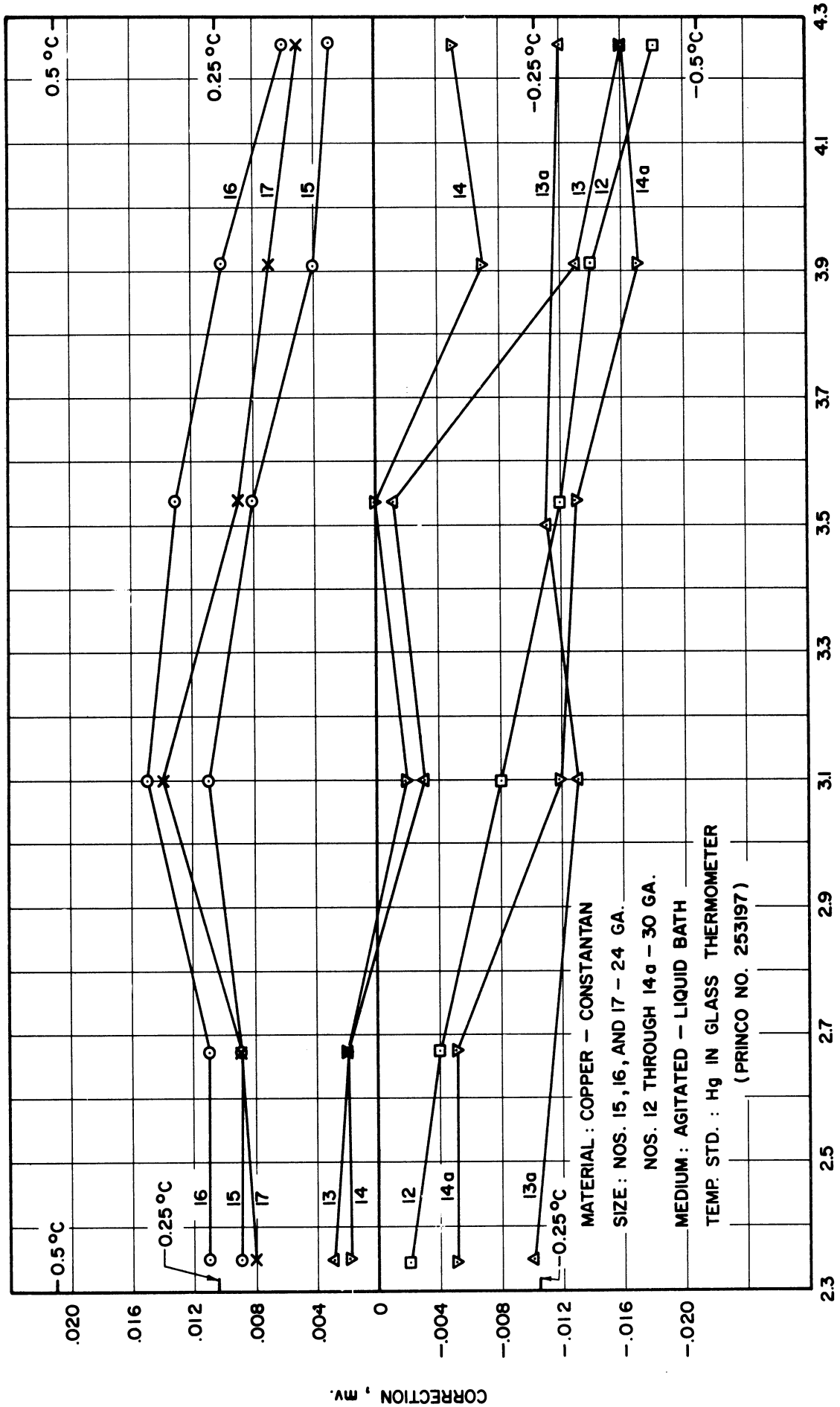

Figure 37. Thermocouple Calibrations.

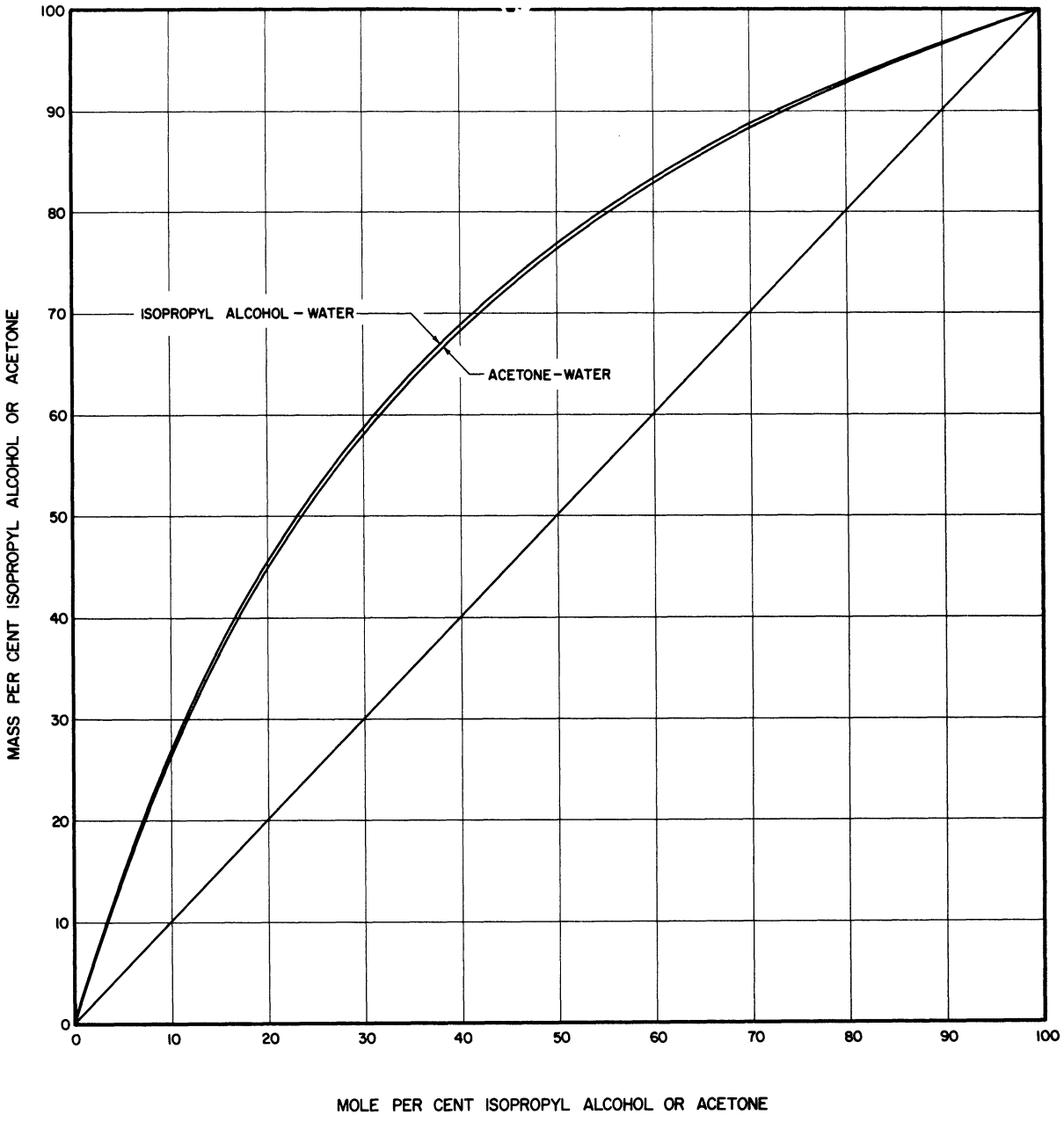

Figure 38. Graph Relating Mole Per Cent to Mass Per Cent.

APPENDIX F

RAW DATA

TABLE XX

RAW DATA FROM ISOPROPYL ALCOHOL-WATER RUNS

Run No.	Time (min.)	Avg. Power (watts)	Net Condensate(g)	Avg. Density (g/cc) at 35°C Condensate	Vap. Liquid	Avg. Temperature (°C) Point 12	Point 13	Point 14	Bar. Press. (mm Hg)
T12-O	27.947	49.587	36.188	Pure Water		90.1	99.4	99.2	737.8
T12-N	29.793	49.569	38.479	Pure Water		90.0	99.4	99.2	737.8
T13-O	30.587	26.851	21.495	Pure Water		95.3	99.3	99.3	738 0
T13-N	28.437	27.364	20.351	Pure Water		94.9	99.2	99.2	738.0
T14-O	25.052	66.448	43.356	Pure Water		88.7	99.3	99.2	738.0
T14-N	28.642	66.238	49.410	Pure Water		88.9	99.3	99.1	738.0
T15-O	30.548	36.637	29.299	Pure Water		92.7	99.2	99.3	740.9
T15-N	25.028	36.975	24.220	Pure Water		92.9	99.2	99.2	740.9
I11-O	14.360	12.300	14.970	Pure Isopropyl Alcohol		70.3	81.6	81.6	738.0
I11-N	24.996	12.286	26.055	Pure Isopropyl Alcohol		70.4	81.6	81.6	738.0
I12-O	17.429	16.355	24.054	Pure Isopropyl Alcohol		68.3	81.6	81.6	737.2
I12-N	22.387	16.344	30.952	Pure Isopropyl Alcohol		68.4	81.6	81.6	737.2
I13-O	19.380	9.477	15.754	Pure Isopropyl Alcohol		73.4	81.7	81.7	740.5
I13-N	20.043	9.455	16.265	Pure Isopropyl Alcohol		73.5	81.7	81.7	740.5
I14-O	15.337	20.237	26.141	Pure Isopropyl Alcohol		67.7	81.7	81.7	740.3
I14-N	22.198	20.219	37.849	Pure Isopropyl Alcohol		67.7	81.7	81.7	740.3
I15-O	15.152	15.913	20.454	Pure Isopropyl Alcohol		68.9	81.6	81.6	734.4
I15-N	22.095	15.916	29.832	Pure Isopropyl Alcohol		69.1	81.6	81.6	734.4
I16-O	14.775	20.270	22.799	0.78552	-	67.0	80.4	80.4	738.4
I16-N	23.110	20.303	35.644	0.78565	-	66.8	80.4	80.4	738.4
I17-O	16.150	13.946	17.265	0.78548	-	69.2	80.3	80.3	735.7
I17-N	23.166	13.953	24.804	0.78570	0.78260	69.2	80.3	80.3	735.7
I18-O	17.740	19.618	24.388	0.79744	-	68.0	79.8	79.9	739.7
I18-N	23.012	19.604	31.624	0.79767	-	68.0	79.8	79.8	739.7
I19-O	14.639	14.703	15.160	0.79751	-	70.2	79.7	79.8	737.9
I19-N	24.461	14.689	25.363	0.79755	0.79481	70.2	79.7	79.8	737.9
I20-O	13.652	25.142	21.880	0.81031	-	67.3	79.8	79.8	736.6
I20-N	23.680	25.112	37.925	0.81043	-	67.2	79.8	79.8	736.6
I21-O	15.297	16.722	16.436	0.81031	-	70.0	79.7	79.7	733.5
I21-N	24.038	16.702	25.806	0.81013	0.81906	70.1	79.7	79.7	733 5
I22-O	15.516	27.902	25.407	0.82192	-	68.2	80.8	80.7	735.7
I22-N	23.730	27.933	38.943	0.82215	-	68.2	80.8	80.7	735.7
I23-O	16.966	17.713	17.873	0.82188	-	72.3	80.8	80.6	738.5
I23-N	25.153	17.726	26.469	0.82195	0.89841	72.3	80.8	80.6	738.5
I24-O	14.075	27.961	20.908	0.83825	-	72.3	84.5	84.5	737.4
I24-N	25.344	27.988	37.767	0.83813	-	72.4	84.4	84.5	737.4

TABLE XX (CONT'D)

RAW DATA FROM ISOPROPYL ALCOHOL-WATER RUNS

Run No.	Time (min.)	Avg. Power (watts)	Net Condensate(g)	Avg. Density (g/cc) at 35°C Condensate	Vap. Liquid	Avg. Temperature (°C) Point 12	Point 13	Point 14	Bar. Press. (mm Hg)
I25-O	14.142	20.174	15.317	0.83869	-	76.1	84.4	84.5	736.7
I25-N	22.405	20.147	24.198	0.83861	0.97119	76.2	84.5	84.5	736.7
I26-O	16.038	33.155	24.954	0.86076	-	75.6	88.3	88.3	739.3
I26-N	23.052	33.084	35.781	0.86072	-	75.6	88.3	88.3	739.3
I27-O	18.137	22.721	19.452	0.86089	-	79.0	88.3	88.3	738.1
I27-N	23.472	22.638	25.164	0.86076	0.98022	79.2	88.4	88.3	738.1
I28-O	20.023	36.252	30.083	0.88558	-	77.5	91.3	91.3	734.6
I28-N	23.401	36.136	35.038	0.88585	-	78.0	91.3	91.3	734.6
I29-O	14.619	25.211	15.347	0.88601	-	79.2	91.3	91.3	733.5
I29-N	22.145	25.208	23.201	0.88597	0.98463	79.2	91.4	91.4	733.5
I30-O	15.062	41.384	23.635	0.90603	-	81.2	93.4	93.3	734.8
I30-N	19.969	40.424	30.429	0.90617	-	79.5	93.5	93.2	734.8
I31-O	12.804	26.353	12.686	0.90630	-	80.5	93.4	93.5	735.1
I31-N	22.419	26.394	22.281	0.90624	0.98727	80.5	93.4	93.5	735.1
I32-O	14.070	48.216	23.018	0.92860	-	75.8	95.4	95.2	737.7
I32-N	20.400	48.082	33.242	0.92866	-	75.7	95.4	95.3	737.7
I33-O	14.577	32.050	15.892	0.92909	-	78.4	95.4	95.2	732.5
I33-N	25.384	32.161	27.809	0.92865	0.98978	78.5	95.4	95.3	732.5
I34-O	15.264	47.326	22.335	0.95177	-	80.3	97.1	97.0	742.5
I34-N	23.032	47.538	33.917	0.95137	-	80.9	97.0	97.0	742.5
I35-O	13.700	33.092	14.024	0.95155	-	81.3	96.9	97.0	741.5
I35-N	21.207	33.109	21.735	0.95154	0.9918[illegible]	81.5	97.0	97.1	741.5
I36-O	15.838	50.448	23.830	0.96153	-	80.5	97.6	97.5	741.0
I36-N	23.053	50.412	34.613	0.96160	-	80.5	97.6	97.5	741.0
I37-O	15.418	34.908	16.087	0.96159	-	81.7	97.5	97.6	736.6
I37-N	26.844	35.058	28.032	0.96146	0.99218	81.6	97.5	97.5	736.6
I38-O	14.020	53.794	21.604	0.96925	-	79.6	98.2	98.1	741.1
I38-N	20.033	53.751	30.862	0.96932	-	79.3	98.3	98.2	741.1
I39-O	15.138	36.921	16.002	0.96938	-	78.8	98.1	98.0	738.6
I39-N	20.352	36.852	21.396	0.96944	0.99278	78.6	98.1	98.0	738.6
I40-O	13.335	56.848	20.921	0.97680	-	81.1	98.6	98.6	738.0
I40-N	20.238	56.859	31.862	0.97664	-	81.5	98.6	98.6	738.0
I41-O	14.127	39.324	15.333	0.97684	-	81.6	98.8	98.6	742.3
I41-N	20.120	39.320	21.847	0.97676	0.99328	81.4	98.8	98.6	742.3
I42-O	12.012	57.856	18.609	0.98495	-	85.4	99.3	99.0	743.3
I42-N	18.871	57.841	29.305	0.98461	-	85.6	99.3	99.1	743.3
I43-O	13.425	38.757	14.004	0.98551	-	87.5	99.3	99.0	741.6
I43-N	22.010	38.858	23.035	0.98528	0.99373	87.2	99.3	99.1	741.6

TABLE XXI

RAW DATA FROM ACETONE-WATER RUNS

Run No.	Time (min.)	Avg. Power (watts)	Net Condensate(g)	Avg. Density (g/cc) at 25 °C Condensate	Vap. Liquid	Avg. Temperature (°C) Point 12	Point 13	Point 14	Bar. Press. (mm Hg)
A1-0	23.583	14.968	40.741	Pure Acetone		48.1	55.3	55.1	734.3
A1-N	17.915	15.000	31.039	Pure Acetone		48.2	55.4	55.2	734.3
A2-0	19.278	12.601	28.121	Pure Acetone		49.5	55.3	55.1	732.6
A2-N	14.155	12.600	20.649	Pure Acetone		49.5	55.3	55.1	732.6
A3-0	21.375	8.895	22.145	Pure Acetone		51.7	55.3	55.3	730.0
A3-N	18.260	8.892	18.873	Pure Acetone		51.7	55.3	55.2	730.0
A4-0	22.796	7.076	18.371	Pure Acetone		52.4	55.3	55.2	731.0
A4-N	20.245	7.068	16.301	Pure Acetone		52.4	55.3	55.3	731.0
A5-0	19.137	14.980	30.019	0.7940	-	48.7	56.3	56.2	737.1
A5-N	13.672	14.956	21.422	0.7938	-	48.9	56.4	56.2	737.1
A6-0	24.165	9.939	25.333	0.7939	-	51.7	56.4	56.2	736.7
A6-N	15.450	9.904	16.147	0.7938	0.7986	51.7	56.4	56.2	736.7
A7-0	18.484	15.541	27.516	0.8049	-	53.8	60.6	60.6	738.7
A7-N	13.784	15.565	20.506	0.8049	-	53.5	60.6	60.6	738.7
A8-0	21.981	11.161	23.645	0.8044	-	55.8	60.7	60.5	738.8
A8-N	13.333	11.176	14.343	0.8045	0.9051	55.9	60.7	60.5	738.8
A9-0	18.060	17.912	28.180	0.8131	-	56.0	65.0	65.4	732.1
A9-N	13.700	17.864	21.208	0.8138	-	56.0	65.3	65.5	732.1
A10-0	21.394	12.262	22.628	0.8147	-	57.4	65.1	65.3	732.3
A10-N	14.200	12.240	14.882	0.8150	0.9559	57.4	65.3	65.6	732.3
A11-0	20.077	23.061	30.992	0.8411	-	55.8	76.6	76.6	733.1
A11-N	15.937	23.057	24.588	0.8412	-	55.9	76.5	76.6	733.1
A12-0	19.714	16.970	22.360	0.8410	0.9816	57.1	76.8	76.5	733.7
A12-N	Run Discarded. Shield Line Plugged.								
A13-0	18.833	28.074	28.903	0.8705	-	58.1	84.7	84.6	736.5
A13-N	16.717	28.027	25.467	0.8708	0.9893	58.0	84.7	84.5	736.5
A14-0	Intermittent plugging of liquid line upset the steady state.								
A14a-0	20.975	32.328	31.468	0.8944	-	58.4	88.6	88.7	726.5
A14a-N	15.375	32.292	23.002	0.8944	-	58.3	88.6	88.7	726.5
A15-0	25.297	22.996	26.811	0.8947	-	59.6	88.5	88.7	723.9
A15-N	15.178	23.116	16.177	0.8947	0.9920	59.4	88.5	88.6	723.9
A16-0	21.012	37.352	31.629	0.9157	-	59.2	91.6	91.6	728.7
A16-N	17.594	37.351	26.546	0.9158	-	59.0	91.6	91.7	728.7
A17-0	21.896	26.066	23.021	0.9155	-	60.8	91.6	91.6	728.0
A17-N	14.835	26.015	15.615	0.9158	0.9929	60.8	91.6	91.6	728.0
A18-0	19.510	42.520	29.973	0.9360	-	61.0	94.2	94.0	744.6
A18-N	18.222	42.419	27.806	0.9362	-	60.6	94.2	94.0	744.6
A19-0	20.123	29.852	21.653	0.9360	-	62.1	94.0	93.9	744.6
A19-N	16.835	29.792	18.028	0.8358	0.9944	61.9	94.0	93.9	744.6
A20-0	22.565	48.343	35.713	0.9535	-	63.4	96.3	96.0	745.0
A20-N	18.032	48.381	28.554	0.9535	-	63.1	96.3	96.0	745.0
A21-0	14.841	30.980	15.047	0.9534	-	64.7	95.9	96.0	743.7
A21-N	15.008	31.138	15.241	0.9535	0.9953	64.4	96.2	96.0	743.7
A22-0	20.145	51.233	30.920	0.9691	-	68.0	96.6	96.6	725.5
A22-N	14.293	51.142	21.833	0.9689	-	68.0	96.7	96.6	725.5
A23-0	20.805	35.682	22.226	0.9689	-	69.2	96.6	96.6	726.8
A23-N	20.200	35.680	21.423	0.9690	0.9962	69.2	96.6	96.6	726.8
A24-0	20.595	54.730	32.252	0.9767	-	71.6	97.8	97.8	742.2
A24-N	17.990	54.724	28.281	0.9766	-	71.6	97.8	97.8	742.2
A25-0	19.799	38.977	22.144	0.9766	-	72.9	97.8	97.8	741.7
A25-N	15.575	38.908	17.378	0.9768	0.9966	72.6	97.8	97.8	741.7
A26-0	19.582	58.251	31.464	0.9831	-	72.7	98.2	98.0	735.7
A26-N	18.432	58.061	29.554	0.9832	-	72.7	98.2	98.0	735.7
A27-0	20.409	39.111	22.065	0.9830	-	75.3	98.2	98.1	737.0
A27-N	16.302	38.979	17.525	0.9831	0.9966	75.0	98.2	98.1	737.0
A28-0	21.065	59.268	33.469	0.9900	-	79.1	98.7	98.6	736.9
A28-N	19.258	59.295	30.531	0.9901	-	79.0	98.7	98.6	736.9
A29-0	22.192	40.354	24.017	0.9901	-	83.1	98.7	98.6	736.6
A29-N	19.187	40.242	20.730	0.9902	0.9969	83.0	98.7	98.6	736.6

BIBLIOGRAPHY

1. Ansell, L.S., Samuels, H. and Frishe, W.C. Chem. Eng., 58, No.4, (1951) 133.

2. Bahlke, W.H. and Kay, W.B. Ind. Eng. Chem., 24, (1932) 291.

3. Brown, G.G., and Associates, Unit Operations. New York: John Wiley & Sons, Inc., (1950) 366.

4. Brunjes, A.S. and Bogart, M.J.P. Ind. Eng. Chem., 35, (1943) 255.

5. Canjar, L.N. and Lonergan, T.E. A.I.Ch.E. Journal, 2, (1956) 280.

6. Chao, K.C. Ind. Eng. Chem., 51, (1959) 93.

7. Cleland, W.W. and Harding, R.S. Rev. Sci. Instr., 28, (1957) 696.

8. Dana, L.I. Proc. Am. Acad. Arts Sci., 60, (1925) 241.

9. Dauphinee, T.M. and Woods, S.B. Rev. Sci. Instr., 26, (1955) 693.

10. Dimmling, W. and Lange, E. Z. Elektrochem., 55, (1951) 322.

11. Dodge, B.F. Chem. and Met. Eng., 35, (1928) 624.

12. Dodge, B.F. Chemical Engineering Thermodynamics. New York: McGraw-Hill Book Company, Inc., (1944) 399.

13. Ibid. p. 558.

14. Doroshevskago, A.G. Zhur. Russ. Fiz.-Khim. Obshchestva, 41, (1909) 958.

15. Duhem, P. Ann. sci. Ecole Norm. super., 3 e serie, 2, (1885) 207.

16. Edmister, W.C. A.I.Ch.E. Journal, 1, (1955) 38.

17. Edmister, W.C. Petrol. Refiner, 27, No. 12, (1948) 656.

18. Ellis, S.R.M. and Thwaites, J.M. Birmingham Univ. Chem. Engr., 6, (1955) 78.

19. Fekula, G.M. Ph.D. Thesis, University of Michigan, Ann Arbor, 1942.

20. Fenner, R.C. and Richtmyer, F.K. Phys. Rev., 20, (1905) 77.

21. Fiock, E.F., Ginnings, D.C. and Holton, W.B. J. Research Nat. Bur. Standards, 6, (1931) 881.

22. Fletcher, J. and Tyrer, D. J. Chem. Soc., 103, (1913) 517.

23. Furukawa, G.T. and McCoskey, R.E. Nat. Advisory Comm. Aeronaut. Tech Note, No. 2969, 1953.

24. Ginnings, D.C. and Corruccini, R.J. Ind. Eng. Chem., 40, (1948) 1990.

25. Green, S.J. and Vener, R.E. Ind. Eng. Chem., 47, (1955) 103.

26. Griffiths, V.S. J. Chem. Soc., (1952) 1326.

27. Handbook of Chemistry and Physics, 36th ed., Chemical Rubber Publishing Co., Cleveland, (1954) 2108.

28. Hobson, M. and Weber, J.H. Chem. and Eng. Data Ser., 2, (1957) 7.

29. Hobson, M. and Weber, J.H. Petrol. Processing, 12, No. 9, (1957) 153.

30. Hougen, O.A. and Watson, K.M. Chemical Process Principles, Part II, New York: John Wiley & Sons, Inc. (1947) 625.

31. Hougen, O.A. and Watson, K.M. Chemical Process Principles Charts. New York: John Wiley & Sons, Inc., 1946.

32. Ibl, N.V. and Dodge, B.F. Chem. Eng. Sci., 2, (1953) 120.

33. International Critical Tables, V, New York: McGraw-Hill Book Company, Inc., (1928) 108.

34. Keenan, J.H. and Keyes, F.G. Thermodynamic Properties of Steam. New York: John Wiley & Sons, Inc., (1936) 16.

35. Kemp, H.S. Ph.D. Thesis, University of Michigan, Ann Arbor, 1944.

36. Kister, A.T. and Waldman, D.C. J. Phys. Chem., 62, (1958) 245.

37. Kobe, K.A., Harrison, R.H. and Pennington, R.E. Petrol. Refiner, 30, No. 8 (1951) 119.

38. Langdon, W.M. and Keyes, D.B. Ind. Eng. Chem., 35, (1943) 459.

39. Lemlich, R., Gottschlich, C. and Hoke, R. Chem. and Eng. Data Ser., 2, (1957) 32.

40. Mathews, J.H. J. Am. Chem. Soc., 48, (1926) 562.

41. McCracken, P.G. and Smith, J.M. A.I.Ch.E. Journal, 2, (1956) 498.

42. Meissner, H.P. Ind. Eng. Chem., 33, (1941) 1440.

43. Nelson, J.M. and Holcomb, D.E. Chem. Eng. Progr. Symposium Ser., No. 7, 49, (1953) 93.

44. Osborne, N.S. and Ginnings, D.C. J. Research Nat. Bur. Standards, 39, (1947) 453.

45. Osborne, N.S., Stimson, H.F. and Ginnings, D.C. J. Research Nat. Bur. Standards, 18, (1937) 389.

46. Osborne, N.S., Stimson, H.F. and Ginnings, D.C. J. Research Nat. Bur. Standards, 23, (1939) 197.

47. Othmer, D.F. Ind. Eng. Chem., 20, (1928) 743.

48. Othmer, D.F. Ind. Eng. Chem., 35, (1943) 614.

49. Othmer, D.F., Chudgor, M.M. and Levy, S.L. Ind. Eng. Chem., 44, (1952) 1872.

50. Pennington, R.E. and Kobe, K.A. J. Am. Chem. Soc., 79, (1957) 300.

51. Perry, J.H. Chemical Engineers' Handbook, 3rd ed., New York: McGraw-Hill Book Company, Inc., (1950) 574.

52. Plewes, A.C., Butler, R.M. and Pugi, K. Can. J. Technol., 34, (1956) 152.

53. Plewes, A.C., Jardine, D.A. and Butler, R.M. Can. J. Technol., 32, (1954) 133.

54. Plewes, A.C., Pei, D.C. and Code, R.K. Can. J. Chem. Eng., 37, (1959) 121.

55. Redlich, O. and Kister, A.T. Ind. Eng. Chem., 40, (1948) 345.

56. Sandonnini, C. and Parravano, S.N. Atti reale accad. naz. Lincei, Serie 6, IV, (1926) 63.

57. Scott, D.W., Waddington, G., Smith, J.M. and Huffman, H.M. J. Chem. Phys., 15, (1947) 565.

58. Scott, R.B., Meyers, C.H., Rands, R.D., Brickwedded, F.G. and Bekkedahl, N. J. Research Nat. Bur. Standards, 35, (1945) 39.

59. Shearer, J.S. Phys. Rev., Series I, XV, (1902) 188.

60. Sinke, G.C. and DeVries, T. J. Am. Chem. Soc., 75, (1953) 1875.

61. Smith, D.A., Kuong, J., Brown, G.G. and White, R.R. Petrol Refiner, 24, No. 8, (1945) 98.

62. Squibb, E.R. J. Am. Chem. Soc., 17, (1895) 187.

63. Stallard, R.D. and Amis, E.S. J. Am. Chem. Soc., 74, (1952) 1781.

64. Stavely, L.A.K., Tupman, W.I. and Hart, K.R. Trans. Faraday Soc., 51, (1955) 323.

65. Stiehl, J.G., Hobson, M., and Weber, J.H. A.I.Ch.E. Journal, 2, (1956) 389.

66. Strickland-Constable, R.F. Proc. Roy. Soc. (London), Series A, 209, (1951) 14.

67. Tallmadge, J.A. and Canjar, L.N. Ind. Eng. Chem., 46, (1954) 1279.

68. Tallmadge, J.A., Schroeder, D.W., Edmister, W.C. and Canjar, L.N. Chem. Eng. Progr. Symposium Ser., No. 10, 50, (1954) 137.

69. Thomas, K.T. and McAllister, R.A. A.I.Ch.E. Journal, 3, (1957) 161.

70. Tyrer, D. J. Chem. Soc., 99, (1911) 1633.

71. Tyrer, D. J. Chem. Soc., 101, (1912) 81.

72. Ibid., p. 1104.

73. Uchida, S., Ogawa, S., Hirata, M., Shimada, G. and Shimokawa, S. Chem. Eng. (Tokyo), 17, (1953) 191.

74. Waddington, G., Todd, S.S. and Huffman, H.M. J. Am. Chem. Soc., 69, (1947) 22.

75. Weber, J.H. J. Chem. Eng. Data, 4, (1959) 301.

76. Weir, H.M. and Eaton, G.L. Ind. Eng. Chem., 24, (1932) 211.

77. Weltner, W. and Pitzer, K.S. J. Am. Chem. Soc., 73, (1951) 2606.

78. West, E.D. and Ginnings, D.C. Rev. Sci. Instr., 28, (1957) 1070.

79. Williamson, K.D. and Harrison, R.H. J. Chem. Phys., 26, (1957) 1409.

80. Wilson, A. and Simons, E.L. Ind. Eng. Chem., 44, (1952) 2214.

81. Worthington, A.E., Marx, P.C. and Dole, M. Rev. Sci. Instr., 26, (1955) 698.

82. Wrewsky, M.S. Z. physik. Chem. (Leipzig), Abt. A, 144, (1929) 244.

83. Zabetakis, M.G., Craig, R.S. and Sterreth, K.F. Rev. Sci. Instr., 28, (1957) 497.